A STUDY OF ARC CONTROL DEVICES FOR MEDIUM POWER AIR-BREAK CIRCUIT-BREAKERS

by

K. D. Srivastava

B.Sc., B.E. (Hons.)

A thesis presented to Glasgow University

for the award of a Ph.D. degree

February, 1957

CONTENTS

PART ONE

DEVELOPMENT OF A LABORATORY POWER SUPPLY

CONTENTS (CONT'D.)

CONTENTS (CONT'D.)

PART THREE

APPENDICES

§§§§§§§§§§

1. INTRODUCTION

Circuit-breakers are designed to open under fault conditions and so isolate the faulty part of the system before more serious damage results. As the contacts part, an arc is drawn between them which must first be safely confined, and finally extinguished, by the recovery of the dielectric in which the contacts are immersed.

The development of circuit-breakers for the high ratings required in modern power systems calls for most expensive trials at a Short-circuit Testing Station, and such development, however successful the results, does not always provide basic data on the phenomena involved in arc control and extinction. In this respect, practice can be in advance of physical theory.

The systematic study of arc control devices is a useful field for post-graduate research, provided suitable laboratory techniques can be devised, and this thesis presents the first stages towards academic research in this field. Certain limitations were accepted at the commencement. The study was to be confined to air circuit-breakers, using the discharge of a tuned capacitor circuit to provide the fault current, and a considerable time would have to be spent in devising suitable operating techniques for this

'synthetic' circuit, with associated oscillographic and photographic techniques. Thereafter, the equipment was to be used for the study of the characteristics of arcs confined in chutes by a series of experiments that would be planned to show the relative importance of such factors as cooling, arc lengthening, and magnetic blow-out phenomena. To do this, it was recognised from the first that experimental chutes would have to be designed for special purposes, and the investigations were not to be confined to chutes of conventional design or practical application.

The thesis is presented in three parts. The first part deals with the development of a synthetic power supply suitable for laboratory research. In the second part a general survey of the present investigation is first given; the data obtained from oscillograms and cine-photographs are presented in the form of tables and graphs etc., and the results are then analysed and conclusions drawn. The last part consists of appendices; these describe the preliminary experiments to study the transfer of a d.c. arc from the main to auxiliary electrodes, and the experimental and photographic techniques. The details of the equipment used are also included in this part.

2. SURVEY OF PUBLISHED INFORMATION

2.1 General

The air-breaker in its modern form made its first appearance in the electric supply industry in the late 1930's. Air-breaker terminology, at the present time, is ambiguous. Various trade names like 'magne-blast' are confused with type designations such as 'deion-breakers'. In the present thesis the term 'air-break circuit-breaker' is used to describe the type of circuit-breaker in which the arc is drawn between suitable arcing electrodes in air, and confined in an arc chute of refractory material, the arc chute being a more elaborate device than the simple chute-box used on low power contactors.

2.2 Nature of the Arc in Air-break Circuit-breakers

The physical characteristics of power arcs in open air have been the subject of many investigations (Refs.1,2). The chief characteristics are briefly summarised below.

The voltage distribution in the arc consists of three principal parts, corresponding to the anode drop, the cathode drop, and the voltage across the actual arc column. The anode and cathode drops are chiefly dependent upon the current, whereas the drop along the arc column is

approximately proportional to the arc length.

Under the action of electric field, electrons are ejected from the hot cathode spot or root, and in their passage to the anode, cause ionisation by collision with neutral molecules. The resulting positive ions are attracted to the cathode. The collision of these ions with the cathode further raises its temperature. Both anode and cathode roots are at a high temperature.

According to Ayrton, the length, l, of the arc column and the voltage, v, between its terminals are related to the arc current, i, by the formula

$$v = \alpha + \frac{\beta}{i} + \left(\gamma + \frac{\delta}{i}\right) l$$

where α, β, γ and δ are constants depending upon the physical properties of the electrode material and the gas surrounding the arc.

Owing to the above relationship it is not possible to produce an arc of any arbitrary length, current and voltage. To maintain the stability of the arc, the energy input to the arc, vi, must never be less than the losses from it. These losses may be due to conduction, convection and radiation, etc.

However, in an a.c. arc, at current-zero, the energy input is instantaneously zero, and once the energy

input ceases the ionisation decays rapidly.

The arc, being a flexible current-carrying conductor, is susceptible to magnetic deformation in accordance with Ampère's Left-hand Rule.

2.3 Basis of A.C. Interruption in Air-break Circuit-breakers

The design of any interrupting device is governed by one or more of the above characteristics. The chief method used for a.c. interruption is a gradual increase in arc resistance until the arc voltage rises to such a value that the available circuit voltage is insufficient to maintain the arc. Alternatively, the dielectric strength of the arcing space recovers at current-zero at such a rate that the available circuit recovery voltage is insufficient to re-establish the arc. In current practice, circuit interruption involves one or both of these methods.

2.4 Classification of Types of Arc Chutes

The voltage wave-form across an opening breaker when a sinusoidal current is flowing has been chosen as the basis for a simple classification (Refs.3,4). Fig.1. shows these wave-forms drawn together with the corresponding current wave.

Type (a): The re-striking voltage, in this type

of arc chute, rises nearly at the rate of the natural frequency of the circuit until the electrode gap breaks down. The arcing voltage during the rest of the half-cycle is fairly low and rises slightly as the next current-zero is reached. The resistance of the arc column at and near current-zero is fairly high, indicating a rapid recovery of the dielectric during this period. To achieve a rapid recovery of the dielectric one or more of the following control devices are generally used:

(a) Metallic arc splitters.

(b) Magnetic system to keep the arc roots in continuous motion.

(c) Induced or artificial air flow to scavenge the inter-electrode space.

Type (b): In this type, due to considerable ionisation existing around the current-zero period, the voltage rises at a rate often much lower than the natural rate of rise of recovery voltage (r.r.r.v.), and having risen at the beginning of the half-cycle, remains nearly at that level throughout the half-cycle, only falling at the end. The arc resistance during the half-cycle may often be higher than in Type (a), since in such chutes, the arc is invariably lengthened considerably. The control devices used to assist in arc lengthening are arcing horns,

insulating, non-gas-forming arc barriers, and magnetic blow-out fields.

2.5 Analysis of Information Regarding Arc Chute Design and Performance

2.5.1 General

Non-gas-forming insulating ceramic material (Micalex, Sindanyo etc.) is almost invariably used for the construction of arc chutes. Copper, iron, insulated iron plates, and insulating refractory material, are mostly used for arc splitters or barriers.

One or more of the control devices mentioned in the previous section are incorporated, but comprehensive data for the choice of any specific method of control are seldom given.

Since the breakers of Type (b) usually employ arc lengthening as the chief method of arc control, the power dissipated in the breaker of this type is much greater than in other types of breaker. The information concerning arc chute interrupting capacity, arc control, and the effect of phase shift of the magnetic field with respect to arc current, is scanty and inconclusive.

2.5.2 Mechanism of Arc Extinction

A few indirect attempts (Ref.5) have been made to examine the physics of arc extinction in air-break circuit-breakers. The basis of all such attempts has been the fundamental work done by Slepian (Ref.6), Cassie (Ref.7), and Mayr (Ref.8), etc. It is widely believed that the mechanism is of the energy balance type (Ref.9), the energy loss from the arc column at and immediately after current-zero having to be greater than the energy input for a clearance to occur.

The precise nature of the physical aspects of arc extinction is still a controversial subject and, in fact, the design of air-break circuit-breakers has so far been largely a matter of ad hoc development.

PART ONE

DEVELOPMENT OF A LABORATORY POWER SUPPLY

POWER SUPPLY

1. General

The conflicting requirements of flexibility, ease of operation, and cost, govern the selection of a suitable power supply for academic laboratory research.

The chief object of the present work was to make a logical study of arc control devices for air-break circuit-breakers; no new design or short-circuit testing of any existing one was ever intended. Moreover, it will be appreciated that the behaviour of an arc in the first few half-cycles of its existence plays a decisive rôle in determining the effectiveness of any arc control device, and therefore, for such investigations, a power supply effective for a few half-cycles is all that is needed. The above considerations led to the development of the 'synthetic' power source discussed below.

2. Synthetic Power Supply

The tuned inductance-capacitance circuit has been used by various investigators in circuit-breaker research. However, the tendency so far has been to use this arrangement mainly for the study of current-zero phenomena (Refs. 4,10,11,12).

The basic circuit used hitherto is shown in Fig.2. The circuit consists of a capacitor, C , and an inductance, L , in series, and tuned to oscillate, on discharge, at the frequency of the power source that it represents; the test gap, G , represents the arc control device being investigated. The voltage, V , to which C is initially charged, from a high impedance d.c. source not shown in the diagram, represents the peak value of the power system voltage. The system fault conditions reproduced by such a circuit are those under which the fault occurs at the peak value of voltage in an inductive a.c. power system, i.e. under zero power factor conditions. This is generally accepted as the most severe condition for a rapid interruption of the arc current, since the rate of rise of recovery voltage (r.r.r.v.) is highest under such conditions.

The frequency of oscillation of the circuit shown in Fig.2. is given by

$$f = \frac{1}{2\pi}\sqrt{\frac{1}{LC} - \frac{R^2}{4L}} \quad \ldots\ldots\ldots \quad (1)$$

Provided the circuit resistance is negligible, the value of the first current peak is $\frac{V}{Z}$, where $Z = \sqrt{\frac{L}{C}}$, and is referred to as source impedance. By a suitable choice of L and C values, the frequency of discharge can be made equal to 50 c/s, and a variety of voltage and current ranges can be simulated.

3. Merits and Demerits of the Synthetic Power Source

The voltage and current relationships are shown in Fig.2.

The decrement, that is the ratio of successive peaks of discharge current or voltage, is determined by the ratio of circuit resistance, R , to inductance, L , (Eqn.1). To keep the decrement low it is therefore necessary to keep R as low as possible, and L as high as possible. Since the product LC is fixed by considerations of frequency, C must be reduced for increasing values of L; consequently, the initial voltage, V , must be increased for a given current.

The resistance, R , in the above discussion consists of circuit and arc resistances; to keep the circuit resistance low is a matter of design, but in later stages of arcing, the arc resistance may become too great for the power supply to remain effective.

The arrangement is simple, easy to handle and very flexible; any of the initial conditions can be varied by proper selection of C, L and V values

4. Extension of Synthetic Circuit Technique to Simulate Point-On-Wave Conditions

The system fault conditions reproduced by the circuit of Fig.2. are those under which the contacts part at the peak value of the system voltage. This gives a set of extreme conditions for the point-on-wave at which the fault may occur, but some data at intermediate values, i.e. for points of arc initiation on the voltage wave other than the peak, are necessary for the better understanding of the phenomena involved.

The desired conditions can be attempted by two techniques:

1. An extension of the synthetic circuit technique.
2. The use of a power transformer to give a conventional power source at 50 c/s.

This section is confined to the first of these methods, and describes the development of a circuit capable of simulating point-on-wave conditions.

5. Point-On-Wave Control Using an Additional D.C. Source

The first circuit used to obtain point-on-wave control is shown in Fig.3a. The high impedance previously used to charge C is replaced by a relatively low impedance d.c. source, E ; resistance, R ; and a series gap, G_2 .

The sequence of operation is that G_2 is short-circuited and C commences to charge by current flowing from E, the rate of growth of voltage being determined by the time constant, CR . At some time, T , subsequent to the short-circuiting of G_2 , the arc in G_1 is initiated, and power current can be supplied by the discharge of C through L and G_1. If the time constant, CR , is small and, at the instant of arc initiation in G_1 , the voltage, V_c , across C is much less than the voltage, E , of the d.c. source, V_c continues to rise. These voltage and current variations with time are shown in Fig.3c, where V_{co} is the voltage to which C has been charged at the instant of arc initiation; thereafter, it oscillates as shown by V_c. The current is shown by the waveform I_L. Both V_c and I_L will have an exponential decrement due to the presence of R, and I_L oscillates about a zero which is displaced from true zero by an amount E/R which is, in fact, the final steady state current.

The circuit analysis in Appendix I gives the equations for V_c and I_L which are the voltage and current conditions in the power system represented, at any time, T , subsequent to the establishment of arc current in the gap, G_1 , namely:

$$V_c = e^{-t/2CR} \cdot E \left[(1-K)^2 + \left(\frac{1-K}{2\omega CR} \right)^2 \right]^{\frac{1}{2}} \cdot \cos (\omega t - \alpha)$$

where $K = e^{-T/CR}$, and $\alpha = \tan^{-1}\left[\frac{1-K}{1+K} \cdot \frac{1}{2\omega CR}\right]$

and $I_L = \frac{E}{R} + \frac{E}{R} \cdot e^{-t/2CR}\left[1 + \left(\frac{RK}{\omega L} - \frac{1}{2\omega CR}\right)^2\right]^{\frac{1}{2}} \cdot \sin(\omega t - \beta)$

where $\beta = \tan^{-1}\left[\frac{2\omega CRL}{2(1-K)\ CR^2 - L}\right]$

The gap, G_2 , having been short-circuited at time, T , prior to t = 0, the initial conditions for C are:-

At t = 0

$$V_c = V_o = E(1 - e^{-T/CR}) = E(1-K)$$

$$I_c = I_o = \frac{E}{R} \cdot e^{-T/CR} = \frac{E}{R} \cdot K$$

The peak value of V_c can be controlled by varying T, E and R, and the point-on-wave at t = 0 by varying T and R, so that the circuit does produce the desired conditions, but with decrement of the wave-forms and a shift of the current-axis. The point-on-wave that can be selected has certain limitations. As $T \longrightarrow \infty$ the value of α approaches asymptotically to a minimum value given by $\tan^{-1}\left(\frac{1}{2\omega CR}\right)$, and this limits the highest point-on-wave that can be selected to a value which is, in practice, some 5-10° below the peak of V_c wave-form. Any point from this limit down to zero on

the rising side of the wave-form can be selected.

6. Point-On-Wave Control Using an Additional Capacitor Source

In this an additional capacitor, C_2 , previously charged from a high impedance source, is used in place of the d.c. supply, the circuit then being as shown in Fig.3b. The functioning of this circuit is clearly similar to that previously described, provided that C_2 is large compared with C_1.

The wave-forms produced by this circuit were similar to those sketched in Fig.3c, except that the V_c and I_L wave-forms oscillate about false zeros which decay exponentially towards the true zero. For the purposes of the present investigation the magnitude of the decrements and the displacement of the current and voltage axes, were not such as to have a significant effect on the data required.

The circuit analysis in Appendix I gives the following expressions for V_{C1} and I_L:

$$C_1 V C_1 = A\, e^{-\alpha_1 t} + B\, e^{-\alpha_2 t} .\cos(\omega t - \beta) \text{ where } \omega = \sqrt{\frac{1}{LC_1} - \frac{1}{4C_1^2R^2}}$$

$$I_L = C\, e^{-\alpha_1 t} + D\, e^{-\alpha_2 t} .\sin(\omega t - \theta)$$

The further treatment of these two equations is most conveniently dealt with by the substitution of numerical values. Limitations to the range of point-on-wave that can be selected are similar to those detailed above.

Fig.4. shows tracing from typical oscillograms using the above methods of point-on-wave control.

7. Experimental Technique and Equipment

In evolving an experimental technique based on the above circuits, various problems of controlled switching, sequence control, and measurement were involved, and the necessary auxiliary equipment was developed. A detailed account of the laboratory techniques and equipment is given in Appendix II.

PART TWO

EXPERIMENTS, RESULTS AND OBSERVATIONS

SECTION A

A GENERAL SURVEY OF THE WORK UNDER REVIEW

1. Introduction

It is intended in this section to outline the logical evolution of the experimental work under review; the experiments performed are presented here in their chronological order. At the commencement, the present state of knowledge of arcing phenomena and current commercial practice was taken into account. Although attempts were made to vary only one parameter at a time, the complicated nature of the phenomena and experimental limitations made this difficult.

The arc chutes used in these experiments are shown in Figs.5a,b. 'Sindanyo', 1/4" thick, has been used throughout for the construction of chutes and insulated arc barriers. Experimental convenience led to the choice of a fixed gap, G , Fig.2., since moving contacts would have introduced the speed of contact travel as an additional variable. The uncertainty of the instant of contact separation and the problem of arc transfer to auxiliary electrodes would have further confused the observations, (Appendix II).

Although a general picture of the arc control

phenomena has emerged, no attempt has been made in this section to analyse the results in detail.

2. Initial Experiments

2.1 Transfer of an Arc from Main to Auxiliary Electrodes

The arc in the early stages of arcing in a circuit-breaker has to be transferred from the main current-carrying contacts to the auxiliary arcing contacts; moreover, at some later stage of this investigation metallic splitters might have been used to raise the arc drop by increasing the number of arc roots in series. Therefore, it seemed that some idea of the mechanism of such a transfer would be useful. A preliminary study of these phenomena was therefore undertaken. Low current d.c. arcs were used because of their relative stability and ease of handling.

Various circuit diagrams and the other experimental details of the above investigation are given in Appendix IV. The main conclusions of this investigation are, however, noted below. The current for this investigation was limited to 15 ampères.

(1) When a metallic splitter, connected to both anode and cathode through resistances, is slowly pushed at right angles into an arc column, a current through it is established. This current consists of both ion and electron

currents. The ion current reaches a maximum steady value as the potential of the splitter is made increasingly negative with respect to the anode. If, however, the potential of the splitter is increased in a positive direction, a potential is reached when these two currents are equal and opposite. This is called the 'floating potential', as it would be the potential assumed by an isolated splitter when in contact with an arc plasma. It is about 40 volts, negative to anode, for a total arc drop of about 50 volts. Now, if the potential of the splitter is made sufficiently positive with respect to the arc plasma at the point of contact, rooting on the splitter occurs.

The splitter can carry currents up to an ampère before rooting occurs. After rooting has taken place the current through the splitter is determined by the resistance, R_1 , between the splitter and the anode, and the voltage across the arc column shunted by the above resistance. The maximum value of R_1 , which would allow rooting on the splitter, is determined by the static characteristic of the arc column and the external circuit constants. The value of R_1 , required for the extinction of the arc shunted by it, decreases as the arc current is increased.

It was not possible to get rooting on a splitter connected only to the cathode through a resistance. This is probably due to the fact that the formation of a cathode

root requires emission of electrons, and hence, high field gradient or temperature, or both, are needed for cathode rooting.

Variations in arc current, for the present range, do not have any appreciable effect on the splitter characteristics detailed above.

(2) Isolated splitters: With the help of the above observations, it may be possible to predict the behaviour of two isolated splitters, connected through a resistance, in an arc plasma.

For rooting on two short-circuited splitters, the spacing between the splitters must be increased until the voltage drop across the arc column between them is greater than the voltage required for the two root drops. The critical resistance between the splitters, for the extinction of the arc column shunted by them, increases with the spacing between them.

It is possible to place two short-circuited splitters at positions along the arc column such that they do not carry any current, i.e. on either side of the point at which ion and electron currents are equal and opposite.

(3) A.C. Arcs: In an a.c. arc, the difficulty of cathode rooting is non-existent, if the arc burns for more than one

half-cycle. In the case of a shunted a.c. arc, the critical resistance required for the extinction of the shunted arc will vary with the rising and falling parts of the current wave-form, due to the difference between the slopes of the dynamic characteristic for the above parts of the current wave.

2.2 Power Supply

A voltage range of 1100 to 4400 volts was chosen for the present work, as being well above the low voltage contactor range.

As mentioned earlier (Section 3, Part I) a long arc in the circuit of Fig.2. could impair the effectiveness of the power supply; therefore, a series of experiments, for Capacitor Bank voltages up to 2200 volts, was carried out to determine the optimum conditions (voltage, current, gap length) which would give maximum duration of arcing in open air. These optimum conditions (2200 V, 2000 amps. and 3/8" gap) were then taken as the starting point for the present investigation.

3. A Study of Arcing in an Enclosed Volume

3.1 General

A preliminary examination of the problem indicated that the first step in arc control should be the confinement

of the arc and the products of arcing, since an uncontrolled arc might lead to multiple short-circuits on a power system.

The study of arcing in a chute was considered in two parts:

1. Arc entry into the chute
2. Arc control by the chute.

3.2 Chute B

It was considered that the two functions of a chute, detailed in the previous sub-section, should, if possible, be considered separately. The first chute was to be just sufficiently big to contain the arc, without in any way affecting its electrical characteristics, the arc voltage and duration of arcing being taken as the criteria of arc control. The first chute, chute B in Figs.5a,b, therefore, conforms to the shape and size of an arc in open air under the voltage and current conditions chosen for this investigation.

This is illustrated in Figs.6a and b. Fig.6a shows an arc between fixed contacts in air, without a chute, while Fig.6b shows arcing in chute B, which is of the same dimensions as the arc in free air. This chute has little effect on the arc characteristics, except that it provided a known boundary for the arc and regulated the upward movement of arc gases. The above figures are reproduced

from cine-films taken for the experiments; only alternate picture frames covering the first half-cycle or arcing are selected. Approximately ten picture frames correspond to a half-cycle of 50 c/s current wave. Details of the cine-technique are given in Appendix III.

3.3 Cooling by Chute Walls - Chute C

The first factor in arc control considered was cooling by loss of heat from the arc to the chute walls. If cooling by the walls is important, it was felt that the arc must be forced into close contact with the 'Sindanyo' walls so that energy could be extracted from the ionised arc column; therefore, chute C, in Figs.5a,b, which is smaller than the previous chute B, was designed.

The cine-films taken for experiments with chutes B and C indicated that the ionised gases at the base of the chute had not been removed; the arc, therefore, re-struck across the shortest path between the contacts. In Fig.6b, prints 6 and 7 show such a re-strike for chute B. The cine-films for tests with chute C indicate that the above tendency, i.e. to re-strike at shorter arc lengths, is increased, thus making extinction difficult. Consequently, the arcing time with chute C was higher (4 to 5 half-cycles) than with chute B (3 half-cycles).

3.4 Arc Entry into the Chute

Some experiments were first performed to determine the position of the chute in relation to the contact assembly, which would make it most effective as a container. Figs.7a to d, show reproductions from the cine-films, and cover the first half-cycle of arcing; only alternate picture frames are selected. Fig.7a shows chute C, which covers the fixed contacts at the lower ends. Print 6 shows conditions near the first current-zero. In Fig.7b, chute C does not enclose the contacts, and thus allows the hot gases to escape outside the chute, which may lead to uncontrolled arcing. This is shown in prints 6 and 7 following the first current-zero.

Figs.7c and 7d show effects similar to Figs.7a and 7b but with chute B.

When the chute was placed with its lower end above the contact assembly as in Figs.7a, 7b and 8b, the arc did not encounter any appreciable difficulty in entering the chute. Some references in the technical press had been made regarding arc entry into chutes (Ref.13). It appeared quite plausible that a chute might offer some 'air impedance' to arc entry into it. It was difficult, at this stage, to say precisely the factors that governed such an impedance; nevertheless, it was felt that the volume and height of a chute might have some bearing on it. To pursue this line of

reasoning chute D was designed, Figs.5a,b. This is 6 inches in height (cf. 3 inches for chutes B and C), and has a volume of 30 cub.in. (cf. 11 and 6 cub.in. for chutes B and C respectively); but in only one of the experiments with this chute was some difficulty in arc entry observed. To consider the effect of increased height alone, chute E was designed. This chute had the same volume as chute B but was nearly twice as tall; but no difficulty in arc entry was observed.

3.5 Arcing in Chutes B, C, D and E

At this stage the work done so far was analysed, and the performance of the above chutes was compared with arcing in free air.

Fig.6a shows an arc between fixed contacts in free air. The arc once initiated travelled to the top of the contacts (Fig.11a) within one millisecond, giving an average arc root velocity of approximately 100 ft./sec. The speed of the cine-camera used prevented any closer estimate (Appendix III). There was an initial delay in the arc movement upwards, and this was usually less than a millisecond. For most of the arc duration the arc roots were situated along the top edge of the contacts and the arc column took up an arbitrary position and shape. Since a high current arc is surrounded by a volume of hot gases, special photographic

techniques employing various light filters were developed (Appendix III). Initially, the arc gases without a chute expanded in all directions with little, but definite, upward movement.

The arc column was surrounded by a volume of highly ionised gases; thus, considerable conductivity existed around the current-zero period. Therefore, the rate of rise of recovery voltage (r.r.r.v.) was considerably reduced; the arc voltage characteristic being of Type b in Fig.1.

The above chutes (B, C, D and E) seemed to have little effect on arc extinction. There was no indication of arc movement downwards, and no difficulty in obtaining arc entry into the chute (with one exception, chute D). In general, arc gases moved upwards (Figs.6 and 7). As can be seen from Figs.8a and 8b the shape of the chute affected the movement of arc gases through it; in these figures alternate picture frames, covering the first half-cycle, are reproduced. Fig.8a shows chute B, with diverging sides, allowing for expansion of the hot gases that moved upwards; prints 5 and 6 cover a current-zero. Fig.8b shows chute B inverted, so that the cross-section diminished with height. The arc movement upwards therefore accelerated as the gases moved upwards. The gas velocity at the top exit with chute B inverted was about 100 ft./sec.

When these chutes were used, the first half-cycle was characterised by a gradual increase of arc voltage, similar to that obtained with opening contacts (Fig.9a). The cine-photographs indicated that the initial delay in arc movement upwards was increased from under a millisecond in open air to about 2 to 4 milliseconds.

The re-strike voltages with these chutes tended to be of Type a in Fig.1; this tendency was more marked with chutes D and E. The re-strike voltages after the first current-zero were about 400-500 volts for chutes D and E, while for chutes B and C, these were usually below 300 volts. This tendency indicated that these chutes were increasing the dielectric recovery of the test gap around the current-zero period (cf. arcing in open air).

Oscillations in the arc voltage of the type shown in Fig.9b were noted with these chutes. This tendency was more pronounced with narrow chutes C and E, and it was particularly marked in the later half-cycles of arcing. A comparison and correlation of the oscillograms with the corresponding cine-films indicated that these oscillations were due to ionised gases at the base of the chutes, which enabled the arc to re-strike across the shortest path between the contacts (Fig.7c, prints 6 and 7). The duration of arcing with chutes C, D and E varied from 4 to 7 half-cycles and was consistently higher than with chute B (3 half-cycles).

This appeared to be due to the recurrent re-strikes of the arc across the shortest path between the contacts, as explained in the preceding paragraph, and was noted mostly with chutes C and E.

Variations in arc current from 2000 to 900 amperes, and 10% variations in the frequency of the synthetic power source, did not have any appreciable affect on the arc voltage characteristic.

3.6 Chute F

Although the impressions of arcing in chutes, gained from these experiments were not precise, it was possible that in the smallest chute used so far (chute C) the arc might not have been sufficiently close to the chute walls to make cooling by them significant. Chute F was therefore designed (Figs.5a,b). This chute has a reduced cross-section compared with chute C, but is equal in height.

No significant improvement in arc control was observed and the arcing time with this chute remained in the region of 4 to 5 half-cycles.

4. Induced Air Flow

The process of heat exchange between the arc and its surroundings was reconsidered, and this could be

classified under three headings:

1. Radiation
2. Conduction
3. Convection

The loss of energy by radiation was considered relatively unimportant (Ref.14). To examine the process of heat exchange by conduction, attempts to minimise induced air currents were made.

4.2 Chutes G and H

It was felt that a chute with constant area of cross-section but decreasing depth, front to back, would help to minimise convection currents, and at the same time, increase the possibility of greater heat extraction by conduction to the chute walls. Chutes G and H were, therefore, designed. These chutes are also 3 inches high. Both areas of cross-section, bottom and top, are 1.5 sq.in. The depth of the chutes, front to back, is 1 inch at the bottom decreasing to $\frac{1}{2}$ inch and $\frac{1}{4}$ inch at the top for chutes G and H respectively. The variation in area of cross-section with height is small; the area of cross-section at the middle being about 1.2 times that of the bottom/top areas.

Oscillograms and cine-films taken for experiments with these chutes were examined. The re-strike voltages for these chutes tended to be of Type a, Fig.1, and were

generally higher than for previous chutes (about 600 volts or more). This might be due to closer contact between the chute walls and the arc column, and therefore, a faster recovery of the dielectric strength of the test gap.

The oscillations in arc voltage characteristic of the type shown in Fig.9b, remained unaltered and, therefore, the arcing time also remained about 4 or 5 half-cycles. These oscillations were due to ionised gases remaining at the bottom of the chute, as illustrated in Fig.10. In this figure, the first ten picture frames covering the first half-cycle or arcing with chute H are reproduced. Approximately 8 frames correspond to a half-cycle of arcing; print 8 shows conditions near the first current-zero. Prints 5 and 7 show the short-circuiting of the arc column.

4.3 Chute I

To remove the ionised gases from near the contacts, three methods were considered: first, the provision of an artificial air flow to remove the ionised gases further upwards; secondly, to provide arc runners to remove the main source of ionisation, i.e. arc roots, upwards; thirdly, to shape the chute in such a manner that the induced air flow through it would be increased. Since the previous experience with chutes B, C and D, etc., (Figs.7a to d and 8a and b) indicated that chute shapes did, in fact, affect the air flow

in the chute, the last method was preferred. Moreover, at this stage, it was premature to resort to additional means of arc control. Chute I was therefore designed (Figs.5a,b). The height, and the area of cross-section at the bottom, are 3 inches and 1.5 sq.in. respectively, equal to those for chutes F, G and H; but the depth of the chute, front to back, decreases with height, from 1 inch at the bottom to $\frac{1}{4}$ inch at the top.

Cine-films and oscillograms taken for the experiments with chute I indicated that the chute was not effective in quickly removing the ionised gases further upwards. This indicated that induced air flow took some time to develop. The arcing time was increased to about 7 half-cycles and the increased tendency for oscillation in arc voltage characteristic corresponded to the recurrent re-striking of the arc at lower arc lengths. The initial delay in arc movement upwards was also increased to nearly 6-7 millisecs.

It appeared that the reduced volume of the chute, 4 cub.in., (cf. 11 cub.in. for chute B) and the narrow top exit, 2" x $\frac{1}{4}$", (cf. 5.5" x 1" for chute B) might be responsible for the poor arc control by chute I, since the products of arcing were confined in a small volume. Furthermore, the narrow top exit might have been blocked by the arc column, thus trapping the ionised gases in the chute.

5. Arcing Horns

The above experiments with chute I indicated that the induced air flow might not be sufficient to reduce the intensity of ionisation at the bottom of the chute near the electrodes. The electrode separation, so far, had been 3/8" and although this value had been chosen because of the characteristics of the main capacitor circuit, it was felt that it might be too small for the voltage used (2200 V). The electrode separation was, therefore, successively increased to 3/4" and then to 1". Due to increased arc length, and therefore, arc resistance, a reduction in the arcing time was expected (Part II, section 2.2) and the experiments that followed confirmed the same. This still was not sufficient to enable the chutes used so far to show any appreciable control of the arcing phenomena. The chutes, by themselves, were not sufficient to exercise appreciable arc control.

The arc roots, for most of the arc duration in the foregoing experiments, were situated along the top edges of the electrodes (Fig.11a). The roots were, therefore, fairly close, 3/4", to the position of minimum-electrode-separation. It was felt that such a close proximity of arc roots was responsible for a high degree of ionisation in this region, and it seemed desirable to move the arc roots further upwards from this region. Arcing horns were, therefore, incorporated (Figs.11b and c).

Some experiments with horns in open air were performed to serve as a basis for comparison with arcing in chutes using horns. The length of the horns was such as to allow the roots to move upwards, away from the minimum-electrode-separation, but at the same time reducing the possibility of the arcing outside the top exit of the chutes used.

In Figs.15a to e, prints are reproduced from the cine-films taken during experiments with arcing on horns in air without a chute. These show horns with varying angles of inclination to the vertical.

Figs.15a,b, show parallel arcing horns 6 inches high and 2 inches apart. Approximately seven picture frames cover a half-cycle of arcing at 50 c/s. The velocity of upward arc movement is about 100 ft./sec., in the early part of the first half-cycle. Fig.15b shows an arc with twice the arc current (4000 amps. first peak), but little difference in the velocity of upward movement is observed.

Fig.15c shows arcing on horns which begin to diverge at the height of 3 inches from the top of the contacts. The arc velocity on the parallel part is of the same order (100 ft./sec.). On the diverging part (Prints 4 onwards) the arc length is increased and the upward velocity of the arc column is reduced, due to its random convolutions. The arc roots, therefore, travel faster than the arc column and have reached

the tip of the arcing horns in print 5. Print 9 shows the condition near the first current-zero.

Fig.15d shows arcing on diverging horns, which begin to diverge at 30^{o} to the vertical, from the start. The arc velocity is definitely reduced; the arc column is only about 3 inches above the contacts throughout the first half-cycle. (Prints 4 and 5, two picture frames between prints 1 and 2, are missing). Print 5 shows the conditions near the first current-zero. Print 7 shows the arc re-striking between the tip of one and the bottom of the other runner, indicating that the gases surrounding the arcing horns are highly ionised.

Fig.15e also shows arcing on similar diverging horns, the angle of divergence being greater, 75^{o} to the vertical, than in Fig.15d. One of the arc roots is seen to travel faster than the other (Print 3). The upward movement of the arc column is slow, about 50 ft./sec., but the arc length has increased to about 6 inches, the contact separation being an inch, in about 4 millisecs., (Print 3). Print 8 shows conditions near to the first current-zero. Print 12 shows arc rooting on other metallic parts of the contact assembly.

The above reproductions show that the arc gases are relatively immobile and, for most of the arc duration, the arc runners are surrounded by a volume of ionised gases, thus

making uncontrolled arcing possible. (Print 7, Fig.15d; Print 11, Fig.15e). Due to considerable ionisation present around the current-zero period, the rate of rise of recovery voltage (r.r.r.v.) is reduced and, therefore, the arc voltage characteristic is of Type b in Fig.1. Arc columns up to 6 inches in length are fairly well defined (Print 3, Fig.15e) but at higher arc lengths the record is diffused. The arcing time in the above experiments was 2 half-cycles.

Some experiments using horns were performed with chutes E, G and H. Figs.12a and 12b show reproductions from cine-films taken for arcing in chutes H and E using horns. In both these experiments the arc burned outside the chute for most of the arc duration. (Print 4, Fig.12a; Print 6, Fig.12b). The arc gases in Fig.12a are not effectively removed from near the contacts, thus enabling the arc to re-strike at a shorter arc length. (Prints 4 and 5). The arc voltage characteristic shows corresponding oscillations (Fig.9b). The arc length towards the end of the first half-cycle is several inches (10-15 inches), while without the arc runners, it was less than 6 inches. (Fig.10, Print 7).

No reduction in arcing time was, however, achieved by using arcing horns with chutes E, G and H. This appeared to be again due to ionised gases near the contacts, enabling the arc to re-strike at shorter arc lengths.

6. Chutes J, J_A and K

It seemed, at this stage, that a chute combining an induced air flow with an intimate contact between the arc column and chute walls might furnish some useful information. Chute J was, therefore, designed. (Figs.5a,b).

Chute J consists of two parts: the bottom part, which encloses the contacts, is similar to chute I; the depth, front to back, decreases from an inch at the bottom to ¼ inch at 3 inches above the bottom of the chute; the top part of the chute is similar to a narrow rectangular 'chimney', ¼ inch deep and 6 inches high. The chute is 2 inches wide throughout.

Experiments with chute J, using arcing horns 6" high, were performed. The arc took a measurable time, usually under 4 millisecs., before any upward movement commenced, and it also paused at the entrance to the narrow upper chamber, the 'chimney' of the chute. Figs.13a to c illustrate the above observations; in these, approximately 8 prints correspond to a half-cycle at 50 c/s.

In Fig.13a, no arc movement commences until Print 7. The arc gases instead of moving upwards through the 'chimney' are noted to escape from the bottom of the chute (Print 4). The arc gases begin to move into the 'chimney' in Print 6, that is, before the arc movement commences. Print 8 shows conditions near to the first current-zero. The

arc has almost reached the top of the runners in Print 9. The arc velocity is approximately 500 ft./sec., the speed of the cine-camera used preventing closer estimate (Appendix III). In Prints 11 to 14, the arc gases generated on the underside of the arc can be seen to be travelling downwards. The height of the 'chimney' (6") prevents these downward travelling gases from re-establishing the arc across the shortest path between the contacts. Fig.13b shows an arc of twice the current value (4000 amps., first peak). The arc movement has commenced in Print 3. The arc gases instead of moving into the 'chimney' escape from the bottom of the chute (Print 4). The arc has reached the top of the runners in Print 7. Though a closer estimate of the arc velocity is not possible, the arc does travel faster at higher currents, and the initial delay in arc movement is also reduced. This presumably is due to the higher self-magnetic blow-out force. Prints 11 to 14 show the arc gases generated on the underside of the arc travelling downwards, but again no short-circuiting of the arc is noted.

The problem of the initial delay in arc movement and the difficulty of arc entry into the 'chimney' was considered in detail. To assess the effects of the height and the depth of the 'chimney', chutes J_A and K were designed. Chute J_A has a chimney height of only 3 inches (cf. 6 inches for chute J), and in chute K, the chimney is 3/4 inch deep

TABLE 1

Record No.	Vol.of the 'chimney'	Height of the 'chimney'	Time taken by arc to enter the 'chimney' as a fraction of half-period ($T/_2$)	Width	Chute
103	1.5 cub.in.	3"	$7/_9$	$1/_4$"	J_A
94	3 cub.in.	6"	$7/_{8.5}$	$1/_4$"	J
106	5.625 cub.in.	3"	$5/_9$	$3/_8$"	L
104	9 cub.in	6"	$5/_{8.5}$	$3/_4$"	K

(cf. ¼ inch for chute J). Table 1 shows a few sample data from these experiments; the total time taken by the arc to enter the 'chimney' seems to be affected by the depth of the 'chimney'.

Fig.13c shows an experiment with chute J_A. The arc movement has commenced in Print 3. Print 5 is of special interest. This shows that the arc had reached the top of the runners sometime between Prints 4 and 5, but the ionised gases at the bottom of the chute have enabled the arc to re-strike at a lower arc length. The height of the 'chimney' is only 3 inches, and therefore the gases generated on the underside of the arc, being unable to escape, can produce this repeated short-circuiting of the arc (cf.Figs. 13a and 13b). Prints 7-8, 11-12 and 13-14 further illustrate the phenomena. Prints 8 and 14 show conditions near the first and second current-zeros respectively. The arcing time with chutes J, J_A and K was about 3 to 4 half-cycles (cf. 2 half-cycles for horns alone).

With the help of cine-photographs, some attempts were made to estimate the effect on arc voltage of close contact between the arc column and the chute walls for chutes J and J_A. The voltage drop across the arc measured for two different positions of the arc, and the corresponding arc length and current are given in Table 3 (p.49a). These results are discussed in detail in Section B.

7. Arc Lengthening

7.1 General

The foregoing experiments were primarily meant to study the effect of cooling by the chute walls on arc control. The provision of arcing horns or runners, etc., was merely to get over the obstacles met in such a study. Experience, however, showed that any increase in the arc voltage or the energy dissipation or the arcing time was invariably due to an increase in arc length. It was therefore felt that, for the simple chutes and for the voltages and currents used in these experiments, arc lengthening might be relatively more important for arc control than cooling by contact with the chute walls. If this was so, chute designs with a view to lengthening the arc were necessary before any control over the arcing phenomena could be expected.

7.2 Chute L

To study the effects of arc lengthening, chute L was designed (Figs.5a,b). The chute is similar to chute J except that the upper chamber has divergent sides instead of being rectangular. Close contact between the arc column and the chute walls, and induced air flow, were retained as design features.

The initial experiments with chute L indicated that the arcing time was equal to that obtained with the arc

runners in open air (2 half-cycles). The arc voltages obtained were also higher when compared with previous experiments. The arc voltage towards the end of the first half-cycle was about 400 V, and the re-strike voltage after the first current-zero tended to be of Type a, Fig.1, and was higher than 800 volts; but towards the end of arcing duration, the arc mainly burnt outside the top exit of the chute (Fig.12c). This chute was not an effective container.

7.3 Insulating Arc Barriers

The arc runners had to be used to prevent the arc from re-forming at the bottom of the electrodes, and these runners had to be divergent to enable the arc to lengthen; at the same time, the arc had to be kept inside the chute. There were two possible ways of satisfying the above requisites; first, to cover the chute top exit partially, leaving some room for the gases to escape; secondly, to insert one or more insulating arc barriers into the upper chamber of the chute. The second of these methods was adopted, since it was felt that restricting the top exit might introduce further complications of pressure rise in the upper chamber, i.e. a higher effective 'air impedance' to arc movement. Moreover, the second alternative would permit a greater arc length within the chute, though some external assistance for arc penetration into the spaces between the

barriers might be necessary. A single arc barrier (2" x 3/8" x 1/8") was therefore incorporated.

Although the arc barrier was held inside the chute merely by friction, the cine-photographs showed that the arc experienced considerable difficulty in travelling upwards; consequently, the arcing duration was increased to about 4 half-cycles. Recurrent lengthening and shortening of the arc column was noted, and the arc voltage characteristic also exhibited relevant oscillations (Fig.9b).

7.4 Magnetic Field System

The arc had to be assisted in penetrating between the arc barriers, thereby increasing in length. A separately excited field was chosen because of its flexibility; care in its design was taken to ensure a uniform field over a reasonable volume of space, at the same time keeping the view for cine-photography clear. Figure 14 illustrates the magnetic field system used. The field system consists of two coils each having 80 turns of VIR cable. The internal diameter of the coils is 12 inches and they are placed 6 inches apart (between centres). The coils can carry currents up to 200 amps. for short durations. The magnetic field strength at 200 amps. is approximately 700 lines/cm.^{2}

Some problems of experimental technique were also considered at this stage; the discharge of the Capacitor

Bank was to be synchronised with the magnetic flux. A method using a synchronous motor and an impulse generator to initiate the arc was developed, the details of which are given in Appendix II. (Fig.17).

7.5 Change of Initial Conditions

The increase in arc length and therefore arc resistance, often made the discharge of the Capacitor Bank (Fig.2) non-oscillatory. Due to the prospect of still higher arc resistances, the Capacitor Bank arrangement was altered to give 4400 volts and 1000 amps. (Fig.2, Appendix II); the critical resistance permissible with this circuit arrangement was thus increased from 2.1 to 8.2 ohms.

Various experiments with chute L were performed. Both a.c. and d.c. magnetic fields were used; the phase angle between the arc current and the magnetic flux was also varied. Increase in the magnetic field was followed by an increase in the number of arc barriers from one to three, since the arc was noted to burn outside the top exit of the chute with higher fields and a single barrier (Figs.12a to e). In some of the above experiments the arcing time was reduced to one half-cycle (50 c/s), but a study of the cine-photographs indicated that for fields greater than 110 lines/ $cm.^2$, and using three arc barriers, the gases issuing from the top exit often made it possible for the arc to form

outside the top of the chute. The arc chute, with three barriers, and placed in a magnetic field of 110 or more lines/cm.^{2} was unable to confine the arc within itself; this is illustrated in Fig.12d: the arc can be seen burning outside the chute from Print 6 onwards.

7.6 Chute M

The necessity of a chute big enough to confine an arc under the above conditions was met by chute M. The principle of design was similar to that of chute L, but this chute was 8½" tall. (cf. chute L 4½"). Experiments similar to those with chute L were performed.

Since the arcing time was now in the region of 2 half-cycles at 50 c/s and the second half-cycle was often distorted, the duration of arcing could no longer be taken as a fair guide to the extent of arc control. Therefore, the arc characteristics obtained, both measured and derived, during the first half-cycle of arcing were chosen as a basis for comparison. Fig.12e shows arcing in chute M, using three arc barriers, and is placed in a d.c. magnetic blow-out field of 500 lines/cm.^{2} Towards the end of the first half-cycle, Print 7, the arc tends to burn outside the top exit.

8.0 Volume Cooling - Chutes N and O

It was felt that since 'Sindanyo' has a poor heat capacity, heat extraction by a volume of air might be more effective; chutes N and O were designed with the above end in view; chute N is similar to chute M, but has a uniform depth, front to back, of 2 inches, while chute O is rectangular (9" x 6" x 2") (Figs.5a,b). Care was taken in the above designs to keep the prospective maximum arc lengths nearly the same (approx. 7 ft., using 7 barriers), though it was recognised that 'air-impedance' to the arc movement, and the mass of 'Sindanyo' used, was different in all the three cases. Experiments similar to those with chute L (variations of magnetic field strength, a.c. or d.c., number of arc barriers, etc.) were performed.

Some ad hoc experiments were performed with an artificial air flow, through and across the top of the chute, and with the top exit partially covered. It was hoped that these would throw additional light on the complicated phenomena in arc chutes. Fig.16b shows arcing in chute N with the top exit partially covered; by comparison with Fig.16a in which the top exit is not covered, it is clear that the resistance to arc lengthening is increased in the case of Fig.16b. Results obtained so far are analysed in detail in the next section. Cine-photography has proved to be a valuable asset; a detailed description of the photographic techniques is given in Appendix III.

SECTION B

ANALYSIS OF EXPERIMENTAL RESULTS

1. General

The precise nature of arc control phenomena in air-break circuit-breakers is still a controversial subject. As mentioned elsewhere, attempts to study the phenomena, from a physical standpoint, have been made by various investigators. In this section it is intended to analyse the relative effectiveness of the various control devices used in the present investigations. For such a study it is necessary to select some specific arc data to serve as a basis for comparison. The nature of the power supply used for these experiments makes it advisable to confine such comparisons mainly to the first half-cycle of arcing. The factors which may be taken as a fairly reasonable guide to the subsequent behaviour of an arc column are:

(1) Arc resistance (r)

(2) The rate of change of arc resistance $(\frac{dr}{dt})$

(3) The instantaneous energy dissipation (w)

(4) The rate of change of energy dissipation $(\frac{dw}{dt})$

TABLE 2

List of Symbols

1.	Voltage across the Capacitor C in Fig.2.	V
2.	Voltage across the above Capacitor C at the first current-zero	V_{1o}
3.	Instantaneous arc voltage and current	v, i
4.	Instantaneous energy input to the arc	w
5.	The energy input to the arc 500 microsecs. before the first current-zero	w_o
6.	The rate of fall of energy input prior to the first current-zero	$\frac{dw_o}{dt}$
7.	The total energy dissipated in the first half-cycle	W_{T1}
8.	Instantaneous arc resistance	r
9.	The arc resistance 500 microsecs. before the first current-zero	r_o
10.	The rate of rise of arc resistance prior to the first current-zero	$\frac{dr_o}{dt}$

$\frac{dr_o}{dt}$ was conveniently assessed by measuring the rise in arc resistance from 500 to 250 microsecs. before the first current-zero.

(5) The available power source voltage (V)

500 Microsecs. before the first current-zero is the particular instant selected for comparison. The time resolution of the oscillographic equipment, the nature of the power supply, and the effect of the d.c. field on the second half-cycle of arcing, led to such a choice. Graphs showing the variation of these parameters over the first half-cycle or near the first current-zero have been plotted for the most interesting cases.

Graphs

Instantaneous values of arc voltage and current are measured from the oscillograms (Appendix II). From these measured values of arc current and voltage, the instantaneous values of arc resistance ($r = e/i$) and energy input ($w = ei$) are derived. V_o, r_o and w_o etc. refer to the values at or near the first current-zero (Table 2).

In Figs.18, 19 and 20, only the period around the first current-zero is plotted; time in these graphs is measured from the current-zero.

In graphs where the complete first half-cycle is plotted, e.g. Figs.21 and 26, etc., time is measured from the beginning of arcing.

The Capacitor Bank in Fig.2 was charged to

approximately 4400 volts; the energy stored in the Bank at this voltage was about 7700 jourles (C = 750 microfarads). The energy dissipated in the first half-cycle, W_{T1}, is given as a percentage of the total energy stored in the Bank. The variations in the initial voltage of the Bank were usually within 5% of the above value.

2. Comparison of Arc Control Methods

2.1 General

The specific arc data enumerated in the previous section i.e. r_o, $\frac{dr_o}{dt}$, w_o and V_{1o} etc. are taken as a basis of comparison for the following control methods:

1. Heat loss from the arc column by contact with chute walls.
2. Arc lengthening, using:
   (a) plain arc runners
   (b) plain arc runners and arc barriers
   (c) plain arc runners, arc barriers and a.c. or d.c. magnetic blow-out field.

The data obtained from such experiments is presented in the form of graphs etc. (Figs.18 to 30).

Since it is not always possible to isolate any of the above methods, simplifying assumptions are made to assess the relative effectiveness of these control methods.

2.2 Cooling by Chute Walls

2.2.1 Experiments with Chutes B, F, G, H and I

It has been mentioned earlier in this thesis that in chutes F, G, H and I, a closer contact between the chute walls and the arc column was intended. Although chutes G and H were also intended to reduce, and chute I to increase, self-induced air flow, cine-films and oscillograms indicated that it is reasonable to assume that such design features would not affect the present analysis unduly. Figs.18a to f show instantaneous values of arc resistance and energy input to the arc column near the first current-zero for the above experiments at 2200 volts and 2000 amps. No arcing horns were employed. From the graphs it will be noted that:

1. The resistance just prior to the current-zero (r_o) is slightly lower (< 1 ohm) in chutes F, G, H, I, Figs.18b to e, than in chute B (1.5 ohms), but the rate of increase of arc resistance near the current-zero, $\frac{dr_o}{dt}$, is higher in chutes F, G, H and I.
2. The total energy dissipation, W_{T1}, is, however, greater in chute B (Fig.18a) than in the others (Figs.18b to f).

2.2.2 Experiments with Chutes M, N and O

Results from the experiments with chutes M, N and O, under similar conditions, are shown in Figs.19a to f.

The prospective maximum arc lengths in all these chutes with seven arc barriers are the same, but the volumes vary widely (18, 85, 123 cub.in. respectively). Since the depth, front to back, of chute M (3/8") is much smaller than either of the other two (2"), the possibility of heat extraction by the chute walls in the case of chute H is much greater than for the other two.

Figs.19a to f show data obtained from experiments with chutes M, N and O, for two values of d.c. blow-out field, other initial conditions remaining the same. Figs. 19a to c refer to a blow-out field of 670 lines/cm.^{2}, while Figs.19d to e refer to a field strength of 470 lines/cm.^{2}.

From these figures it is clear that with chutes N (Figs.19b and e), and O (Figs.19c and f), which are deeper than chute M (Figs.19a and d), both resistance prior to the current-zero (r_o) and the total energy, W_{T1}, are higher than with chute M. However, the rate of rise of resistance, $\frac{dr_o}{dt}$, is greater for chute M.

2.2.3 Experiments with Chute J

From oscillograms and corresponding cine-films taken for experiments with chute J, arc voltage, current and length are measured at two successive instants during the first half-cycle. These two instants are so selected that at the first instant the arc is in the lower chamber, and, at

TABLE 3

Measurement of Arc Voltage/inch in Chute J.

Nos.	Lower Chamber				Upper Chamber (Chimney)			
	Arc length	Arc voltage	Mean Arc drop/inch	Current	Arc length	Arc voltage	Mean Arc drop/inch	Current
93	2.6 in	57.7 V	22.2 V/in	1065 A	6 in	162 V	27 V/in	1300 A
94	2.6 in	69.3 V	26.8 V/in	1300 A	4.8 in	173 V	36 V/in	900 A
100	2 in	69.3 V	35 V/in	2370 A	4.0 in	162 V	40 V/in	1850 A
102	2 in	86.5 V	43.25 V/in	1650 A	8.0 in	277 V	34.7 V/in	1850 A

the second, in the upper chamber of the chute. Moreover, the instants chosen are not too close to the current-zero. Table 3 shows these data for four typical cases.

It can be seen from Table 3 that the current values for the two instants, for a given experiment, are not widely different. From these data it can be seen that the arc drop, for a given experiment, at these two instants is almost directly proportional to arc length, although the arc column, for the latter of these two instants, is in much closer contact with the chute walls.

The oscillograms taken for experiments with chute J were also compared with those with arcing horns in open air, under similar conditions, and it was noted that:

The re-strike voltages in the case of arcing horns in open air were about 200 volts and were of Type b, Fig.1; while with chute J, the re-strike voltages were about 300-500 volts and tended to be of Type a, Fig.1; the duration of arcing was, however, longer for experiments with chute J (3-4 half-cycles as against 2 half-cycles for horns alone).

2.2.4

From the preceding analysis of experiments with chutes B, F, G, H, I; M, N, O and J, it is clear that the effect on arc characteristics of confining the arc between chute walls is most evident around the current-zero period

(higher re-strike voltages for chutes J and M, and higher $\frac{dr_o}{dt}$ for chute M, Figs.19a to f). No significant difference in arc resistance or arc drop per unit length is noted for the major part of the half-cycle. The significant cooling effect noted around the current-zero period is due to the greater susceptibility of the arc to temperature changes during this period; a temperature change of about 30°C. can alter the degree of ionisation by a factor of two. (Ref.17).

2.3 The Effect of Arc Lengthening in Chutes

It has been mentioned earlier that arc runners, arc barriers and magnetic blow-out field have been used to assist arc lengthening in a chute. The effects of such devices on arc characteristics in the case of chute M are shown in Figs.20a to g. Only the period near to the first current-zero is plotted. It will be noted that:

(1) The resistance prior to the first current-zero (r_o) gradually increases from about half an ohm with plain electrodes in open air (Fig.20a) to nearly seven ohms with chute M using arc runners, seven arc barriers, and a magnetic blow-out field of nearly 500 lines/cm.^{2} to assist arc lengthening (Fig.20g). Similar increases in the rate of rise of arc resistance prior to the current-zero, $\frac{dr_o}{dt}$, energy dissipation near the current-zero, w_o, and

the total energy dissipation, W_{T1} , are also noted.

(2) An increase in the number of arc barriers from three to seven (Figs.20f,g) reduces both the arc resistance, r_o, and the total energy dissipation, W_{T1}, but the rate of rise of arc resistance near the current-zero, $\frac{dr_o}{dt}$, is increased.

It would appear that the reduction in r_o and W_{T1} is due to higher resistance to arc movement, (which results in smaller arc length), offered by the chute with seven barriers as compared with that having three, and the increase in $\frac{dr_o}{dt}$ is due to a closer contact between the arc column and the chute walls and therefore effective cooling near the current-zero. An increase in the number of arc barriers would therefore necessitate an increase in the blow-out field to insure arc penetration into the spaces between the arc barriers, and therefore, arc lengthening.

2.4 Magnetic Blow-out Phenomena

2.4.1 D.C. Blow-out Field

Figures 21 to 23 show the data obtained with chutes M, N and O using a d.c. blow-out field. The blow-out force on the arc during the second half-cycle will blow the arc downwards; comparisons are therefore confined to the first half-cycle. The field strength is varied from 200 to 700

lines/cm.^{2}. As the blow-out field is increased, the following tendencies are noted:

1. In the earlier part of the first half-cycle the rate of change of energy input, $\frac{dw}{dt}$, increases. The total energy dissipated, W_{T1}, also increases, (Figs.21-22); however, the rate of rise of W_{T1} with the field decreases (Figs.22a,b,c).

2. Although the general level of arc resistance over the major part of the half-cycle rises, $\frac{dr_o}{dt}$ falls (Figs.21-23).

Cine-photographs taken for these experiments indicate that the arc velocity in the beginning of the half-cycle increases with the blow-out field. An increased arc velocity would mean a quicker rise in arc length and hence arc resistance, since the change in arc current is relatively slow. The above process might also increase the total energy dissipation, since:

Instantaneous energy input is given by

$$i^2r = \frac{V^2r}{r^2 + x^2}$$ where V is the power source voltage and x the circuit reactance, and r is composed mainly of arc resistance.

An analysis of the above relationship shows that the energy input increases as r increases, reaching a maximum

when r = x; a further increase in r would reduce the energy input.

Since the total energy dissipated over the half-cycle, $W_{T1} = \int_0^{T/2} i^2 r \, dt$, a rapid increase in arc resistance in the earlier part of the half-cycle, noted with a d.c. blow-out field, might reduce the total energy dissipation, W_{T1}. The maximum field used by the author (700 lines/cm.^{2}) was not sufficient to reduce W_{T1} with increasing blow-out fields; but the decrease in the rate of rise of the total energy, W_{T1}, with increasing d.c. blow-out fields is due to the above effect (Fig.22).

The lowering of the rate of rise of arc resistance prior to the current-zero, $\frac{dr_o}{dt}$, with increasing magnetic blow-out fields, Fig.23, might be due to the following causes:

1. The increase in the energy input during the last few millisecs. of the first half-cycle, Fig.21, with the field strength, would increase the ionisation near the first current-zero, and therefore reduce $\frac{dr_o}{dt}$.
2. Since the arc velocity increases with the magnetic field, it is likely that the arc column reaches its highest position in the chute earlier in the half-cycle if the blow-out field is sufficient. The upper part of the chute gets heated, and since the

chute walls are poor conductors of heat, the heat-extracting effect of these walls would be reduced near the first current-zero.

2.4.2 A.C. Blow-out Field

A comparison of d.c. and a.c. magnetic blow-out fields is shown in Fig.24. To avoid undue complications of phase variation, the a.c. fields in phase with the arc current are compared and the r.m.s. values are quoted.

With d.c. fields the total energy dissipated in the first half-cycle, W_{T1} , is higher than with a.c. (r.m.s. values). This might be due to higher arc velocity obtained with d.c. field. A higher arc velocity would give a higher rate of increase of arc length, and therefore higher arc resistance; and so long as the circuit resistance is lower than the circuit reactance, an increase in arc resistance would also increase the energy input.

With a d.c. field the above reasoning would also apply to higher observed values of the arc resistance near the current-zero, r_o. However, the higher values of the rate of rise of arc resistance prior to the current-zero, $\frac{dr_o}{dt}$, are possibly due to the higher blow-out field available prior to the current-zero, which keeps the arc column close to the chute walls.

2.4.2.2 Phase Variations

Most of the experiments with lagging or leading blow-out fields, as compared to in-phase fields, have shown effects which may prove to be of use in obtaining arc extinction. No significant downward arc movement is noted for phase variations up to 30-40° lag or lead in spite of the reversed blow-out force during part of each half-cycle.

Figs.25,26,27 show the data obtained. Some of these graphs show the variation of arc resistance, energy input and the magnetic blow-out force over the first half-cycle; the blow-out force plotted is that experienced by a unit length of the arc perpendicular to the blow-out field.

Leading and lagging blow-out fields affect arcing quite differently. With a leading field, as the angle of lead is increased, it is noted that:

(1) Up to about 40° lead there is in general an increase in the total energy dissipated over the first half-cycle, W_{T1}. The proportion of this energy dissipated during the earlier part of the half-cycle also increases (Figs.25-27), and therefore the instantaneous energy input prior to the current-zero, w_o , decreases..

(2) At low field strengths (approximately 250 lines/cm.^{2}) (Figs.26a,b,c), there is little change in the arc resistance prior to the current-zero, r_o . However, at high field

strengths (approximately 700 lines/cm.^{2}), the arc resistance prior to the current-zero, r_o , first increases and then decreases. This changeover generally occurs at about 10-15^o lead (Figs.27a,b,c,e,h,i).

(3) The rate of increase of arc resistance prior to the first current-zero, $\frac{dr_o}{dt}$, decreases.

With a lagging field, the following tendencies are noted, as the angle of lag is increased:

(1) The total energy dissipated during the first half-cycle, W_{T1}, decreases, and the proportion of this energy dissipated during the later part of the half-cycle increases. The instantaneous energy, w_o , also increases. (Fig.27d).

(2) The arc resistance, r , shows little variation at low field strengths (approximately 250 lines/cm.^{2}, peak) (Figs.26a,d,e); but at high field strengths (approximately 700 lines/cm.^{2}, peak) (Figs.27c,d,e,f,g), the arc resistance, r , first increases then decreases. The changeover generally occurs at about 10-15^o lag (Figs.27f,g).

(3) The rate of increase of arc resistance prior to the current-zero, $\frac{dr_o}{dt}$, also increases.

The changes in the amount and distribution of the total dissipated energy, mentioned in the preceding paragraphs, might be due to the difference in the arc movement during the

early part of the half-cycle. Compared to an in-phase blow-out field, the arc would move faster and slower with leading and lagging fields respectively. In the next section possible explanations of the effects of magnetic blow-out fields, around the current-zero period, are advanced.

The effects of phase variations in the case of chutes M, N and O are substantially similar.

2.4.3 The Effects of Magnetic Blow-out Field Near Current-zero

The magnetic blow-out force on a flexible current-carrying conductor confined between two insulating plates is shown in Figs.28a and b. The magnetic flux is perpendicular to the plane of the paper, and the positive direction of the flux is from front to back. In all the experiments for this investigation the positive direction of the arc current is from left to right. A horizontal current-carrying conductor, therefore, experiences an upward force when both the flux and the arc current are positive. The above figures show the blow-out force on the arc for both similar and dissimilar polarities of arc current and magnetic flux.

For d.c. and lagging a.c. fields, the blow-out force prior to the first current-zero is outwards (Fig.28a), and therefore the arc column is forced in close contact with the chute walls. This would tend to increase the rate of

rise of arc resistance, $\frac{dr_o}{dt}$, (sections 2.4.1 and 2.4.2.2), since a small fall in temperature near a current-zero could reduce the ionisation considerably (Ref.17). With d.c. (Figs.20a-g) and lagging a.c. (Fig.27f) blow-out fields, the arc resistance sometimes rose several hundred ohms, immediately following the first current-zero. Some typical oscillograms are reproduced in Figs.29a-f. However, the magnetic blow-out force after a current-zero is negative, and the arc column would tend to contract (Fig.28b). With d.c. blow-out fields, after the first current-zero the arc column would travel downwards as the inwards blow-out force increases, while with lagging a.c. blow-out fields the arc column might move downwards if the angle of lag is sufficiently large. For small angles of lag ($< 30^{o}$) the arc would begin to move upwards as the magnetic blow-out force changes sign. The negative inwards force (Fig.28b) would delay the initial arc movement when a lagging blow-out field is used. The rate of increase of arc length and therefore the voltage drop across the arc column would be reduced; the rate of heat extraction from the arc column might also be reduced since the close contact between the arc column and chute walls is delayed; these factors could make arc extinction difficult.

With a leading a.c. blow-out field the force on the arc column before a current-zero is inwards (Fig.28b). If

the angle of lead is sufficiently great ($> 40^{o}$) the arc column would travel downwards before the first current-zero. This tendency of the arc column to contract before the first current-zero would reduce the contact between the arc column and chute walls and hence the heat extraction from the arc column near the first current-zero. This is reflected in the value of $\frac{dr_o}{dt}$, which is low (Figs.27b,c). However, after the current-zero, the blow-out force is positive and the arc column would tend to expand, and better contact with chute walls would be possible, and since the arc is most susceptible to cooling around the current-zero period, arc extinction might be effected in some cases. Figs.29f and 27a show measured and derived arc characteristics for an experiment with chute O using a 40^{o} leading magnetic blow-out field; the arc has been extinguished in one half-cycle and considerable post-arc conductivity also occurred.

In experiments with a.c. magnetic blow-out field it is observed that where no downward movement occurs around the first current-zero, the maximum value of the angle of lead (about 40^{o}) is higher than for lagging fields (about 30^{o}). This might be due to substantial air currents present towards the end of the first half-cycle which would tend to offset the downward blow-out force on the arc column in the case of leading blow-out fields. (Ref.16).

From the preceding discussion it is evident that the

periods immediately before and after the current-zero are critical. But for d.c. and lagging a.c. blow-out fields, the period immediately before, and for leading a.c. blow-out field, the period immediately after the current-zero is relatively more important.

2.5 Effects of an Artificial Air Flow

Results from experiments with an artificial air flow through chute N of about 2000 ft./min. are shown in Figs.22b and 30a,b. The increase in W_{T1} is small for low blow-out fields, but increases for high blow-out fields (Fig.22b). This is so because the arc at high blow-out fields attains its final position in the chute in the earlier part of the half-cycle, and therefore, the air flow assists in keeping the arc column close to the chute walls; moreover, the surface area of the arc column is higher, due to increased arc lengths.

Figs.30a-b show that there is a slight increase in the arc resistance towards the end of the first half-cycle, r_o; however, $\frac{dr_o}{dt}$ increases considerably. This effect of air flow around the current-zero period is due to the greater susceptibility of the arc column to temperature changes during this period.

3. Criteria of Arc Extinction in a Chute

It is observed that often in experiments performed with various arc control devices, arcing duration was reduced to one half-cycle. For arc extinction to occur at a current-zero, the arc resistance, r_o , and the rate of rise of arc resistance, 500 microsecs. prior to the current-zero, $\frac{dr_o}{dt}$, should be high; also, for a given value of r_o and $\frac{dr_o}{dt}$ the possibility of arc extinction is reduced if energy input to the arc prior to the current-zero is increased. Since instantaneous energy near current-zero generally falls uniformly to zero, the value of the instantaneous energy input 500 microsecs. prior to the current-zero, w_o , can be taken as a measure of the energy input just prior to the current-zero. Moreover, the possibility of arc extinction is further decreased if the power source voltage available at the current-zero, V_{lo} , is increased. It would, therefore, appear that for a critical arc extinction

$$f\left[\frac{r_o \cdot \frac{dr_o}{dt}}{w_o \cdot V_{lo}}\right] = \text{a constant}$$

A large number of experiments are required to determine tha above criteria accurately, and the experiments in the present investigation were not designed for such a purpose. An analysis was, however, carried out to determine

the value of

$$\frac{r_o \cdot \frac{dr_o}{dt}}{w_o \cdot V_{lo}}$$

for various sets of conditions.

The analysis is shown in Fig.31. It will be noticed that the value of

$$\frac{r_o \cdot \frac{dr_o}{dt}}{w_o \cdot V_{lo}}$$

for experiments in which arc extinction occurred at the first current-zero are consistently higher than the rest. It will also be noticed that the values for an arcing duration of two half-cycles are higher than those for three or more half-cycles and so on. There are, however, a few boundary cases.

As stated earlier, the present investigation is inadequate to determine the criteria accurately. It is felt that the above criteria can provide a very useful guide in chute design, since it is possible to determine the effect of various arc control devices, e.g. arc barriers, magnetic blow-out field, etc., on the above parameters by simple ad hoc experiments.

4. Conclusions

A technique for laboratory research on arcing phenomena for medium powers has been developed, and has yielded useful information on arc control measures, (Part I). A certain pattern of the arc control phenomena has emerged, and the broad tendencies therefrom are noted below.

4.1 Arc Chute as a Container

The necessity of providing an arc chute merely as a container for the arc column and gases has become evident. A chute can confine and then guide the arc gases upwards, thereby preventing uncontrolled arcing (Figs.7a to d). However, if due care to the design of a chute is not given, the following problems may arise:

First, the configuration of a chute and the low heat conductivity of chute walls may not allow quick removal and cooling of the ionised gases at the bottom of a chute. These gases at the bottom of a chute may then enable the arc to re-strike across the shortest path between the electrodes (Figs.7b and c, 9b).

Except for low powers, cooling of arc gases in a chute is relatively more difficult than in open air, and therefore, it is advisable to remove the sources of ionisation, i.e. arc roots and arc column, further upwards. Arc runners and possibly air flow at velocities greater than

about 40 ft./sec. through a chute are quite effective for the above purpose.

Secondly, in a chute the arc may take a measurable time before any movement commences (up to about 5 millisecs., for the chutes used by the author). Moreover, the arc may experience considerable difficulty in entering narrow parts of a chute (chutes J, K, L and M).

Arc movement upwards is due to self-magnetic blow-out force and the buoyancy of hot air currents (Ref.16). It appears that a chute offers some sort of 'air impedance' to the establishment of streamlined air flow in it. It is difficult to assess various factors governing the magnitude of this impedance. However, from the study of viscous flow in pipes it appears that the expression

$$\frac{\text{pressure drop}}{\text{air velocity}}$$

may provide a reasonable basis for comparison of 'air impedance' of chutes.

Regarding the smooth entry of the arc into narrow slots, the formula, shown below, has been developed by Reece (Ref.15):

$$\text{minimum width of a slot} = .02\sqrt{I} \text{ cm.}$$

where I is the maximum prospective r.m.s. value of the current to be handled. For an arc current of 2000 amps., the minimum slot width required by the above formula is about

1 cm. It is interesting to note that for experiments in which some difficulty in arc entry has been noticed, the slot width is of the order given by the above formula, (chute J, 0.7 cm.; spacing between arc barriers in chute O, 1 cm.).

Thirdly, when a high current arc of thousands of ampères is confined in a narrow slot, the gases generated on the underside of the arc column may move downwards; the arc may then re-strike across the shortest path between the electrodes, and thus retard arc extinction (Figs.13a to c). Therefore, the spacing between arc barriers, or the depth of a chute, front to back, may prove to be a limiting factor unless some arrangement for removing these gases is incorporated.

In spite of the difficulties mentioned above the velocity of upward arc movement in a chute with runners, in the later part of the first half-cycle, is much higher (500 ft./sec., Figs.13a-c) than on plain runners in air (100 ft./sec., Figs.15a-c). This is due to the self-induced flow, which has had time to establish, of hot arc gases. These gases have to move upwards through the chute. Since arc velocity in a chute can be fairly high, relatively slow artificial air flow (40 ft./sec.) does not affect the arc movement in any significant way.

4.2 Arc Control Methods

Arc lengthening and cooling by chute walls have been chiefly employed for arc control in this investigation. During the major part of the first half-cycle, arc lengthening is most effective in raising the voltage drop across the arc (Figs.20a-g). However, the close contact between the arc column and chute walls does increase the deionisation losses around the current-zero period (Figs.18 and 19; section 2.2, p.48). Arc barriers with magnetic blow-out field are reasonably effective for arc lengthening. For a given current the resistance offered by a chute to upward arc movement, and therefore, to arc lengthening is dependent on chute dimensions. This resistance increases as the depth of a chute, front to back, or the spacing between the arc barriers is reduced (Table 1, p.37a, Figs.20f,g). Although formulae giving minimum depth or spacing for a given current have been developed, (Ref.15), for better arc control, a detailed investigation and analysis of this phenomenon is needed.

Under given conditions, the arc velocity in the early part of the half-cycle is highest with the d.c. blow-out fields; the arc resistance, and therefore the energy dissipation during the first half-cycle, W_{T1} , is also high. Over the range of d.c. blow-out field covered by this investigation (200-700 lines/cm.^{2}), W_{T1} gradually increases

with the field; but with still higher fields the arc resistance may rise at such a rate that the total energy $\int_0^{T/2} i^2 r \, dt$ begins to decrease (Figs.22a-c; section 2.4.1, p.52).

4.3 Current-zero Period

Experiments with varying angles of phase between the blow-out field and the arc current have furnished some useful information concerning the process of arc extinction. In most of the cases the arc resistance during the period immediately preceding the current-zero was of the order of tens of ohms. Arc extinction after the first current-zero was achieved under a variety of conditions. In all such cases, it is felt that the arc must reach a critical state just prior to the current-zero. Moreover, it is possible to describe the physical state of an arc column at any instant by its resistance, rate of change of arc resistance and the energy input. Particular methods of arc control, e.g. blow-out fields, chute dimensions and arc barriers etc., affect any one of the above parameters (r_o , $\frac{dr_o}{dt}$, w_o) quite differently; it seems that it is the combined effect of a particular control method on these parameters which determines its effectiveness. Criteria for arc extinction dependent upon these parameters have been suggested and are noted below.

For extinction to occur in one half-cycle

$$f\left[\frac{r_o \cdot \frac{dr_o}{dt}}{w_o \cdot V_{lo}}\right] > \text{constant}$$

where V_{lo} is the power source voltage available at the first current-zero. The data available from the present investigation is inadequate to determine the criteria accurately; but if accurately determined it would provide reliable guidance in arc control.

In the early part of a half-cycle, the effect of buoyancy due to hot air currents assists the upward arc movement. Phase variations of a.c. blow-out field, up to 30^{o} lag or 40^{o} lead, do not cause a downward movement of the arc when the blow-out force is reversed.

Finally, more data concerning the interaction of the types of loss which occur from the column is needed; the effects of the previous history of the arc column in determining the critical conditions for arc extinction also need to be studied. Some suggestions for further work along these lines are given in the next section.

5. Further Work

The investigation under review broadly shows the relative effectiveness of various arc control processes, e.g. cooling by chute walls, arc lengthening and magnetic blow-out phenomena, etc., but to develop principles of effective arc control more exact data is required.

Experiments to gather such data would need to be specially designed. Some suggestions for future experiments are given below:

1. Experiments with d.c. arcs to study the effect of rapid arc movement through air.
2. Experiments with arcs in a confined space to study the process of heat extraction by the confining material. These experiments would be similar to those done by T.E.Browne, Jr. (Ref.5).
3. (a) Experiments with magnetic blow-out field to correlate for a given arc current, driving force, arc length and the resistance offered by a chute to arc movement.
   (b) Simple experiments to study the current-zero phenomena, using both d.c. and a.c. blow-out fields.

An improved cine-photographic technique would be of much help and might illuminate the process of arc movement in a magnetic field. The oscillographic technique would have to be extended for accurate recording around current-zero.

Finally, the above experiments would permit an accurate evaluation of the criteria mentioned in section 3, p.62.

6. Acknowledgements

The present investigation was conducted in the Electrical Engineering Department of the Royal College of Science and Technology, Glasgow, under the guidance of Professor F.M.Bruce, M.Sc.,Ph.D.; the author wishes to thank the staff of the above department for their kind and valued help. The author is much indebted to the Council of Scientific and Industrial Research, New Delhi, for the award of an Assam Oil Company Maintenance Scholarship, and also to Messrs. A.Reyrolle & Co.Ltd., and Belmos & Co.Ltd., for providing technical assistance and chute material for the present investigation. Finally, the author especially wishes to thank Professor F.M.Bruce and Mr.J.T.Pender for their interest, encouragement and guidance during the investigation and in the preparation of this thesis.

7. References

1. Gaseous Electrical Conductors; J.D.Cobine, McGraw Hill, 1941.

2. Physical Properties of Arcs in Circuit-breakers; Emil Alm, Stockholm, 1949.

3. Circuit-breaking; H.Trencham, Butterworth Scientific Publications, London, 1953.

4. Air-break Arc Chute Circuit-breakers: Discussion of Published Information on Modern Types; M.P.Reece, B.Sc.(Eng.); E.R.A. Report G/XT 135, 1952.

5. A Study of Conduction-phenomena Near Current-zero for an A.C. Arc Adjacent to Refractory Surfaces; T.E. Browne, Jr., and A.P.Strom, Transc.A.I.E.E., 1951, Vol.70, p.407.

6. Extinction of a Long A.C.Arc; J.Slepian, Transc.A.I.E.E., 49, No.2, pp.421-31.

7. Circuit Severity - A New Theory; A.M.Cassie, C.I.G.R.E., Paris, Session 1939, Paper No.102.

8. Beitrag zur Theorie das Statischen und des Dynamischen Lichtbogens; Archiv für Electrotechnik, (Berlin), 1943, 37, p.588.

9. Some Researches on Current Chopping in High Voltage Circuit-breakers; A.F.B.Young, Proc.I.E.E., Vol.100, Part II, 1953.

10. Synthetic Testing of Circuit-breakers; Maury and Renaud; Parts I and II, R.G.E., Oct. and Nov. 1948, Vol.57.

11. Severity of Circuit-breaker Test Conditions. Some Interesting Results Using a Discharging Condenser as Power Supply. F.O.Mason, E.R.A.Report G/T 230, 1949.

12. Indirect Circuit-breaker Tests; E.Vogelsangers, C.I.G.R.E., P. No.122, Session 1948.

13. Passage of the Electric Arc into the Arc Quenching Grid; N.A.Babakov, Vestn. Electroform, 1947, 18, x , p.15.

14. Application of Heat Transfer Data to Arc Characteristics; C.G.Suits and H.Portisky, Phys.Rev., 55, (1939), p.1184.

15. Arc Chutes for A.C.Contactors; Some Notes and Data for Design; M.P.Reece, E.R.A.Report G/T 304, 1956.

16. Magnetic Blast in Circuit-breakers; W.Rieder and A.Eidinger; C.I.G.R.E., Session 1956, Paper No.107.

17. Arc Interruption by Cooling; G.E.Review, Sept.1939, Vol.42, p.375.

PART THREE

APPENDICES

The final expression then becomes:

$$q_3 = e^{-t/2CR} \cdot C \cdot \left[V_o^2 + \left(\frac{V_o}{2\omega CR} + \frac{I_o}{\omega C}\right)^2\right]^{\frac{1}{2}} \cdot \cos(\omega t - \alpha)$$

$$\text{where} \quad \alpha = \tan^{-1}\left(\frac{V_o + 2RI_o}{2\omega CRV_o}\right)$$

Since

$$V_c = \frac{q_3}{C} \ ,$$

$$V_c = e^{-t/2CR}\left[V_o^2 + \left(\frac{V_o}{2\omega CR} + \frac{I_o}{\omega C}\right)\right]^{\frac{1}{2}} \cdot \cos(\omega t - \alpha) \quad ..(1)$$

A similar analysis gives the current I_L flowing through the inductance, namely,

$$I_L = \frac{V_o}{R} + I_o + \left[\left(\frac{V_o}{R} + I_o\right)^2 + \left(\frac{V_o}{\omega L} - \frac{I_o}{2\omega CR}\right)^2\right]^{\frac{1}{2}} \cdot e^{-t/2CR}$$

$$\cdot \sin(\omega t - \beta) \quad \ldots\ldots\ldots\ldots (2)$$

$$\text{where} \quad \beta = \tan^{-1}\frac{\frac{V_o}{R} + I_o}{\frac{V_o}{\omega L} - \frac{I_o}{2\omega CR}}$$

In these equations, the switch s_2 having closed a time, T , before t = 0, the initial conditions for the capacitor are:

$$V_o = E(1 - K) \qquad \text{where } K = e^{-T/CR}$$

$$I_o = \frac{E}{R} \cdot K$$

Substitution in equations (1) and (2) gives:

$$V_c = E\left[(1 - K)^2 + \frac{(1 + K)^2}{(2\omega CR)^2}\right]^{\frac{1}{2}} \cdot e^{-t/2CR} \cdot \cos(\omega t - \alpha)$$

$$\text{where} \quad \alpha = \tan^{-1} \frac{1 + K}{1 - K} \cdot \frac{1}{2\omega CR}$$

$$I_L = \frac{E}{R} + \frac{E}{R}\left[1 + \left(\frac{R(1 - K)}{\omega L} - \frac{1}{2\omega CR}\right)^2\right]^{\frac{1}{2}} \cdot e^{-t/2CR} \cdot \text{Sin}(\omega t - \beta)$$

$$\text{where} \quad \beta = \tan^{-1} \frac{2\omega CRL}{2CR^2(1 - K) - L}$$

Analysis of circuit shown in Fig.3b.

The two switches S_1 and S_2 replace gaps G_1 and G_2, and S_2 is closed a time, T , before S_1 closes. The three circuit equations are:

$$Ri_1 + \frac{1}{C_2}\int i_1 dt - \frac{1}{C_1}\int i_3 dt = E$$

$$i_1 + i_3 = i_2$$

$$L\frac{di_2}{dt} + \frac{1}{C_1}\int i_3 dt = 0$$

Writing the instantaneous charge on C_1 as $q_3 = \int i_3 dt$, solution of the above equations gives:

$$\frac{d^3q_3}{dt^3} + \frac{1}{C_oR}\frac{d^2q_3}{dt^2} + \frac{1}{C_1L}\frac{dq_3}{dt} + \frac{1}{C_1C_2RL} = 0$$

$$\text{where} \quad C_o = \frac{C_1C_2}{C_1 + C_2}$$

which has the solution:

$$C_1VC_1 = q_3 = A \cdot e^{-\alpha_1 t} + B \cdot e^{-\alpha_2 t}\cos(\omega t - \beta)$$

$$\text{where} \quad \omega = \sqrt{\frac{1}{LC_1} - \frac{1}{4C_1R^2}} \qquad \ldots\ldots\ldots\ldots(1)$$

If t = 0 at the instant of closing S_1, and the capacitor voltage and current are then V_o and I_o, the initial

conditions are:

$$q_3 = C_1 V_o$$

$$\frac{dq_3}{dt} = -I_o \qquad \text{at} \quad t = 0$$

$$\frac{d^2 q_3}{dt^2} = \frac{V_o}{L} + \frac{I_o}{C_1 R}$$

The constants A, B, α_1 , α_2 and ß can be evaluated by the substitution of above values in equation (1). A similar analysis gives the current I_L flowing through the inductance L as:

$$I_L = C \cdot e^{-\alpha_1 t} + D \cdot e^{-\alpha_2 t} \sin (\omega t - \theta) \quad \ldots\ldots (2)$$

In these expressions, the switch S_2 having closed a time, T , before t = 0, the initial conditions for the capacitor C_1 are:

$$V_o = E \frac{C_o}{C_1} (1 - K)$$

where $K = e^{-T/CR}$

$$I = \frac{E.K}{R}$$

APPENDIX II

Equipment and Experimental Techniques

1. Main Power Source

1.1 Capacitor Bank

This consists of 8 centre tapped units of 1500 mfd. each, thus giving the total capacitance of 12000 mfd. The Bank can be charged to a maximum of 1100 volts d.c. per section, and then discharged through an inductance and test arc in series, the circuit (Fig.1.) being tuned to give an oscillatory discharge at 50 c/s. The various modes of initiating the test gap are discussed later in this appendix.

The Bank can be connected in various series and parallel arrangements to give the required current and voltage conditions (Fig.2.). The maximum current available when all the units are connected in parallel is approximately 4000 amps. at the first peak. Due to resistance of the circuit the current wave-form has an exponential decrement. The circuit resistance consists of:

1. Resistance of connecting leads.
2. Resistance of coil.
3. Arc resistance.

To keep the decrement as low as possible, thick copper strap is used for various connections, and a heavy section of cable has been used for the tuning coil.

1.2 Tuning Coil

The inductance of the coil, the capacitance of the bank and the frequency of discharge are connected by the relation:

$$f = \frac{1}{2\pi}\sqrt{\frac{1}{LC}}$$

neglecting the circuit resistance. The various values of inductance required for 50 c/s, for different arrangements of the Bank were calculated.

The design of the coil is greatly affected by the mode of arc initiation. In the case of initiation by fuse or a moving contact there is not any necessity for extra insulation, and a double cotton-covered cable is suitable, but in the case of impulse initiation the coil must be designed to withstand the impulse voltage. The impulse insulation level of VIR cable used was 120 kV between cores.

The coils are designed to give maximum Q.

1.3 Charging Circuit

This consists of a full-wave rectifier, supplied by a 4-0-4 kV transformer controlled by a variac on the primary side. A charging resistor has been placed on the output side of the rectifier to limit the initial charging current (Fig.3.).

1.4 Protection

As will be appreciated (Fig.2.), any short circuit between the busbars or any fault in any one of the units will cause the whole Bank to discharge through it. The magnitude and frequency of these currents will be very high (>16kA, 5.8 kcs.); hence, it was essential to incorporate some form of protection.

One way which suggests itself at the first instance is to split up the tuning inductance into coils to be placed in between the units and busbars. This necessitates much bigger coils ($L \propto {}^{1}/C$) and many coils instead of one.

The other alternative is to use H.R.C. fuses in place of copper links as shown in Fig.2. A study of inverse time characteristics (Fig.4.) of H.R.C. fuses indicated that fuses below 35A rating may operate before the prospective peak on short-circuit is reached. It was found that a 35A fuse can replace a link carrying 500A first peak and a 25A fuse a 250A link. The fuses could carry well over a dozen discharges without any appreciable deterioration.

It is also necessary to ensure that the Bank is not overcharged, so an automatic tripping circuit was installed with the charging circuit. The voltage setting can be varied by changing the resistance in series with the moving coil relay in Fig.3.

1.5 Other Sources

As is clear, the above source can only supply heavy currents for a short duration. The sources of continuous supply are:

1. A.C. welding generator to give 600 amps. continuously.
2. D.C. motor-generator set to give 300 amps. continuously at 50 volts.

2. Initiation of Arcs

The arc can be initiated by any of the following methods:

1. Fuse - the test gap is shortened by a thin fuse wire of the same metal as the electrode.
2. By drawing an arc between moving contacts.
3. By breaking down a fixed gap by an impulse voltage.

The first one is the simplest, but it introduces the unknown factor of metallic vapour in the gap and the arc is established at a late point on the current wave, due to the fusing time that is involved.

In the second case, any effects due to movement of the electrode at the beginning of arcing would have to be considered.

These difficulties can be avoided by using an impulse to initiate the arc. If the energy input to the

gap by the impulse source, and the energy available from the current source, are sufficient for transfer from a spark to an arc, the power follow will take place.

Referring to Fig.1., the impulse is applied to the non-earthy side of the test gap. The simple Marx circuit used for impulse generation, along with its charging accessories is shown in Fig.5.

On application of the impulse to the non-earthy side of the gap, the output of the generator oscillates at a frequency determined by the output capacitance of the generator and tuning coil in series. This frequency in the present case was 77 kcs. The resistance required to damp this out would be very high, but for this application it is not necessary to have a smooth impulse wave-form. The output resistance of the generator was 200 ohms. Due to the above reasons there is a lowering of the voltage available at the gap for breakdown. The open-circuit output of the generator had to be increased considerably to break down gaps up to 3 cm. (150 kV approx.).

To get a smooth output from the generator it was necessary to isolate the impulse from the current source, which was not easy. The method suggested by Durnford and McCormic (p.27 Proc.I.E.E. Part II, Feb. 1952) could not be adopted due to comparatively low current source voltage (1100 V).

It is essential that the tuning coils should be designed to withstand the impulse voltages.

3. Measuring Equipment

3.1 Low Frequency Work

Cambridge Six Element Dudell Oscillograph (Fig.7a.)

Data

Item	D.C. Sensitivity	Natural Frequency in Air	Resistance	Viscosity of Silicone
L.F. Vibrators	3.6 mm/mA at 65 cms.	3000 c/s (approx.)	2.8 ohms	91 cs. at 20°C
H.F. Vibrators	0.36 mm/mA at 65 cms.	10000 c/s (approx.)	2.4 ohms	265 cs. at 20°C
Wattmeter Vibrators	1.1 mm/mA at 60 cms. with 5 amps in Field coil	3000 c/s (approx.)	2.8 ohms	91 cs. at 20°C

Field Coil: No. of turns 40; Burden 1.25v.A. at 5 amps. R.M.S.

Wattmeter: Resistance 0.09 ohms; Inductance - 110 microhen. at 800 cps.

Vibrator: Insulation, coil to coil, 1000 V. R.M.S. for 1 minute.

Continuous Paper Camera

This can be operated either by hand or automatically

by cams. Maximum paper speed is 2 metre/sec.

Drum Camera

Circumference = 0.5 metre.

Maximum paper speed = 12.5 metre/sec.

Calibration marks appear at an interval of .01 sec., and are provided by a Neon discharge tube maintained by a tuning fork.

3.2 Transient Voltages

Slow Transients: TR 30 (Southern Instrument Co. Ltd.)

This is a 4 channel, 4kV Cathode Ray Oscillograph, accompanied by a 4 channel D.C. Amplifier (Fig.7b.). Three channels are meant for signal records while the fourth is for a time marker. Timing calibration marks are derived from a square wave oscillator controlled by a 100 kcs. crystal. Three frequencies are available for the time marker, i.e. 1, 10 and 100 kcs.

The time base is provided by a high speed, 70 mm., drum camera, the length of a record is 36 inches, and the maximum speed of the drum is 10,000 r.p.m., i.e. a temporal resolution of 6 inches/millisec.

Full scale deflection is obtained at 400 volts peak to peak. The time of exposure can be varied from 5 to 150 millisecs.

D.C. Amplifier

This has 4 channels; maximum gain is 890, which can be reduced to 32, in 11 equal steps, by a sensitivity switch. The frequency response is linear up to 30 kcs. A separate unit for calibrating the record, when the amplifier is being used, has been built into the unit (Fig.7b.).

Faster Transient: TR 10 (Southern Instrument Co. Ltd.)

This is a single channel, 10 kV Cathode Ray Oscillograph, and is fitted with a detachable 35 mm. camera. The sweep time can be varied from 1 microsec. to 1000 microsecs. Full scale deflection is obtained at 600 volts, peak to peak (Fig.7c.).

3.3 Pendulum Timing Switch

This device was used for initiating the events in a predetermined sequence (Fig.7a.). Up to twenty contacts can be operated in one swing of the compound pendulum. The minimum time interval obtainable is 20 millisecs., and the maximum is about 1.5 sec. The time intervals can be varied by adjusting the sliding weights on the pendulum.

3.4 Shunts and Potential Dividers

Resistance for the measurement of discharge currents had to be kept low to keep the decrement of discharge as low

as possible. Care had been taken to secure low non-inductive resistances; the lowest value of the resistance used was as low as 0.00005 ohm.

Potential Dividers

Resistance potential dividers have been used, being the simplest for low frequency work. The resistance has been kept below 100 kilo-ohms to minimise errors due to shunt capacitances.

In the case of impulse initiation the divider is across the Bank before the arc is initiated, and the lower the value of resistance divider, the greater will be the fall of voltage across the Capacitor Bank. Total divider resistance of 200 kilo-ohms gives a time constant of 20 minutes with 12000 mfds. Carbon resistances were used to minimise inductance effects.

For an impulse initiation it is necessary to protect the fecording equipment against the high impulse voltages appearing across the gap before the arc has formed. As suggested by Alston, metrosil was therefore placed across the low voltage arm. (Proc.I.E.E.; Vol.103, Part A, No.7, Feb. 1956). Metrosil was preferred to glow discharge tubes for the following reasons:

1. It is instantaneous in action.

2. The currents are not limited to quite such small values as in the case of glow discharge valves.
3. There is little change in performance with time.

To avoid undue interference in recording and measurement, and heavy induced voltages due to electrostatic and electromagnetic fields of the impulse plant, it is essential that every unit equipment should be separately earthed by non-inductive copper leads to a common datum point.

A complete circuit arrangement is shown in Fig.6.

4. Variation of the Phase Angle between Discharge and A.C. Blow-out Field Currents

The first gap of the impulse generator, used for arc initiation, was replaced by a rotary gap, Fig.7d. The rotary gap consisted of a rotating arm, with a sphere at its end, mounted on the shaft of a synchronous motor. The position of the arm relative to the shaft could be varied. The above sphere was made to pass between two other spheres, which constituted the first gap of the impulse generator. If this gap was properly adjusted, the generator fired as the rotating sphere passed through it. Movement of the rotating arm, relative to the motor axis, alters the position, in space, of the motor rotating field, at which the generator fires, i.e., it varies the phase of arc initiation, relative to the rotating field, and therefore, to the blow-out field,

if the blow-out field system and the synchronous motor are supplied from the same a.c. source. Thus, by suitable calibration the phase angle between the discharge and the blow-out field currents could be varied over full 360^{o} by moving the rotating arm relative to the motor shaft.

APPENDIX III

High Speed Photographic Techniques

1. General

The appearance and movement of the arc during the circuit-breaking process are of vital interest. The arc is drawn in air at atmospheric pressure. Although the arc is normally hidden from view, it is usually possible to photograph it by making one side of the chute of transparent material. Ordinary still and high speed cine-cameras can be used to obtain photographs of the arcs during their very short life.

A framing rate of 1000-2000 frames/sec. was considered suitable. The drawback of the commercial designs available for the above framing rate was that these were of the spooled film type, taking about 100 feet of film and requiring a wastage of about 30 feet; moreover, the necessity of developing a long length of film limited the number of observations possible in a given time. It was, therefore, decided that a drum camera using approximately three feet of film per exposure would be advisable. A suitable design for a High Speed Drum Camera using the well known rotating-block type of optical compensator was kindly made available by A.Reyrolle and Company, Ltd., Hebburn-on-Tyne (Ref.1).

Fig.1. shows the camera. The essentials are a

rotating drum carrying a strip of 35 mm. photographic film on the outside of its rim, and an optical system designed to form an exact number of image frames over the complete length of the film. The drum rotates about a horizontal axis in a light tight casing which also carries the lens system (Fig.1.), the exposure time being controlled by a shutter incorporated in the lens system. The shutter can be tripped electrically by means of a solenoid mounted above the lens. Two normal framing rates have been used, namely, 0-1000, with a total of 80 frames, 10 mm. by 25 mm., or 0-2000 frames per second with a total of 160 frames, 5 mm. by 25 mm.

The camera consists of two units. The camera-unit consists of a drum, a casing and an optical system and the base unit includes a motor drive and auxiliary electrical components. This arrangement has enabled the camera-unit to be made as light as possible; the camera-unit can be removed to a dark-room for film-processing.

2. Optical System

This consists of a lens, a shutter and a rotating glass-block compensator. The lens has a focal length of 75 mm. and f = 1.8, and the shutter which is built into the lens is of the normal Compur type. Three forms of rotating-block compensator are used (Fig.2.):

(a) With two faces clear and two opaque when using 10 x 25 mm. frame size.

(b) With four clear faces when using 5 mm. x 25 mm. frame size.

(c) As with arrangement (a) but with the block cut into three equal parts by two opaque planes parallel to the opaque faces.

It was found necessary to develop the triple block of type (c) to deal with very contrasty subjects; this reduces the blurring of the image due to the relative movement of the image and film (Ref.1). Reducing the aperture of type (a) by painting the edges black was also tried but with little success.

3. Focussing and Aligning

The field of view and focus can be checked by means of a focussing screen and microscope mounted in a projection on the door of the casing. This screen can be swung into position for viewing, only when the drum is removed (Fig.1.).

The camera can be rotated about the axis of the drum to give alignment in altitude.

4. Photographic Technique

The subjects associated with the present work included both self-luminous parts, and parts requiring external

illumination.

To record the details within the chute, one side of the chute was made of acrylic resin (Perspex). Care, was, however, taken to avoid spurious reflections from the perspex surface, when external lighting was used.

The arc chute with arcing horns and barriers was first photographed with external lighting. Front surfaces of arc barriers and chute walls were painted black to give a clearer picture. Daylight flood-lamps were used for the lighting.

The next stage of photographing the self-luminous arc was fairly simple. The camera lens was fitted with a suitable filter to cut down exposure, and the shutter was opened a short time before the test sequence began. When the arc appeared the film was exposed; the possibility of the exposed frames overlapping on the film was reduced by adjusting the speed of the camera to insure that one revolution of the drum takes longer than the estimated life of the arc. Kodak red filter (x10) was used in the beginning; Ilford U.V. filter 18B was, however, found to be more effective.

5. Processing

Films were usually processed in the standard daylight developing tanks. As the optimum aperture setting of

the camera lens was difficult to assess in arc photography, the exposure and subsequent processing of the film was often governed by previous experience rather than by careful calculation. Fast pancromatic films have been used throughout this work.

6. Colour Photography

Ferrania-Color process was also used for some of the experiments. The results obtained showed a definite improvement over the black and white process; the arc column was easily discernible from arc gases, but the time required for processing made its frequent use impracticable.

Analysis of the cine-films was made from the negative itself. An Aldis projector was sometimes used to project the film on to a large screen. Further impressions of the work being studied were often obtained by slow motion projection of the film on to a screen. The film for this purpose was cemented at its ends to form a loop, thus enabling continuous repetition.

The author wishes to express his gratitude to the staff of the Research Department, A.Reyrolle and Co. Ltd., Hebburn-on-Tyne, for their help and guidance in evolving a photographic technique for the present investigation.

Ref.1. Some Photographic Techniques in Industrial Electrical Research; A.F.B.Young,B.Sc.,A.M.I.E.E. and D.Legg,B.Sc.: Reyrolle Review, 160, Dec.1954, pp.2-15.

APPENDIX IV

Transfer of Arc from Main to Auxiliary Electrode

The work on the present series was started as a preliminary to arc chute development. The circuit shown in Fig.1. was employed throughout the present series of experiments, except for the study of the stability of shunted arcs, in which case the splitter was connected to the anode only through a resistance.

The order of the magnitudes of the resistances R_1 and R_2 was determined by using Ayrton's equation and constants given by Rudenberg, (Refs.1,2).

$$v = \alpha + \frac{\beta}{i} + (\gamma + \frac{\delta}{i})l$$

where $\alpha = 30$ V, $\beta = 10$ V/A, $\gamma = 10$ V, $\delta = 30$ V/A

For arc lengths of 1, 2 and 3 cm. respectively,

$$v = 40 + 40/i \quad \ldots\ldots\ldots\ldots (1)$$

$$v = 50 + 70/i \quad \ldots\ldots\ldots\ldots (2)$$

$$v = 60 + 100/i \quad \ldots\ldots\ldots\ldots (3)$$

Solving these equations with

$$v = 240 - iR \quad \text{(Mains Voltage 240 V)}$$

the resistance values obtained are 250, 180 and 81 ohms respectively.

In most of the experiments of the present series, a resistance of 40 ohms was used in series with the splitter.

Resistance, r , was about 2 ohms and was for the measurement of splitter current. The validity of the above calculations was also verified.

The Dudell oscillograph was used for recording arc voltage, arc current, and splitter voltage and current. Both the continuous paper camera and the drum camera were used.

Splitter Characteristic

To begin with, it was assumed that the splitter characteristics (Fig.2.) should have shapes similar to the probe characteristics used for the study of discharge plasma (Ref.2).

It was intended to study the effects of varying currents, electrode materials etc., on this characteristic, but due to difficulty in obtaining the full curve it was decided to concentrate on the specific portions of the characteristic, such as 'floating potential' and 'rooting potential'.

Records PC 40-42 (Table 3) refer to the 'floating potentials' for three different currents.

Determination of the 'rooting potential' was not simple, due to the ever changing values of the arc length, current and voltage, etc. It was then decided to record rooting and non-rooting conditions by pushing the splitter

through a burning arc (Records PC 32-39; Table 2).

The instability of the arc is evident from the table of observations attached. It was not possible to take any readings for arcs over 15 amps., although all the available means of stabilising the arc were employed. The arc was drawn vertically, and a carbon arc projector assembly was used.

As regards the stability of shunted arcs (Fig.3.), a few experiments were carried out on the basis of the traditional arc theory, and the observed values were in agreement with the calculated values. The time taken by the unstable shunted arc to extinguish itself will depend on the time constant of the loop thus formed.

If the unshunted arc characteristic (Fig.4.) is given by

$$E = E_A + \frac{B}{I}$$

then for the half of the shunted arc

$$E = E_A + \frac{B}{2i}$$

$$\text{But } R = \frac{E - E_A}{ir} ,$$

thus giving the critical value of R. e.g. For a 6 cms. arc with 10 amps. in the unshunted arc (3 cms.) the critical resistance is 4 ohms (Fig.4.).

For a 2 cms. arc, shunted at the middle and

carrying 5 amps. in the unshunted branch, the critical resistance is about 8 ohms.

Conclusions

1. When the splitter, B , is pushed into the arc column, AC , it can carry currents up to an ampère before extinction or rooting occurs. (On some occasions currents up to 1.5 amps. were observed which may have been due to a third root.) (Fig.1.; Table No.2).

2. After rooting has taken place on the splitter, B , (Fig.1.) and before the extinction of the arc, AB , the splitter current is only limited by the resistance drop across R_1 (between B and A), in relation to the voltage drop of the shunted arc AB.

3. Before rooting, the current through the splitter, B , consists of both ion and electron currents. The ion current reaches a maximum steady value (Fig.2.) as the potential of the splitter B is made more and more negative with respect to the anode A. If the potential of the splitter is then increased in the positive direction, a potential F is reached, when these two currents are equal and opposite in magnitude. This is called the 'floating potential', as it would be the potential assumed by an isolated splitter, when in contact with an arc plasma. It is about 40 V, negative to anode,

for a total arc drop of about 50 V. (Table 3).

If now the potential of the splitter is made positive, with respect to the arc plasma at B, a potential point R is reached (Fig.2.), when the potential of the splitter, relative to the plasma, is sufficiently positive to allow the formation of an anode root on the splitter.

4. Variations in the arc current at low current values do not have any appreciable effecf on the characteristic. (Table 3).

5. After rooting on the splitter, lower values of the resistance R are required for the extinction of the shunted arc AB, (Fig.3.) at higher arc currents.

6. It was not possible to get cathode rooting at the splitter (Fig.5.). This is probably due to the fact that the formation of a cathode root requires emission of electrons, and hence higher field gradient or temperature, or both, are needed.

Isolated Splitters

With the help of the above observations, it may be possible to predict the behaviour of two isolated splitters in an arc plasma connected through a resistance.

For rooting on two short-circuited splitters (Fig.6.)

at higher arc currents, the spacing between the splitters must be increased until the voltage drop along the arc length between them is greater than the voltage required for the two root drops.

The critical resistance between the splitters, for the extinction of the arc shunted by them, increases with increased spacing.

It may be possible to place two short-circuited splitters at positions such that they do not carry any current (Fig.6).

A.C. Arcs

Obviously in an a.c. arc the difficulty of cathode rooting is non-existent provided the arc burns for more than one half-cycle. In the case of a shunted a.c. arc, the critical resistance for the extinction of the shunted arc will vary on rising and falling currents, due to the difference between the slopes of the dynamic characteristics.

Finally, for some of the practical applications, it may be necessary to determine the complete characteristic. The work on this series had to be suspended due to the instability of the arc.

Ref.1. Physical Properties of Arcs in Circuit-breakers; Emil Alm, Stockholm, 1949.

Ref.2. Gaseous Electrical Conductors; J.D.Cobine, McGraw Hill, 1941.

TABLE 1

S.No. PC	Arc Current (Amps.)	Arc Volts (Volts)	Splitter Volts negative to anode	Splitter current (m.A)	Remarks
1	10	58	56	-1.22	
2	10	58	47	-.02,1.8	Splitter current reverse
3	10	56	41.7	1.89	
4	10	64	44	1.50	Records 1-10b exhibit a superimposed 50c/s oscillation on the splitter current, probably due to a pickup from the mains.
5	10	54	30.7	1.05	
6	10	52	30.5	1.2	
7a	10	59	32.8	0.87	
7b	6.66	102	54.8	1.5	The arc seems to have bent round the splitter, and hence lengthened itself.
8	9	76	50.4	1.2	
9a	10	64	34	9.0	
$10a_1$	11.4	64	20.8	6.44	
$10a_2$	10.7	76.7	24.1	3.44	
10b	8.6	68	18.7	4.19	
13	6.13	44	19.7	9.56	These records show an oscillation in the splitter current. The current oscillates between the two extreme values noted in column 4, at a frequency of approx. 30 c/s.
14	6.55	60	17.5	6-20.3	
16	7.13	60	15.3	13.5-21	
18	5.7	68	11.1	25.7	
19	4.8	80	66.0	2.92	
20	5.7	68	39.4	0.9	The splitter current seems to reverse.
21	6.55	64	20.8	11.0	
22	5.75	80	21.8	12.4	

The splitter, in this series of experiments, was fixed, and its potential, relative to the anode, was varied by changing the resistance R_2 (Fig.1.). No complete transfer occurred in any one of these experiments, and the resistance R_1 was 40 ohms

TABLE 2

S.No. PC	Arc Current (Amps.)	Arc Volts (Volts)	Splitter Volts negative to anode	Splitter current (Amps.)	Remarks
33	5.0	79.5	51.5	0.960---	Rooting takes place, the splitter current is measured just before rooting occurs.
34	7.12	71.4	55.1	1.07 ----	No rooting occurs. The value refers to the tip of the splitter current before extinction occurs.
35	7.12	86.3	44.6	0.78 ----	Rooting occurs, the splitter current is measured just before rooting.
36	12.8	63.0	38.3	0.975)	No rooting occurs, the splitter current being measured just before extinction
37	11.4	68.5	42.7	0.55)	
38	9.18	75.3	55.8	1.48 ----	The reading noted here refers to the first extinction. The main arc between A and C re-struck as the splitter was withdrawn after rooting. This process of arc transfer and re-ignition was repeated thrice on the same record.

The splitter, in this series of experiments, was pushed into the plasma until the arc was extinguished or rooted on the splitter. The Drum Camera was used, and the total exposure time was in the region of about six seconds. The resistance in the splitter circuit was 40 ohms.

TABLE 3

Determination of the Floating Potential

S.No. PC	Arc Current (Amps.)	Arc Volts (Volts)	Splitter Volts negative to anode	Splitter current (m.A)	Remarks
40a	-	49.4	41.6	0	The splitter was fixed at the centre of the arc length, for these experiments. The potential of the splitter, relative to the anode, was varied until the ammeter in series with the splitte showed zero deflection. A central zero ammeter was used. In record 40a the arc current was not recorded.
40b	4.43	54.6	44.6	.4	
41	8.94	46.7	41.6	0	
42	12.75	46.7	43.8	0	

Illustrations.

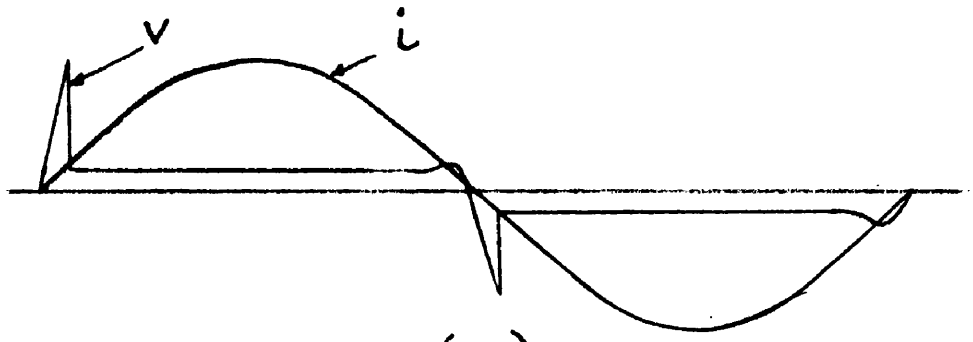

TYPE (a)

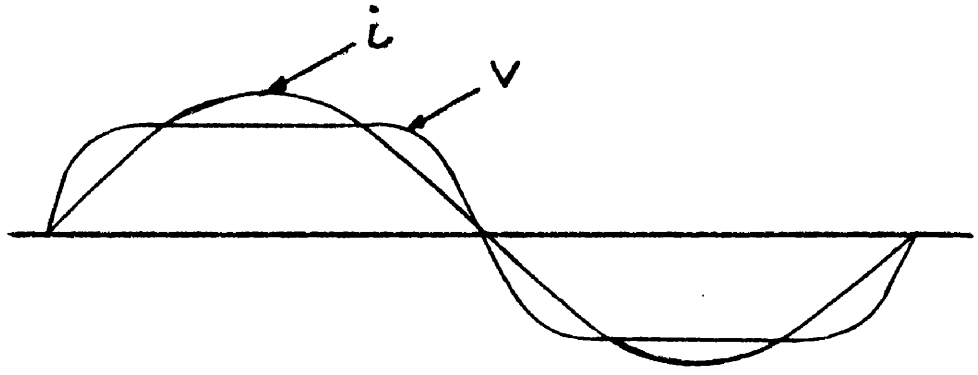

TYPE (b)

Fig. 1 IDEALISED ARC VOLTAGE WAVE-FORMS

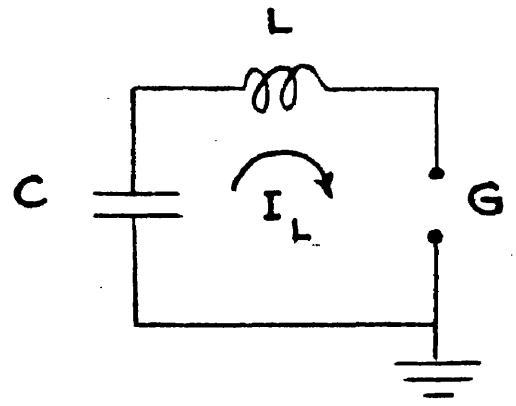

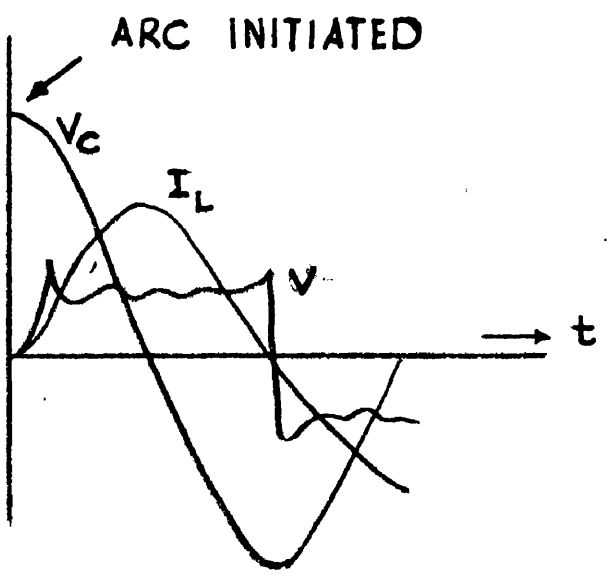

Fig. 2.

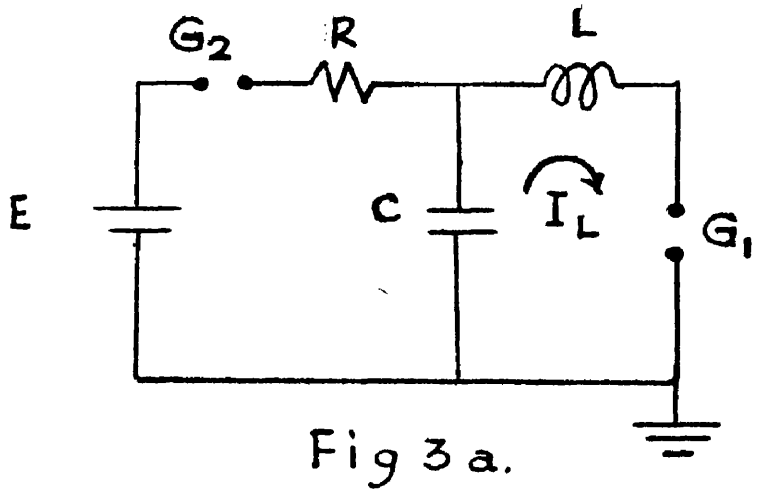

Fig 3a.

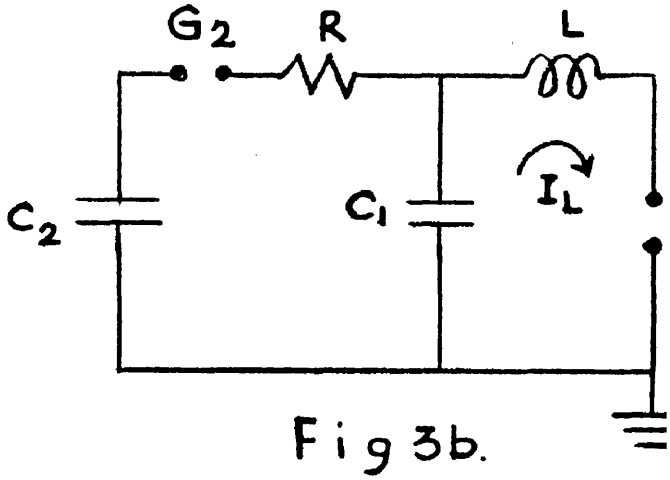

Fig 3b.

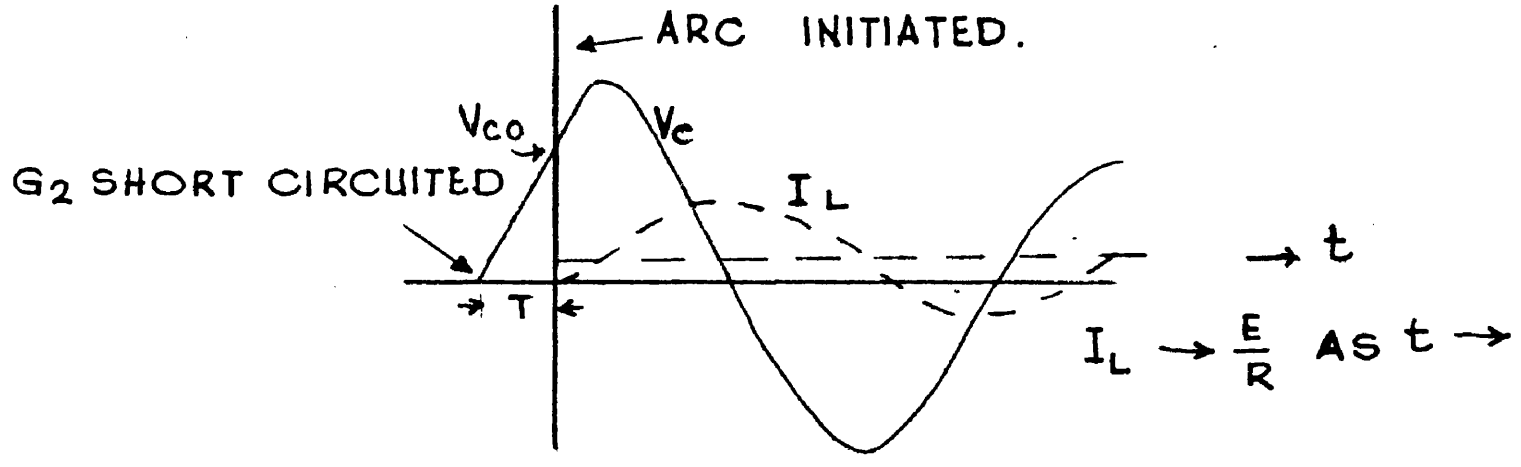

Fig 3c.

POWER SUPPLY.

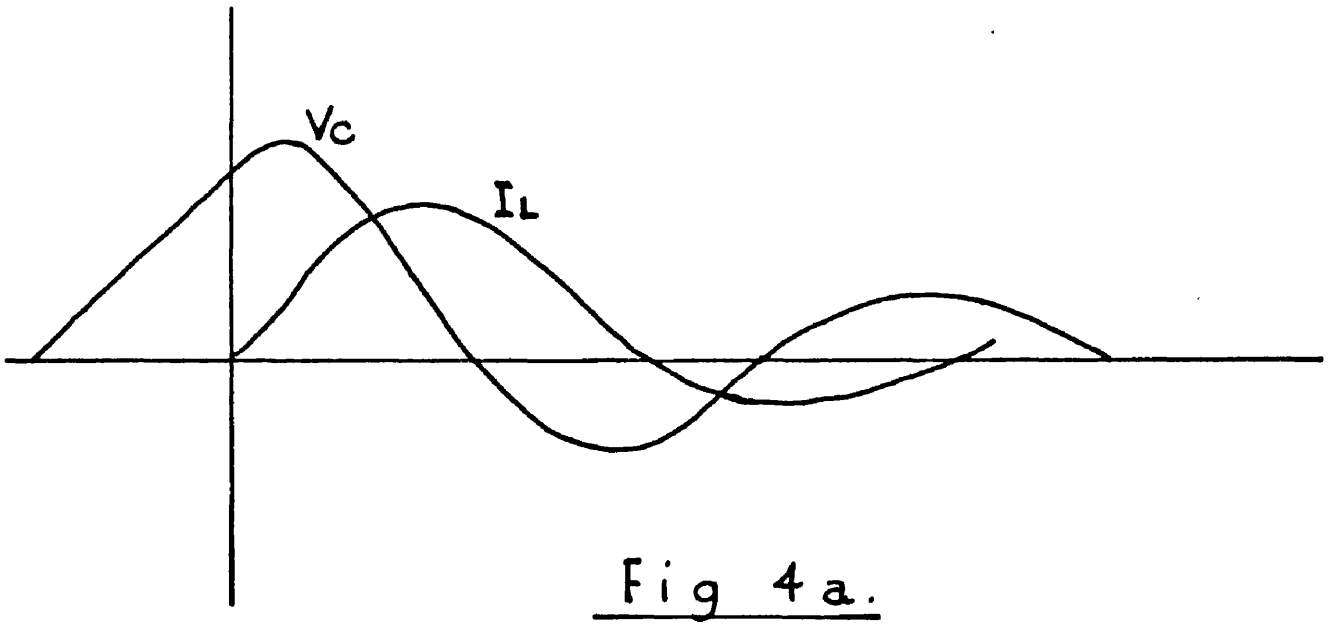

Fig 4a.

TRACING OF OSCILLOGRAMS SHOWING POINT-ON-WAVE SELECTION USING A 500v d.c. SOURCE IN THE CIRCUIT OF Fig.3

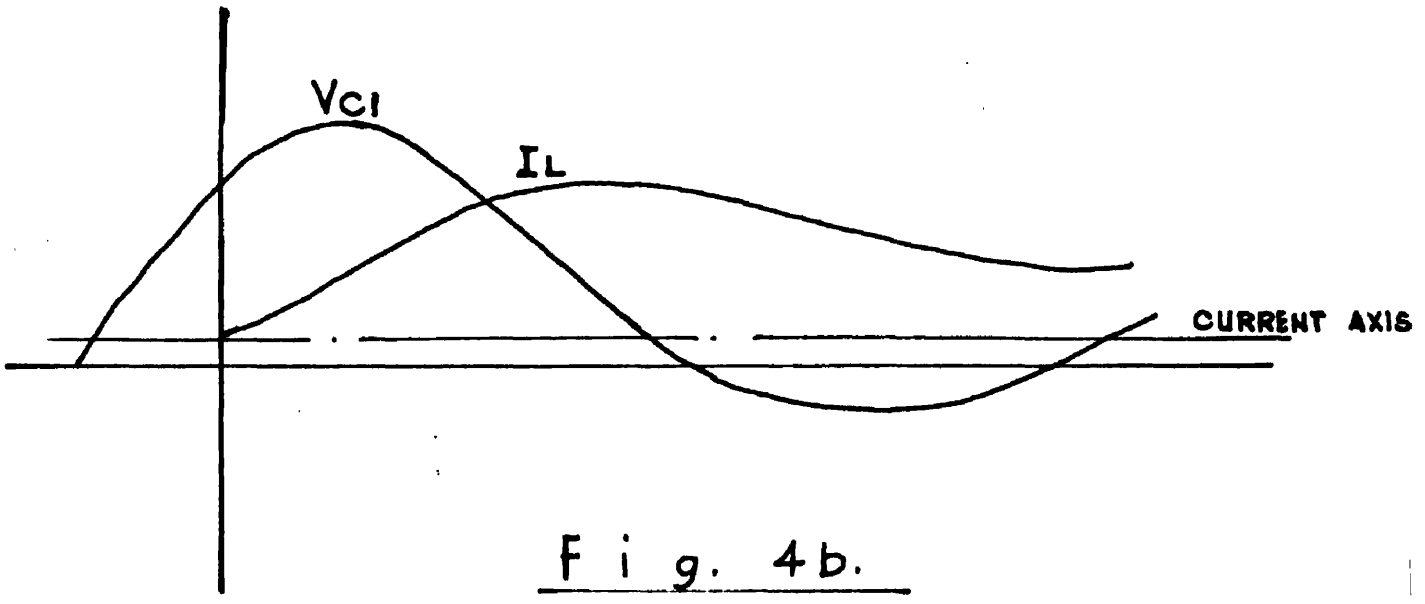

Fig. 4b.

TRACING OF OSCILLOGRAMS SHOWING POINT-ON-WAVE SELECTION USING A 750 μF CAPACITOR (C_2) CHARGED TO 200c IN THE CIRCUIT OF Fig. 3b.

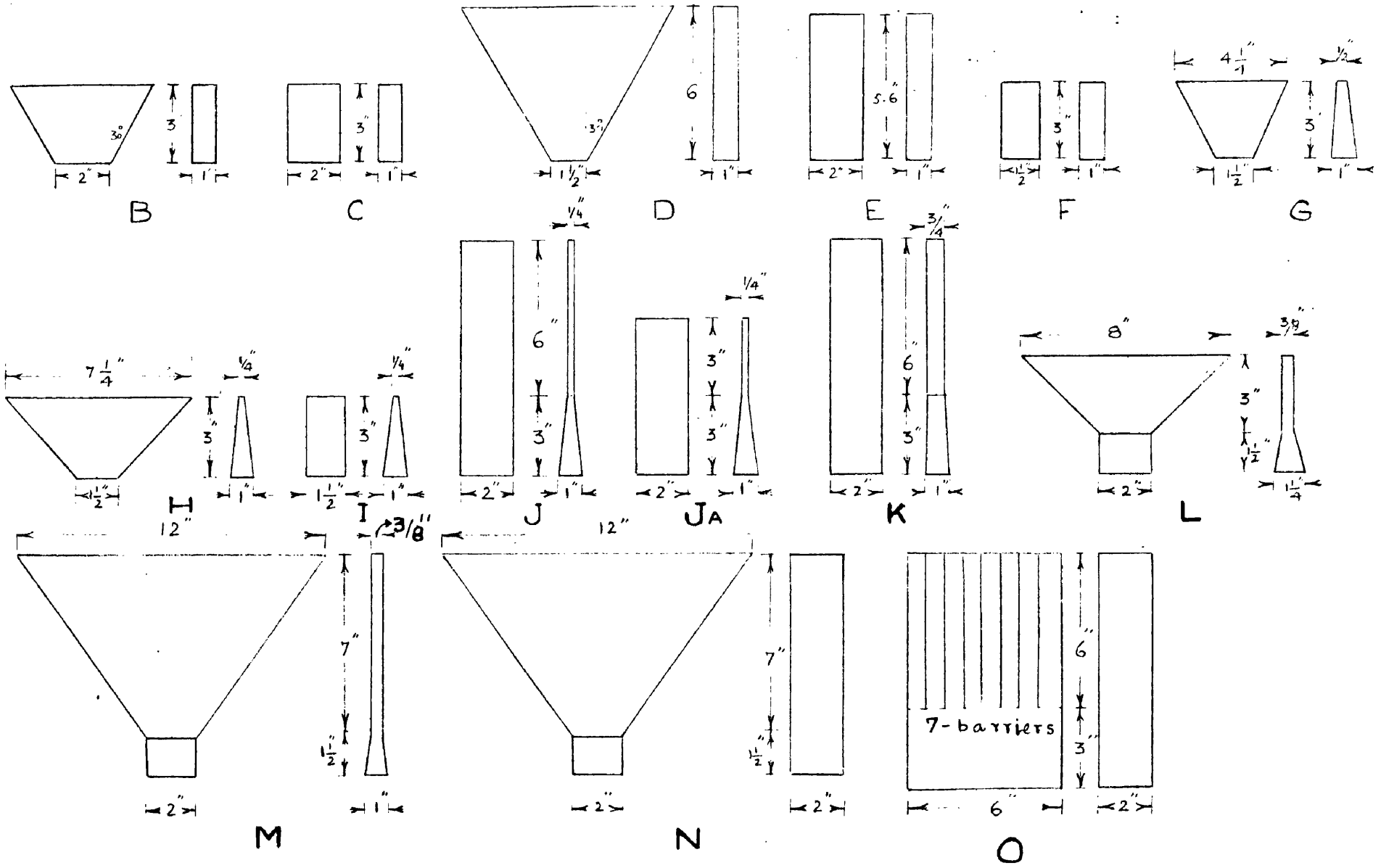

Fig. 5a. Dimensions of experimental Arc Chutes used.

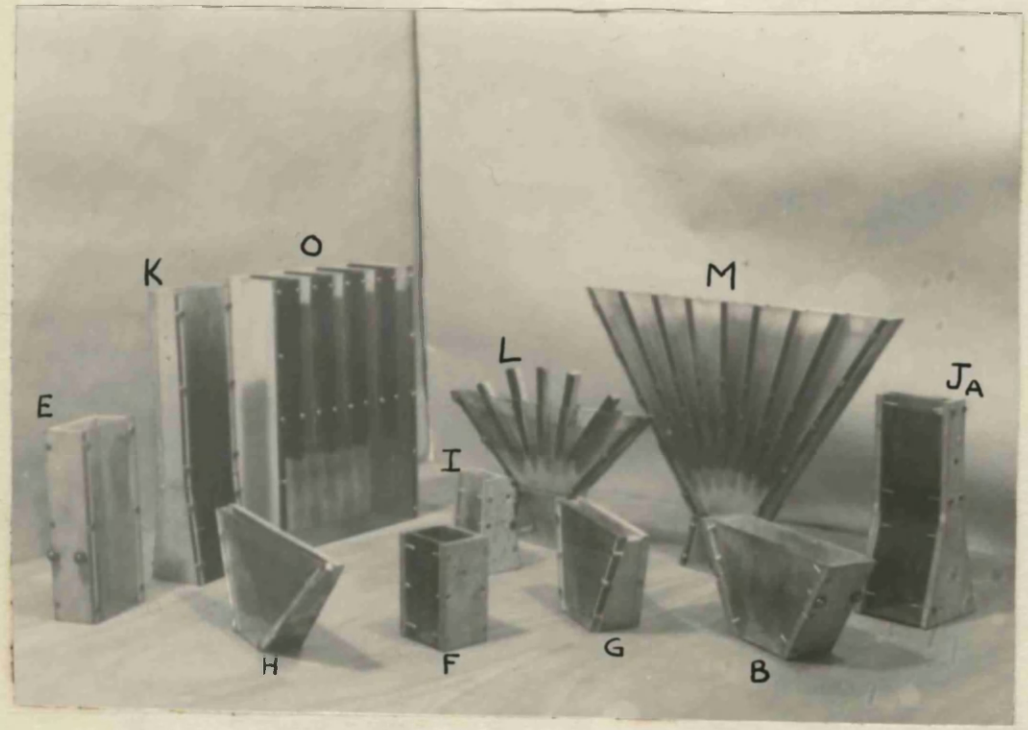

FIG.5b: A pictorial view of the experimental arc chutes used.

1. 2. 3. 4. 5. 6. 7.

FIG. 6a

FIG. 6a shows an arc between fixed contacts in air, without a chute, while FIG. 6b shows arcing in chute B, which is of the same dimensions as the arc in free air. Only alternate picture frames are reproduced. Print 6 in FIG. 6a and Print 5 in FIG. 6b show conditions near the first current-zero.

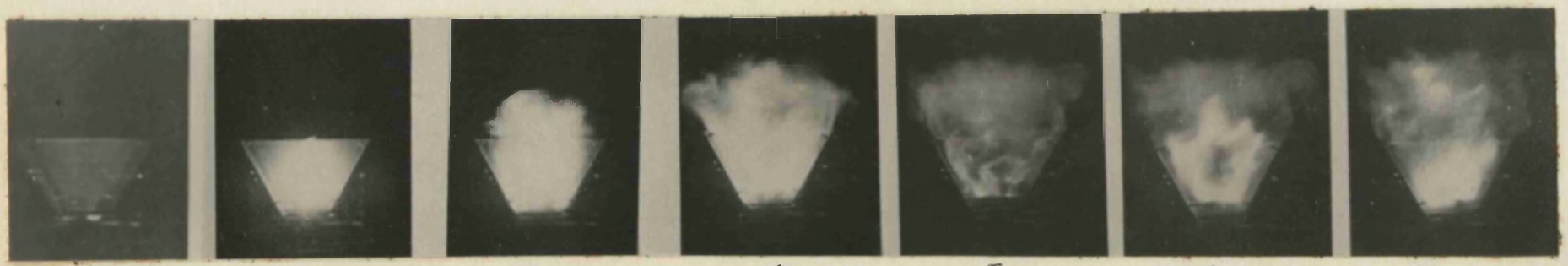

1. 2. 3. 4. 5. 6. 7.

FIG. 6b.

FIG. 7a.

1 2 3 4 5 6 7

FIG. 7b

1 2 3 4 5 6 7

FIG. 7c.

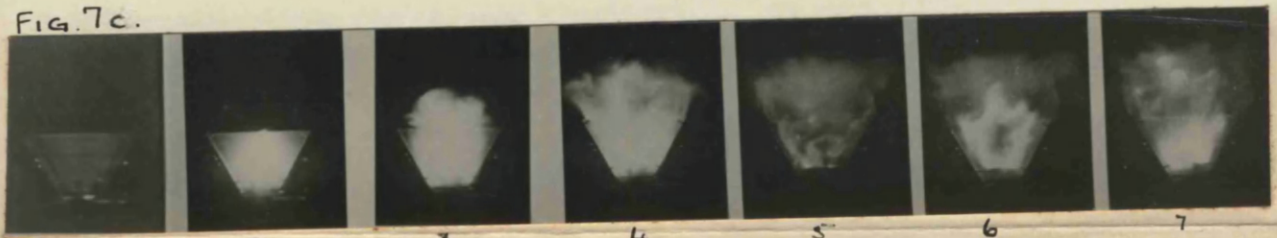

1 2 3 4 5 6 7

FIG. 7d

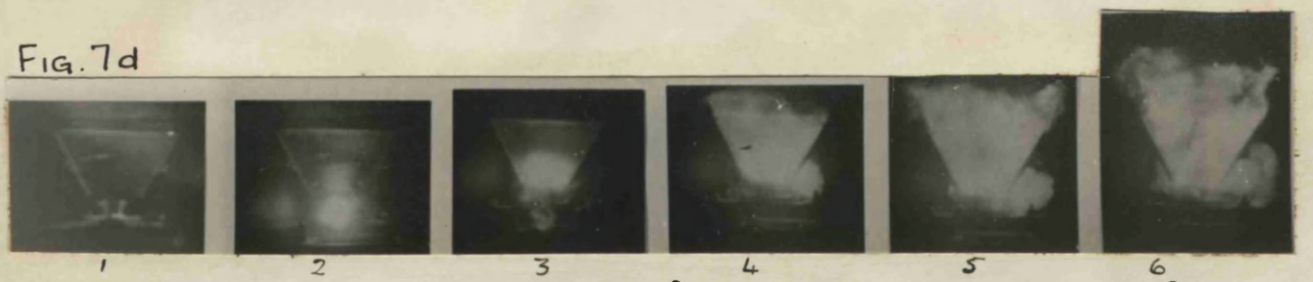

1 2 3 4 5 6

Figs. 7a to d cover the first half-cycle of arcing; only alternate picture frames are selected. Fig. 7a shows Chute C, which covers the fixed contacts at the lower ends. Print 6 shows conditions near the first current-zero. In Fig. 7b, Chute C does not enclose the contacts and thus allows the hot gases to escape outside the chute which may lead to uncontrolled arcing. This is shown in prints 6 and 7 following the first current-zero.

Figs. 7c and 7d show effects similar to Figs. 7a and 7b but with Chute B.

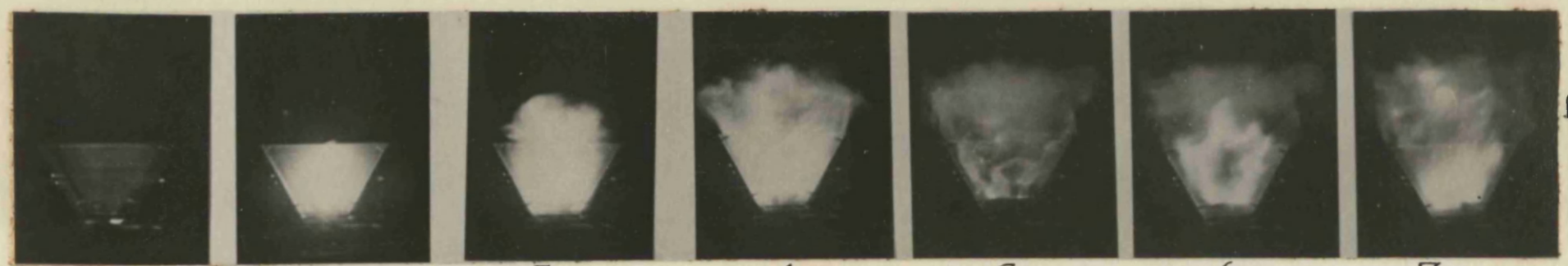

Fig. 8a.

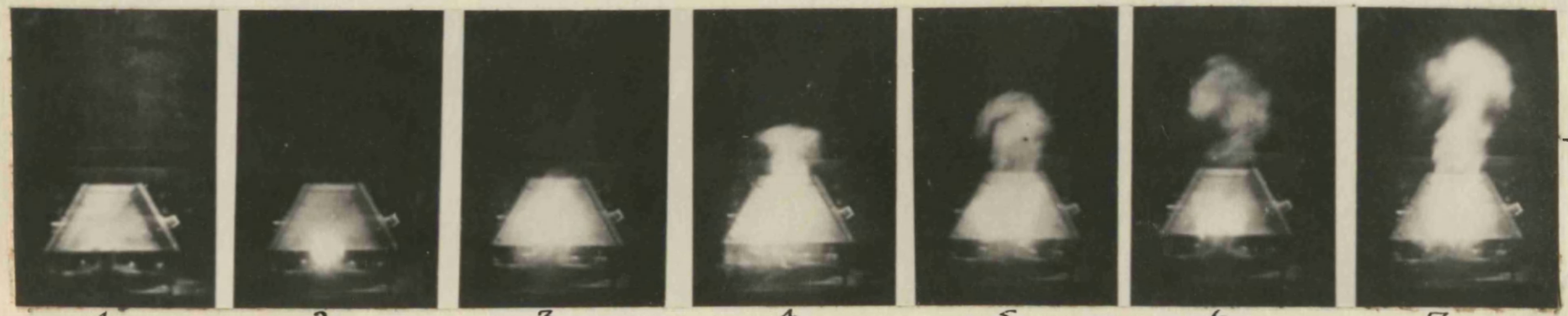

Fig. 8b.

Fig. 8a shows Chute B with diverging sides, allowing for expansion of the hot gases that moved upwards; prints 5 and 6 cover a current-zero. Fig. 8b shows Chute B inverted, so that the cross-section diminishes with height. The arc movement upwards therefore accelerated as the gases moved upwards.

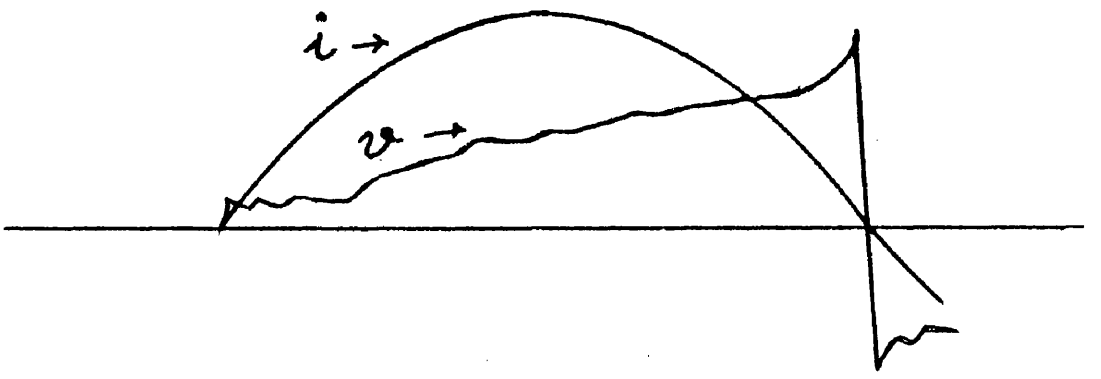

Fig. 9a: Diagram showing the form of arc voltage and current over the first half-cycle, when a chute was used.

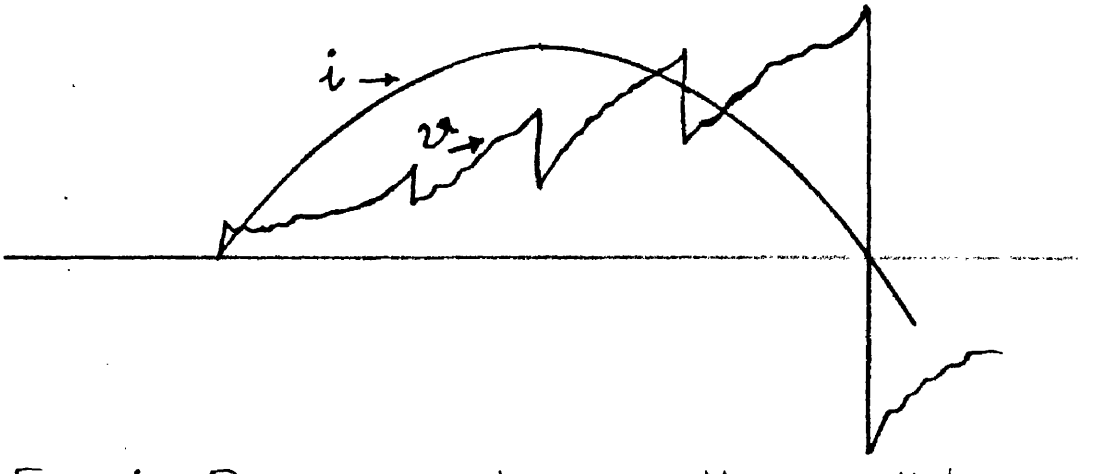

Fig. 9b. Diagram showing the oscillations on the arc voltage characteristic, due to the restriking of the arc across the shortest path between the contacts.


1.


2.


3.

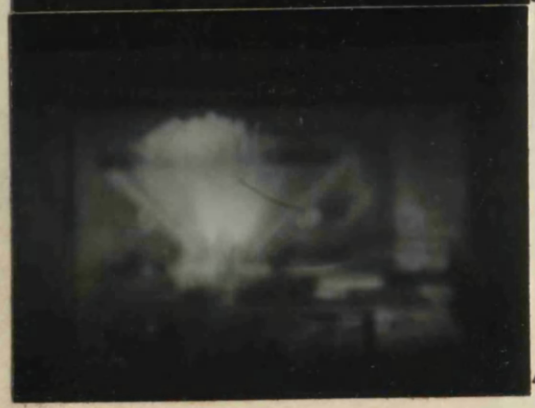
4.

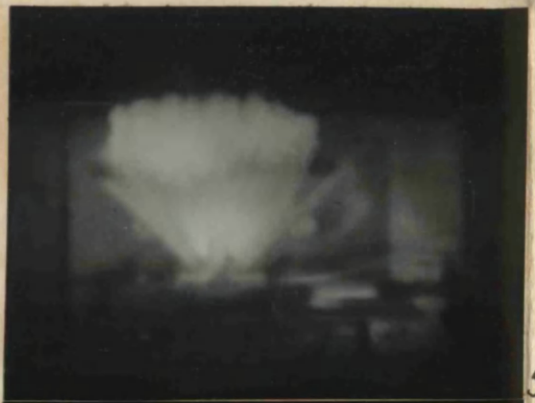
5.


6.


7.


8.


9.


10.


11.

FIG. 10: Showing the first half-cycle of arcing with Chute H; approximately 8 frames correspond to a half-cycle. Print 8 shows conditions near the first current-zero, while Prints 5 and 7 show the short-circuiting of the arc column.

Gap = 3/8"; V_c (max.) = 2200 v; I_L (max.) = 2000 A.

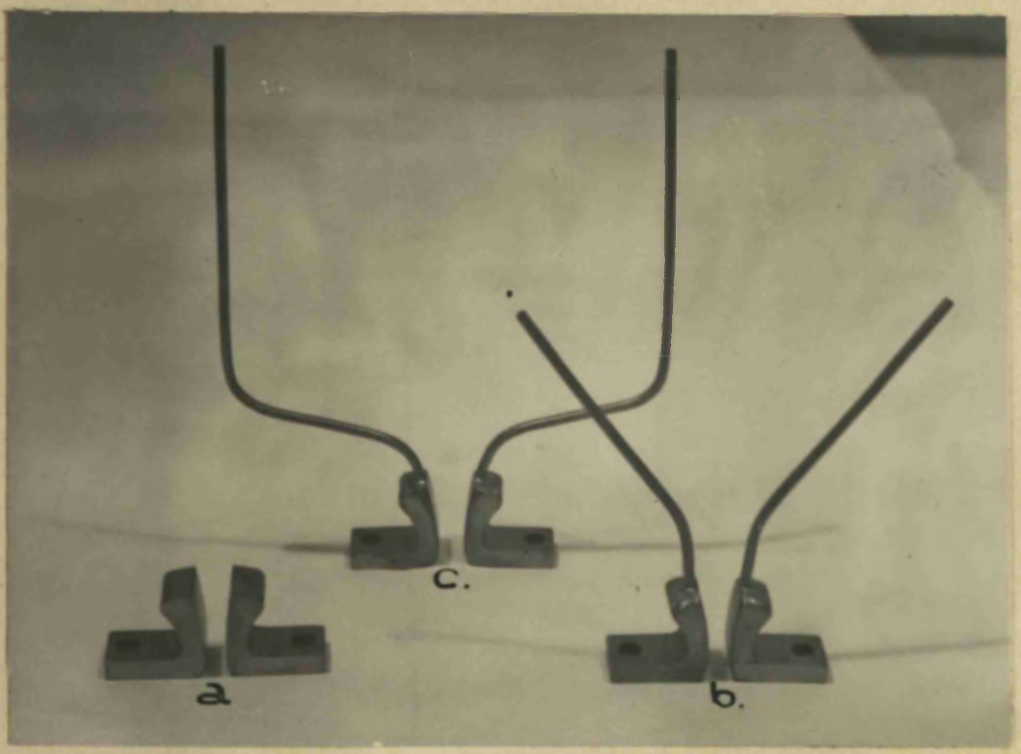

FIG. 11: Showing experimental arcing horns used.

Fig. 12a Showing Chute H with horns; the arc burns outside the chute from print 5 onwards.

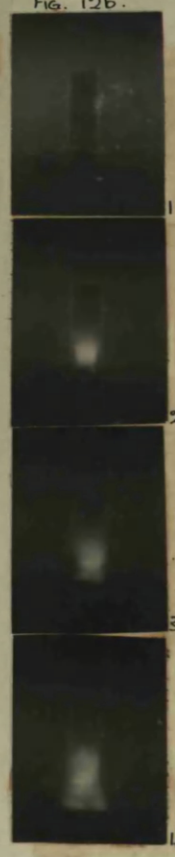

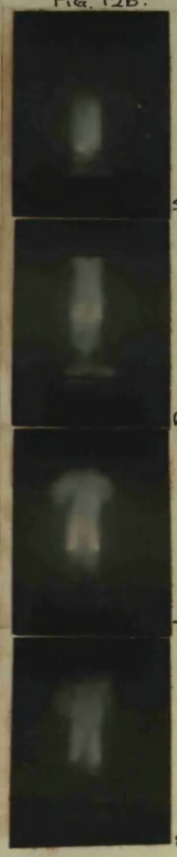

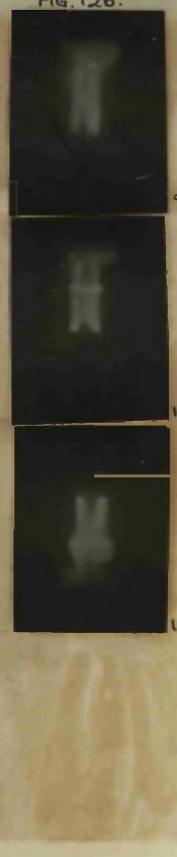

Fig. 12b. Showing Chute J with horns.

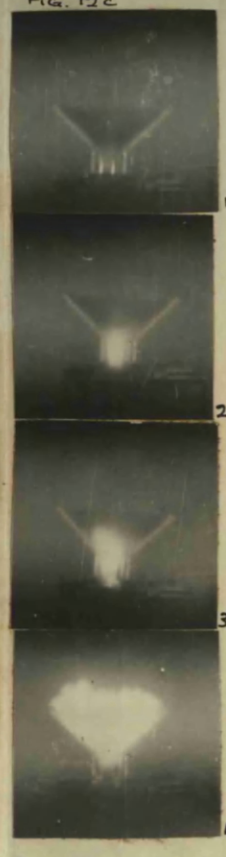

Fig. 12c Showing Chute L with horns; the arc burns outside the chute from print 6 onwards.

Figs. 12a to e. Illustrating the effectiveness of a chute as a container. Only the photographs covering the first half-cycle are reproduced.

FIG. 12c

FIG. 12d.

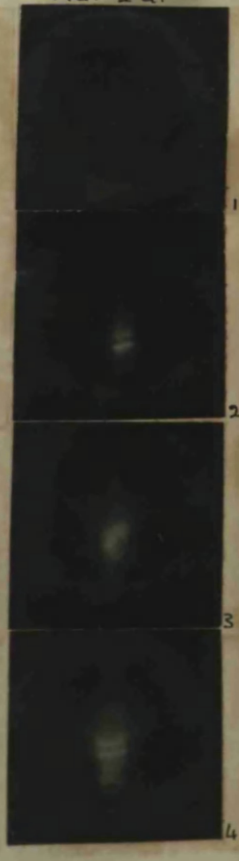

FIG. 12d.

FIG. 12d.

hute from print 6 onwards.

Fig. 12d. Showing Chute L with three arc barriers, horns, and d.c. magnetic blow-out field of 110 lines/cm².

2 are reproduced. About 8 picture-frames correspond to a half-cycle.

FIG. 12e. 1-4

FIG. 12e 5-8

FIG. 12e. 9-11

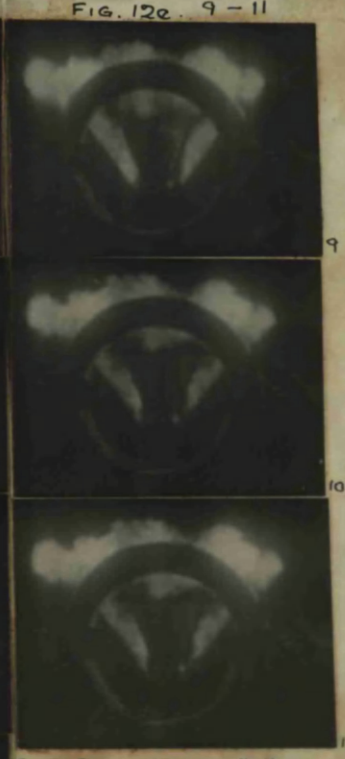

Fig 12e. Showing Chute M with three arc barriers, horns, and a d.c. magnetic blow-out field of 500 lines/cm². The arc burns outside the chute from print 6 onwards.

FIGS. 12a – e.

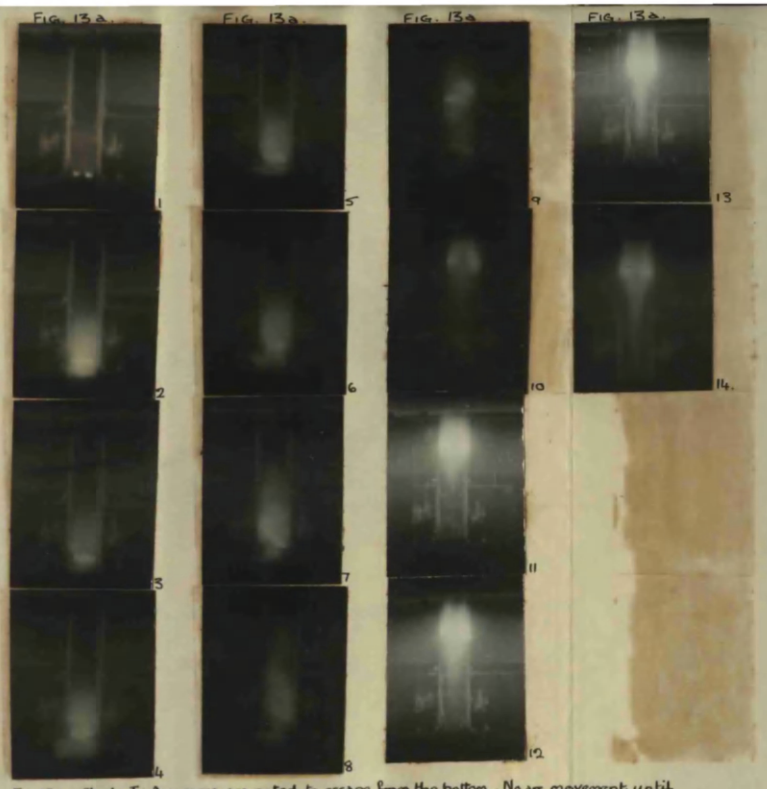

FIG. 13a.

FIG. 13a.

FIG. 13a.

FIG. 13a.

Fig. 13a. Chute J: Arc gases are noted to escape from the bottom. No arc movement until print 7. Arc gases travel downwards through the chute in prints 11-14. Print 8 shows conditions near the first current-zero.

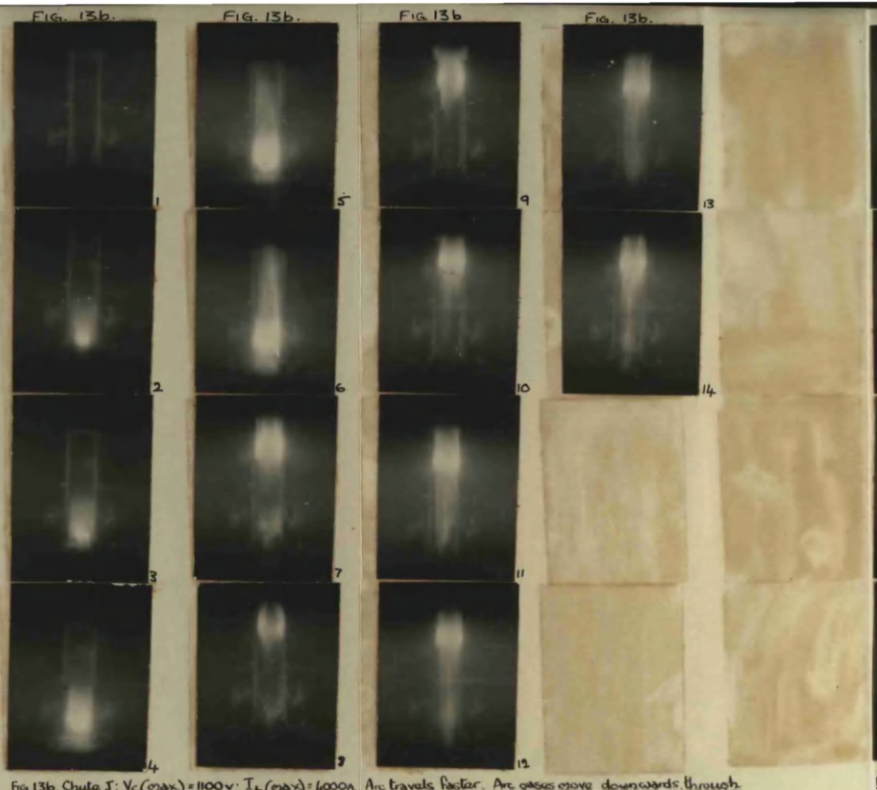

FIG. 13b.

FIG. 13b.

FIG. 13b

FIG. 13b.

Fig. 13b. Chute J: V_c (max) = 1100v; I_L (max) = 6000A. Arc travels faster. Arc gases move downwards through the chute in prints 10-14. Print 8 shows the conditions near the first current-zero.

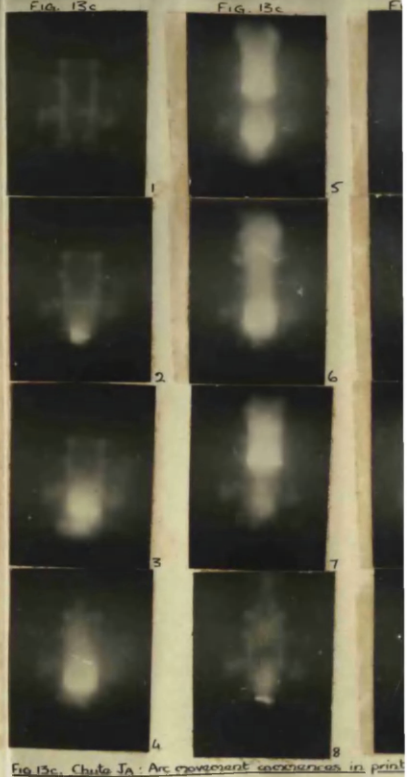

FIG. 13c.

FIG. 13c.

Fig. 13c. Chute J_A: Arc movement commences in print 4 at the bottom. Prints 7-8, 11-12, and 15-16, show conditions near the first current-zero.

FIGS. 13a-c. Showing the first half-cycle of arcing with chutes J and J_A, using horns six inches tall. Approximately 8 picture frames cover a half-cycle. V_c (max) = 2200v; I_L (max) = 2000A;

FIG. 13b

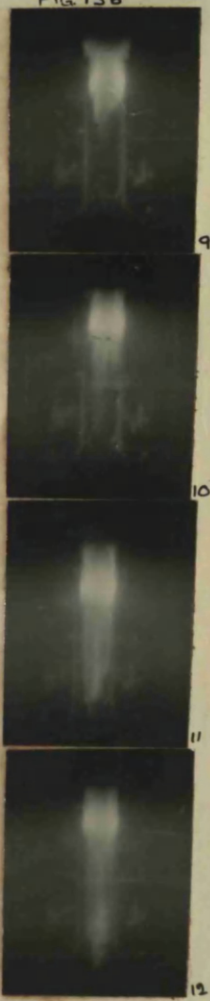

FIG. 13b.

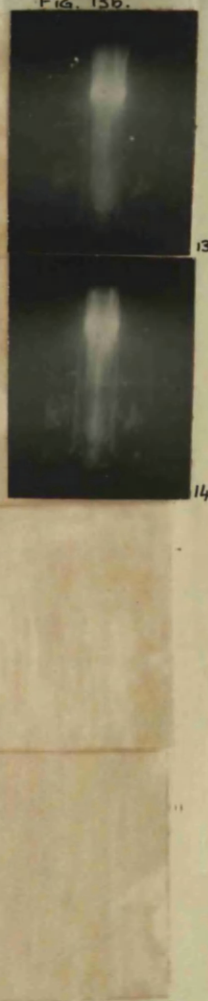

Arc travels faster. Arc gases move downwards through
ws the conditions near the first current-zero.

FIG. 13c

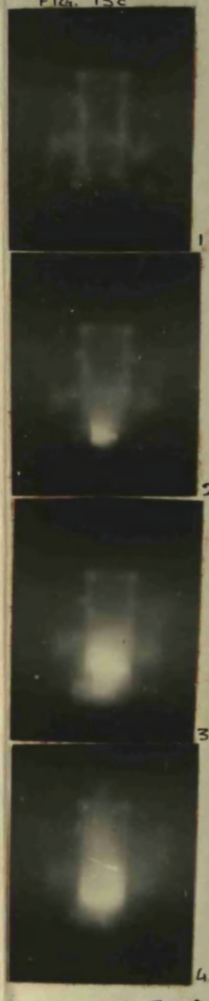

FIG. 13c

FIG. 13c

FIG. 13c.

FIG. 13c. Chute JA: Arc movement commences in print 3. Print 5 shows the arc re-striking at the bottom. Prints 7-8, 11-12, and 13-14, show more restrikes. Print 8 shows conditions near the first current-zero.

x inches tall. Approximately 8 picture frames cover a half-cycle. V_c (max) = 2200v; I_L (max.) = 2000a; Gap = 1".

FIGS. 13a-c.

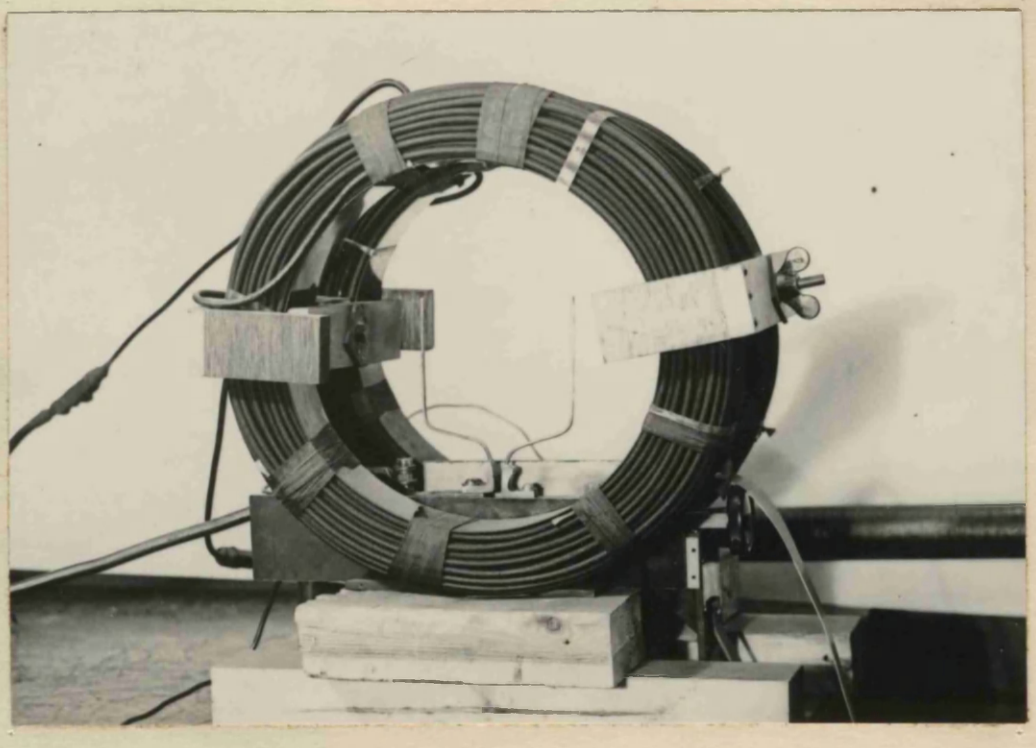

FIG. 14: Showing the magnetic field system.

(Inside dia. = 12". Distance between centres of coils = 6".)

FIG. 15a. Parallel horns, six inches tall, two inches apart. Print 9 shows the conditions near the first current-zero.

FIG. 15b. Parallel horns six inches tall, two inches apart. $I_L(max.) = 4000$ A. $V_c(max) = 1100$ v. Print 7 shows conditions near the first current-zero.

FIG. 15c. Showing horns that are parallel up to a height of 3 inches, then begin to diverge. Print 8 shows conditions near the first current-zero.

FIG. 15d. Showing horns that diverge at 30° conditions near the first current

FIGS. 15a to e. Shows the first half-cycle of arcing on horns in free air. The arc movement upwards is slow, and the arc g to remain in the vicinity of the horns. [$I_L(max) = 8000$A; $V_c(max) = 2200$v; Gap = 1"]

FIG. 15d.

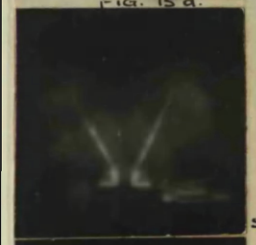

5.

6.

7.

8.

diverge at 30° to the vertical. Print 5 shows first current-zero.

1 the arc gases can be seen.

FIG. 15d.

9.

10.

11.

FIG. 15e. 1–4

FIG. 15e. 4

8

FIG. 15e. 9 – 12

12.

FIG. 15e 13 – 14

14.

FIG. 15e. Showing horns that diverge at 75° to the vertical. Print 8 shows conditions near the first current-zero.

FIGS. 15a-e.

FIG. 16a


1.


2.


3.

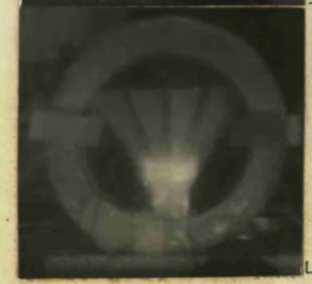
4.

FIG 16a

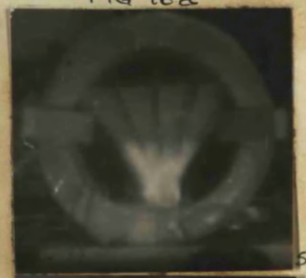
5.


6.


7.

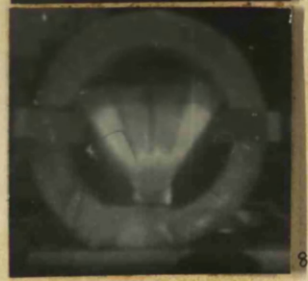
8.

FIG. 16a.

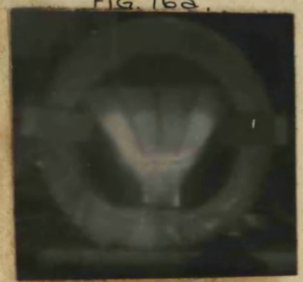
9.


10.


11.

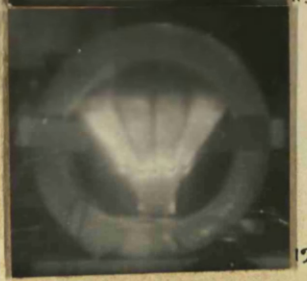
12.

FIG. 16b


1.

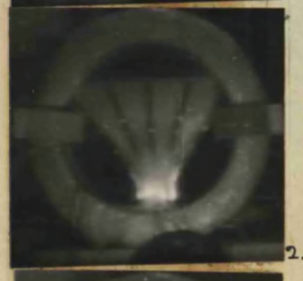
2.


3.


4.

FIG. 16b.


5.


6.


7.

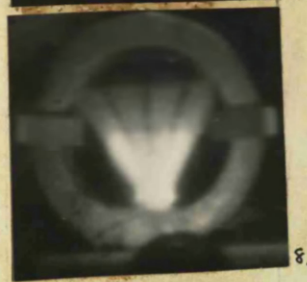
8.

FIG. 16b.


9


10.

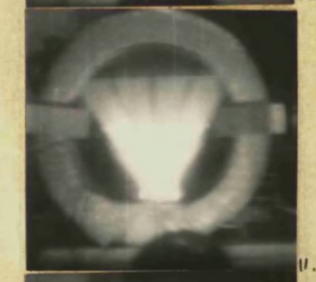
11.

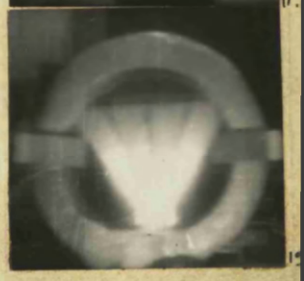
12.

FIG. 16b.

5.

6.

7.

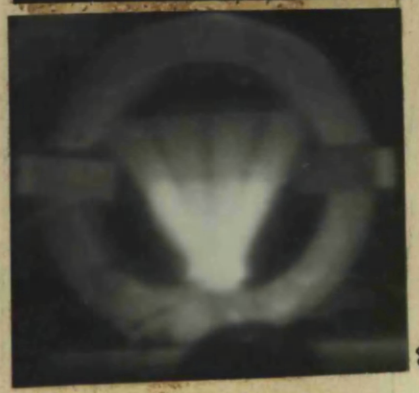

8.

FIG. 16b.

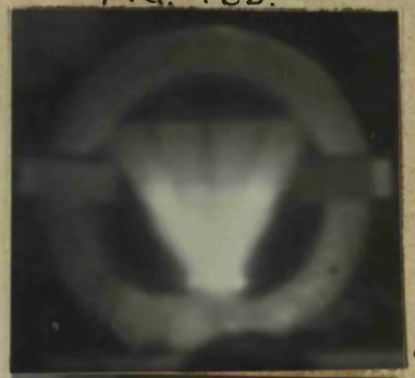

9.

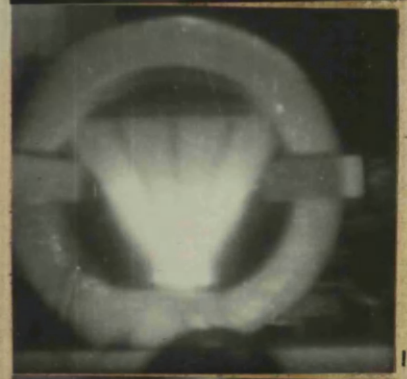

10.

11.

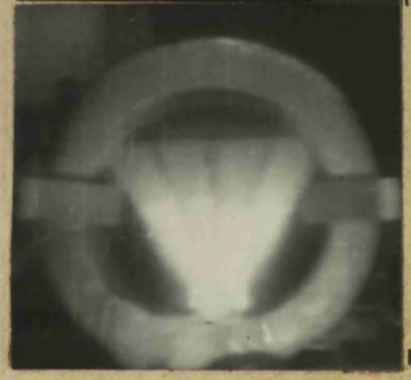

12.

FIGS. 16a, b. Illustrating the effect on arc movement of covering the top exit in Chute N. Only the prints covering the first half-cycle are reproduced. In Fig. 16b the top exit is partially covered (shown below.) The arc movement upwards can be seen to be retarded.

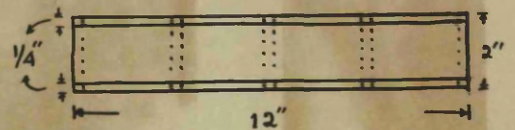

FIGS. 16a, b.

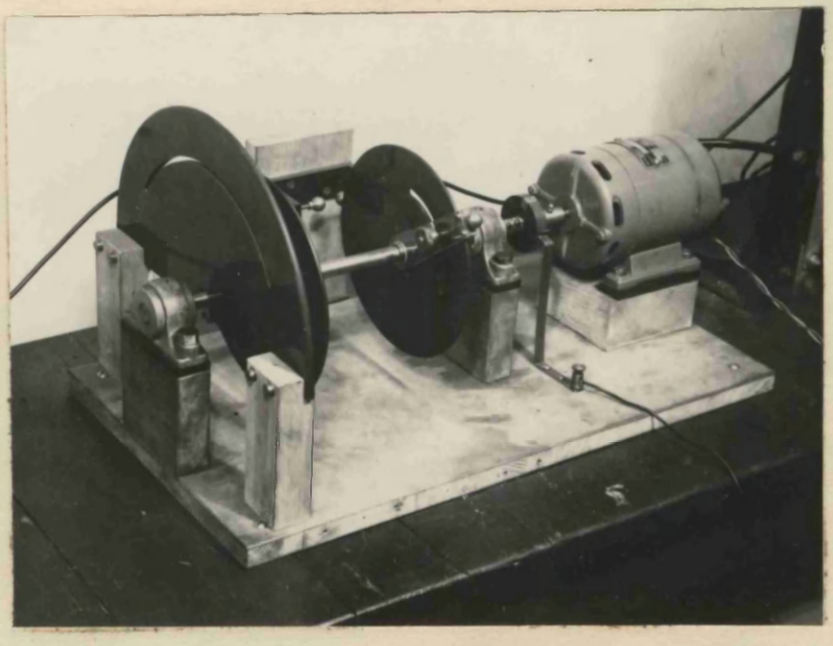

FIG. 17: Showing the Synchronous Rotary Switch.

NOTE

In Figs.18, 19, 20, 25 and 27e-i only the last 1500 millisecs of the first half-cycle are plotted. Time is measured from the first current-zero.

In Figs.21, 24, 26 and 27a-d, the first half-cycle is plotted. Variations in the duration of the half-cycle are due to damping of the discharge current from the Capacitor Bank.

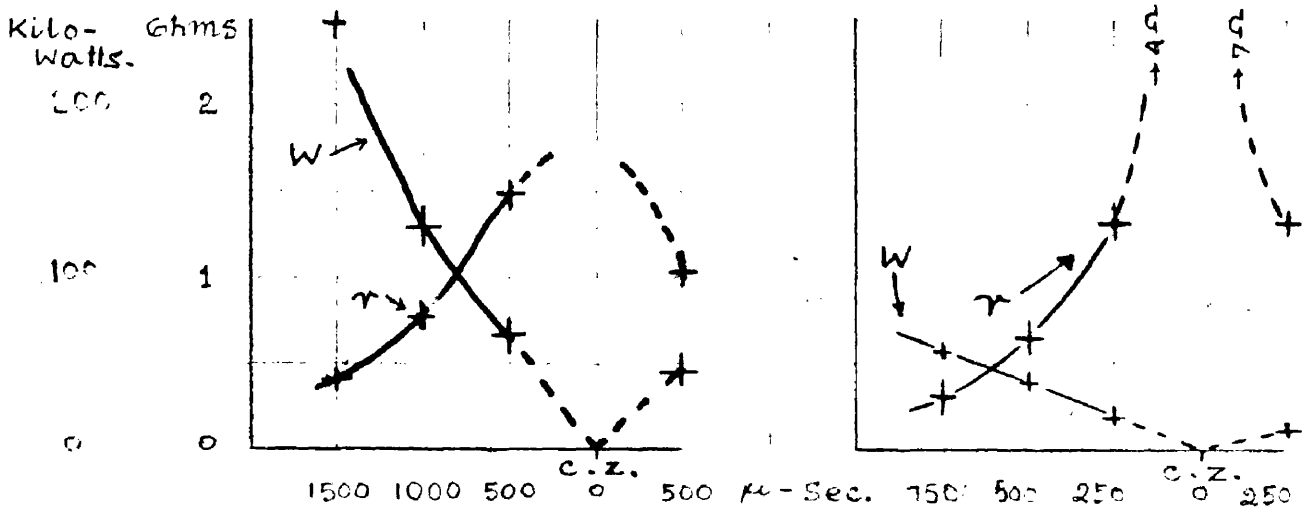

FIGS. 18. a-f

V_c(max) 22(

I_L(max) 20(

V_{10} = 1520V W_{T1} = 55%

V_{10} = 1630V W_{T1} = 36%

a. CHUTE-B

b. CHUTE-F

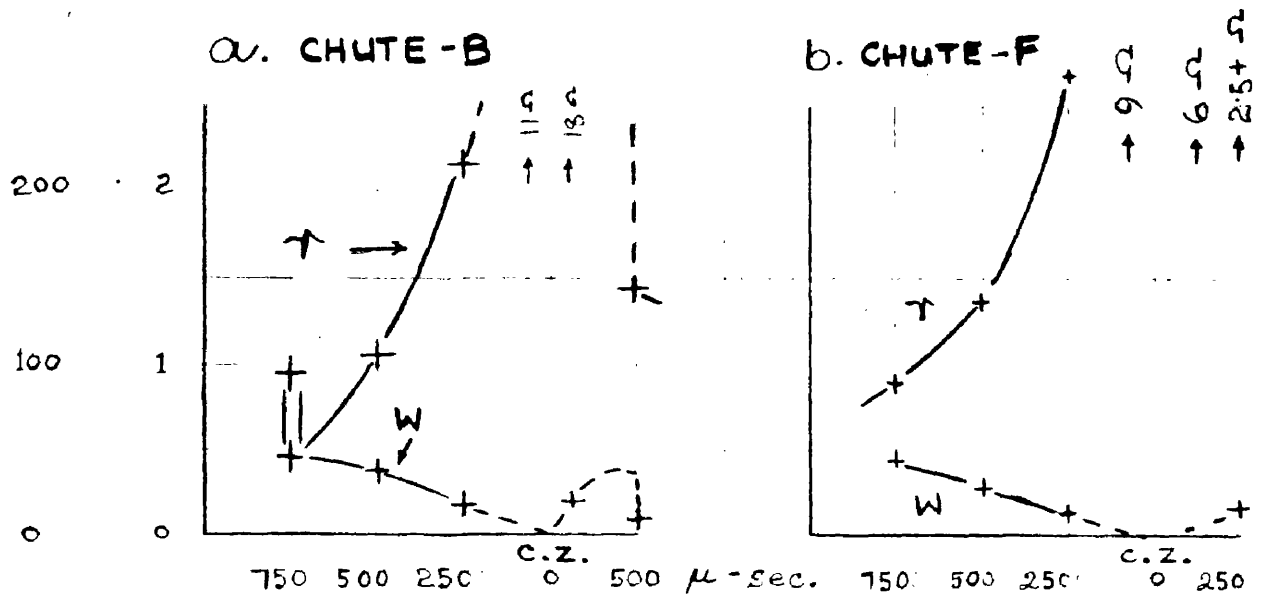

V_{10} = 1800V W_{T1} = 34%

V_{10} = 1800V W_{T1} = 34%

C. CHUTE-G

d. CHUTE-H

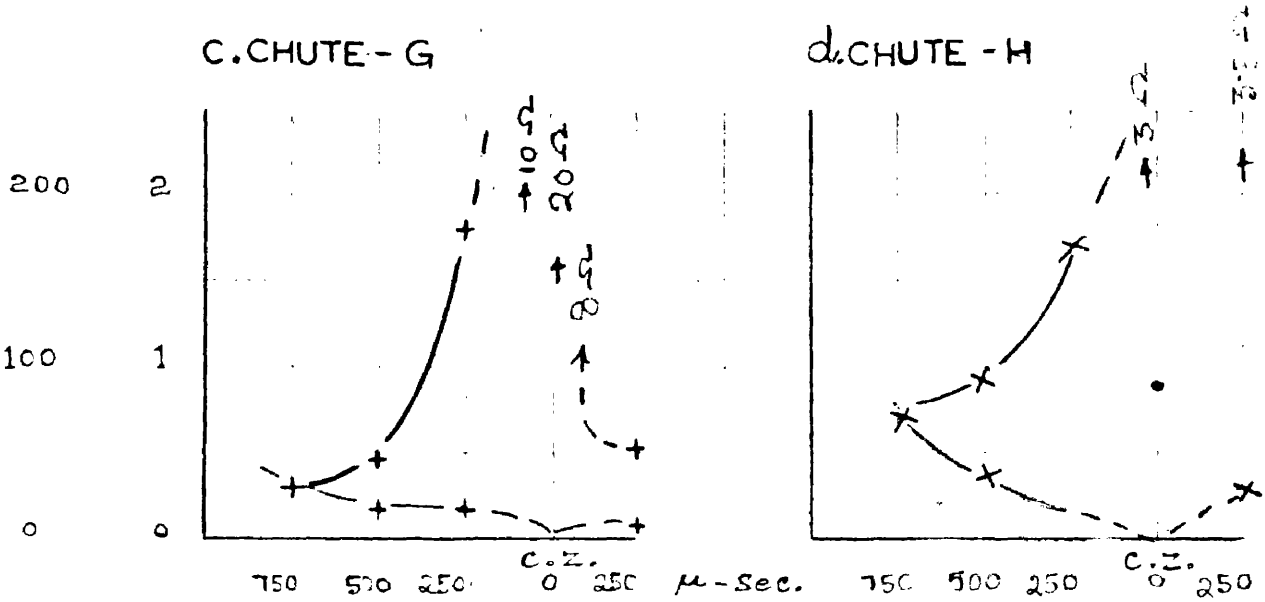

V_{10} = 1940V W_{T1} = 26%

V_{10} = 1500V W_{T1} = 56%

e. CHUTE-I

f. PLAIN ELECTRODES

FIGS. 19.
a-f

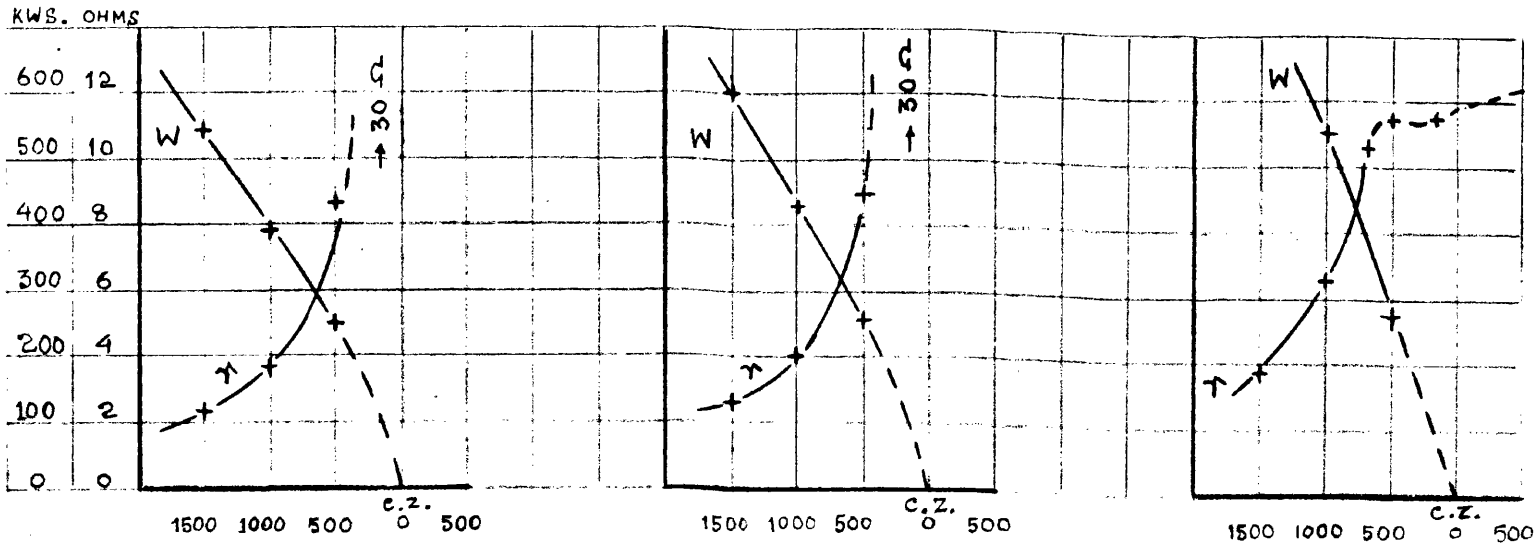

V_C (max) = 4400V
I_L (max) = 1000A.

V_{10} = 2530V, W_{T1} = 68%

a. CHUTE-M

V_{10} = 2430V, W_{T1} = 71%

b. CHUTE-N

V_{10} = 2000V, W_{T1} = 80%

c. CHUTE-O

Blow-out Field 670 lines/cm²

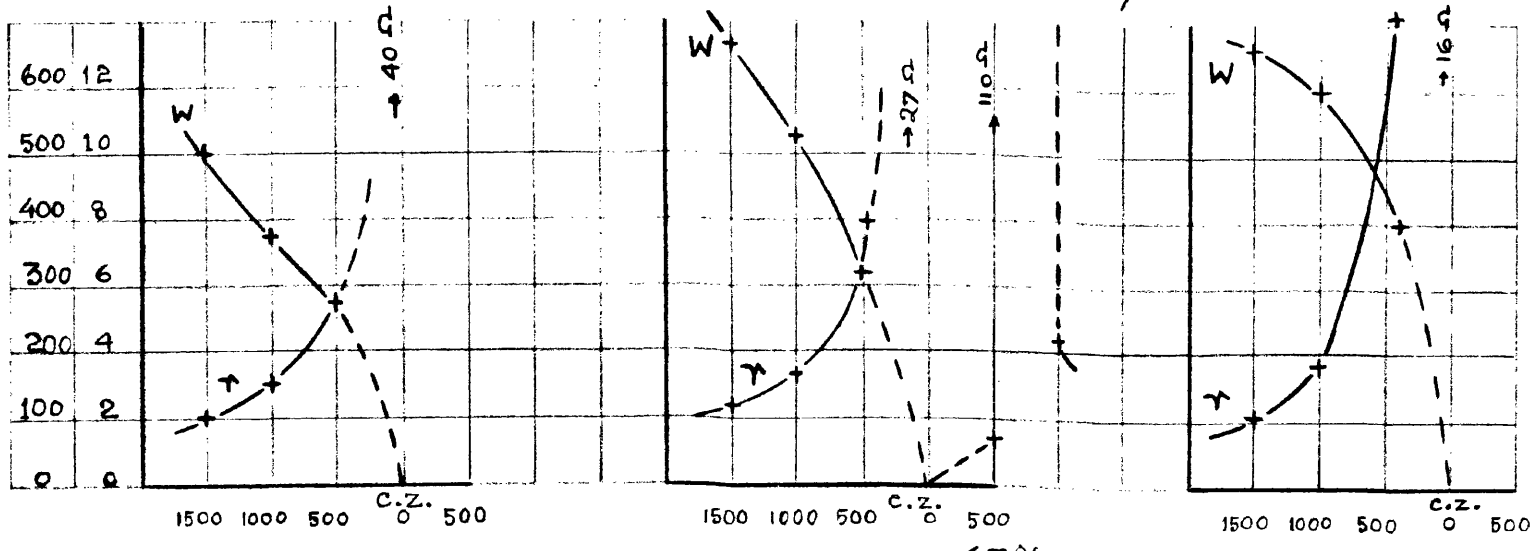

V_{10} = 2850V, W_{T1} = 55%

d. CHUTE-M

V_{10} = 2740V, W_{T1} = 63%

e. CHUTE-N

V_{10} = 2220V, W_{T1} = 75%

f. CHUTE-O

Blow-out Field 470 lines/cm²

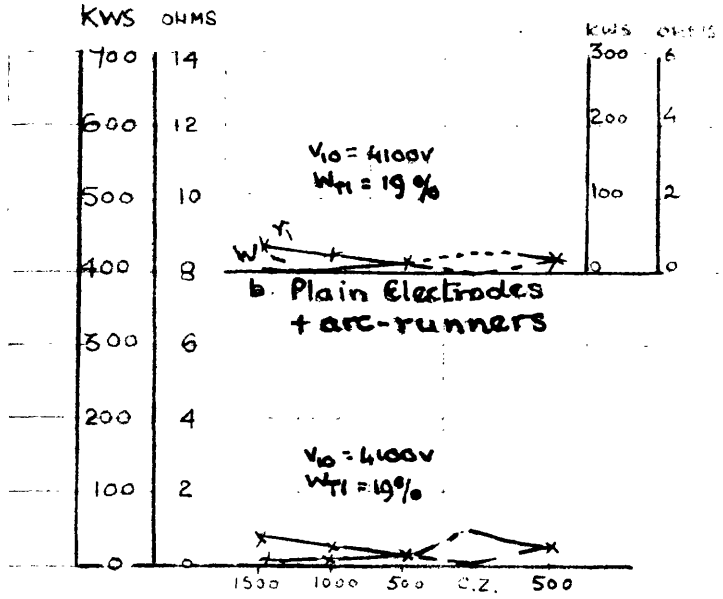

a. Plain electrodes.

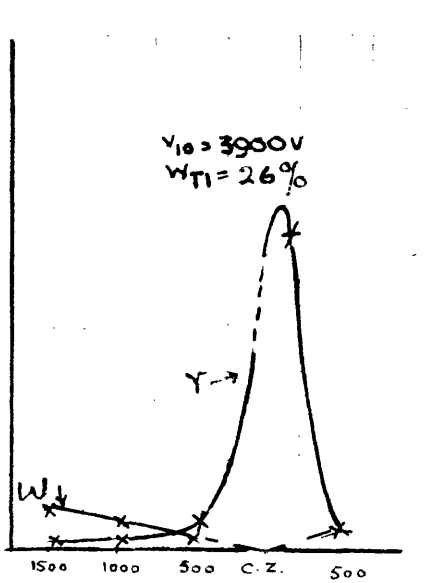

c. Chute M with arc-runners.

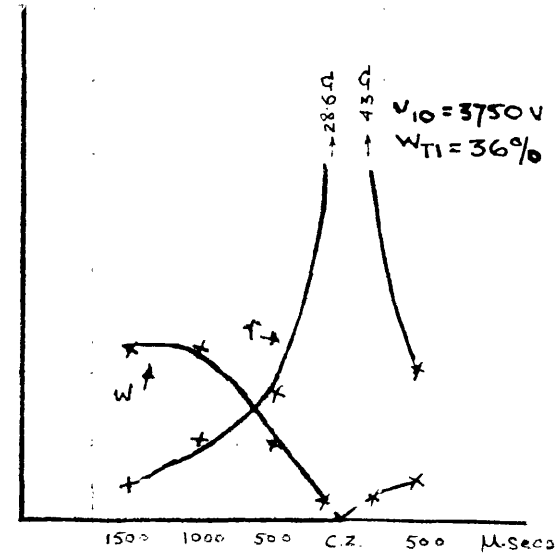

d. Chute M + arc-runners + 3 arc-barriers.

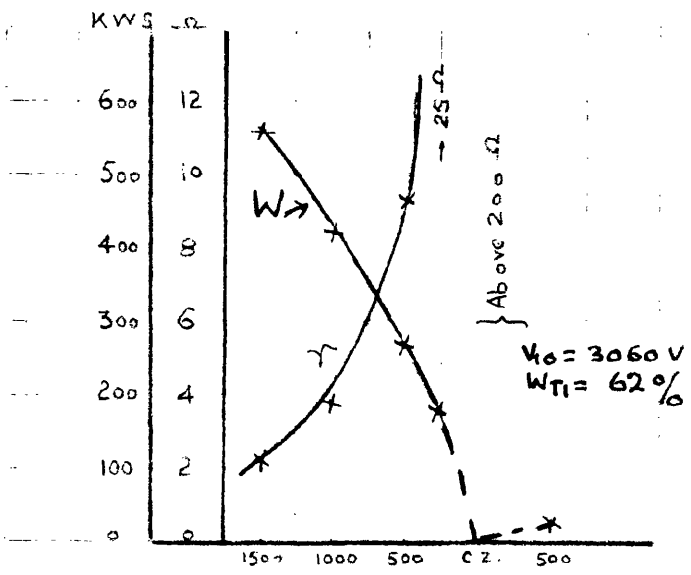

e. Chute M + arc-runners + 3 arc-barriers + d.c. blow-out field - 270 lines/cm^2.

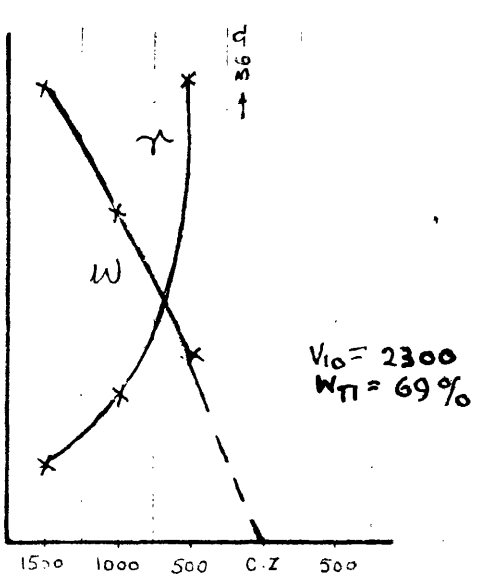

f. Chute M + arc-runners + 3 arc-barriers + d.c. blow-out field - 510 lines/cm^2.

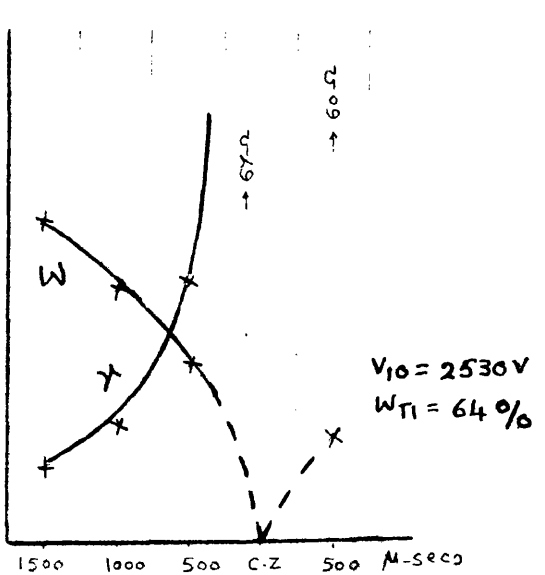

g. Chute M + arc-runners + 7 arc-barriers + d.c. blow-out field - 510 lines/cm^2.

FIGS 20a-g: Showing variation of arc-resistance and instantaneous energy

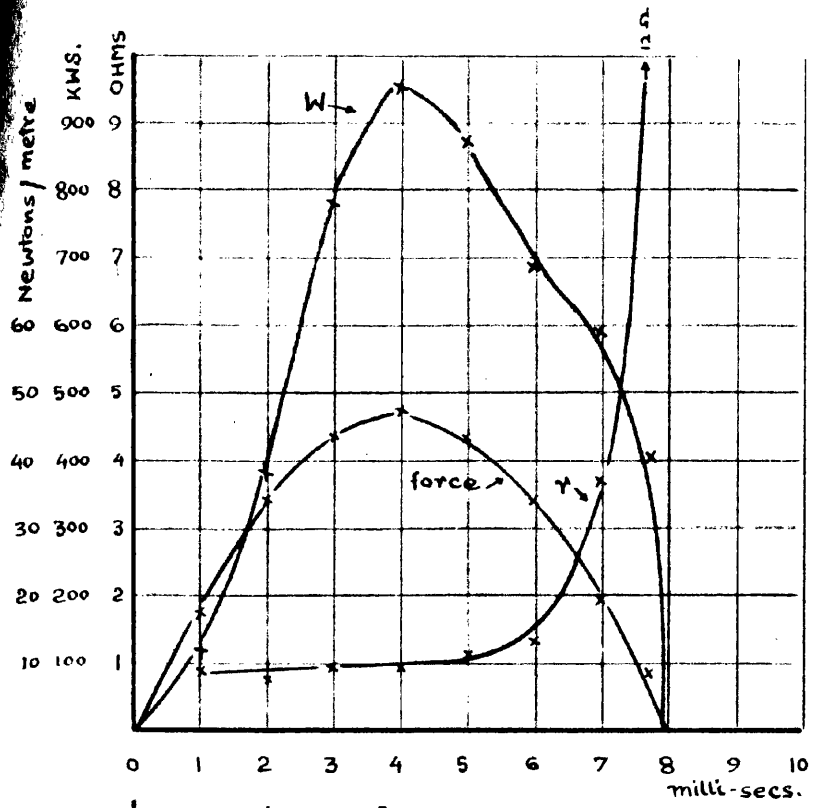

b . 470 lines/cm². ; V_{IO} = 2400 V ; W_{TI} = 75 %

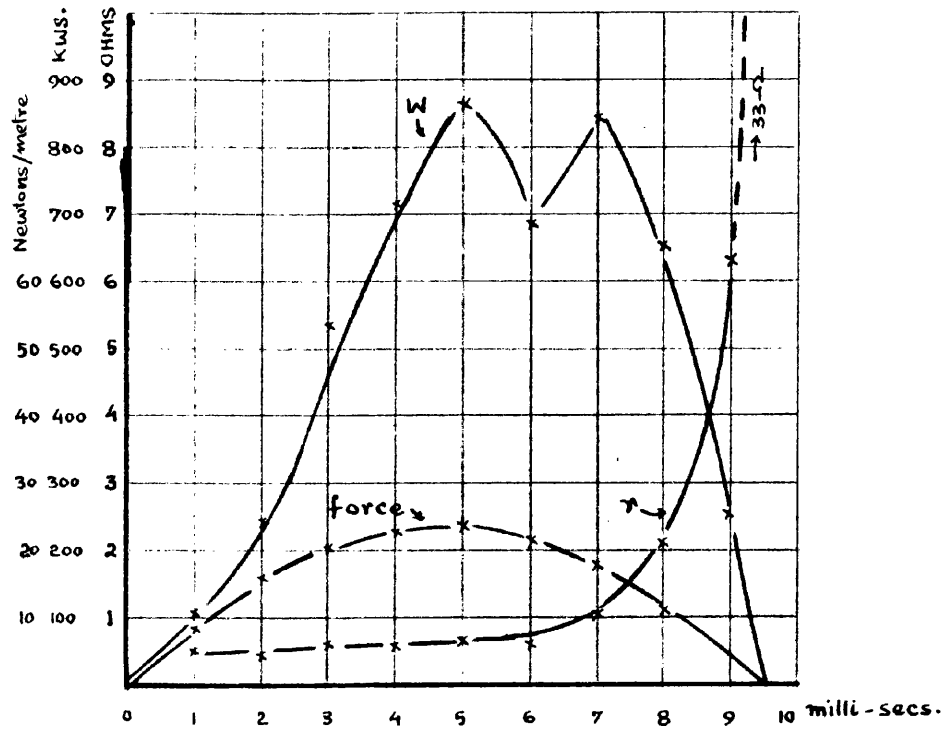

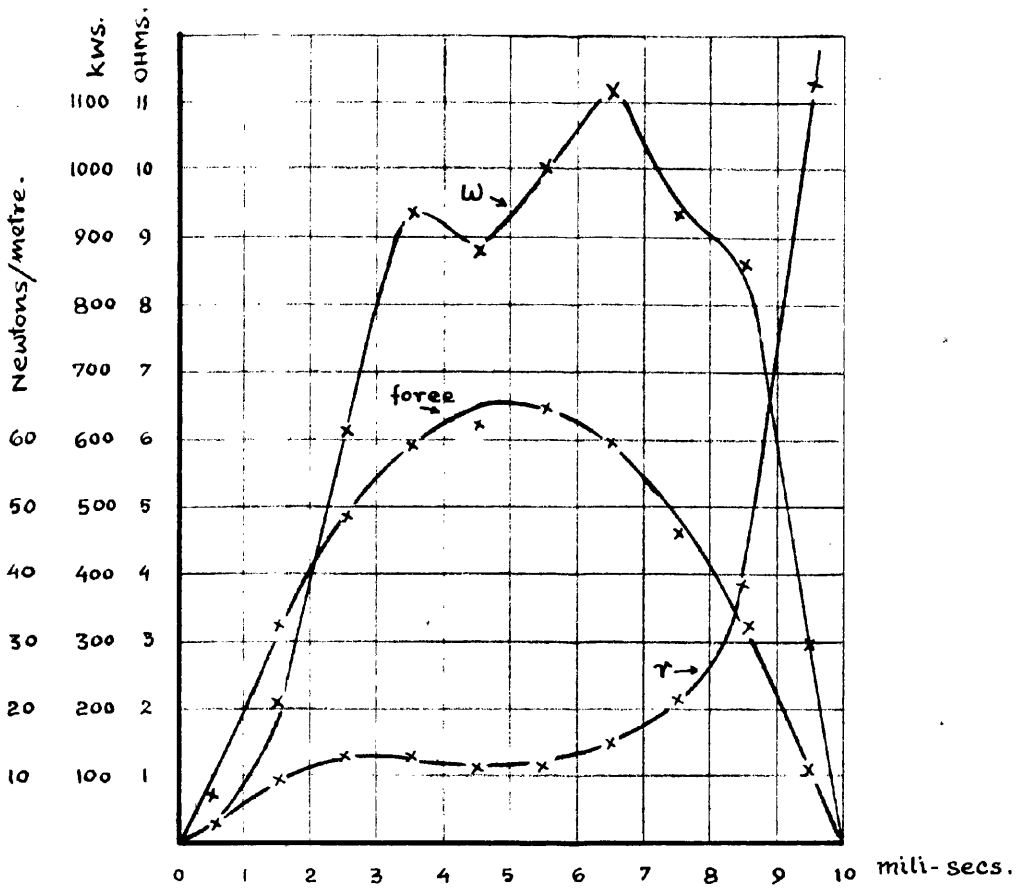

C . 670 lines/cm². ; V_{IO} = 2100 V ; W_{TI} = 80 %

FIGS. 21 a-c : Showing variation of arc resistance, instantaneous energy input, and blow-out force over the first half-cycle for Chute O with d.c. blow-out field.

Initial conditions: Gap = 1" ; 7 arc-barriers ; V_c (max) = 4400
I_L (max.) = 1000 Amps.

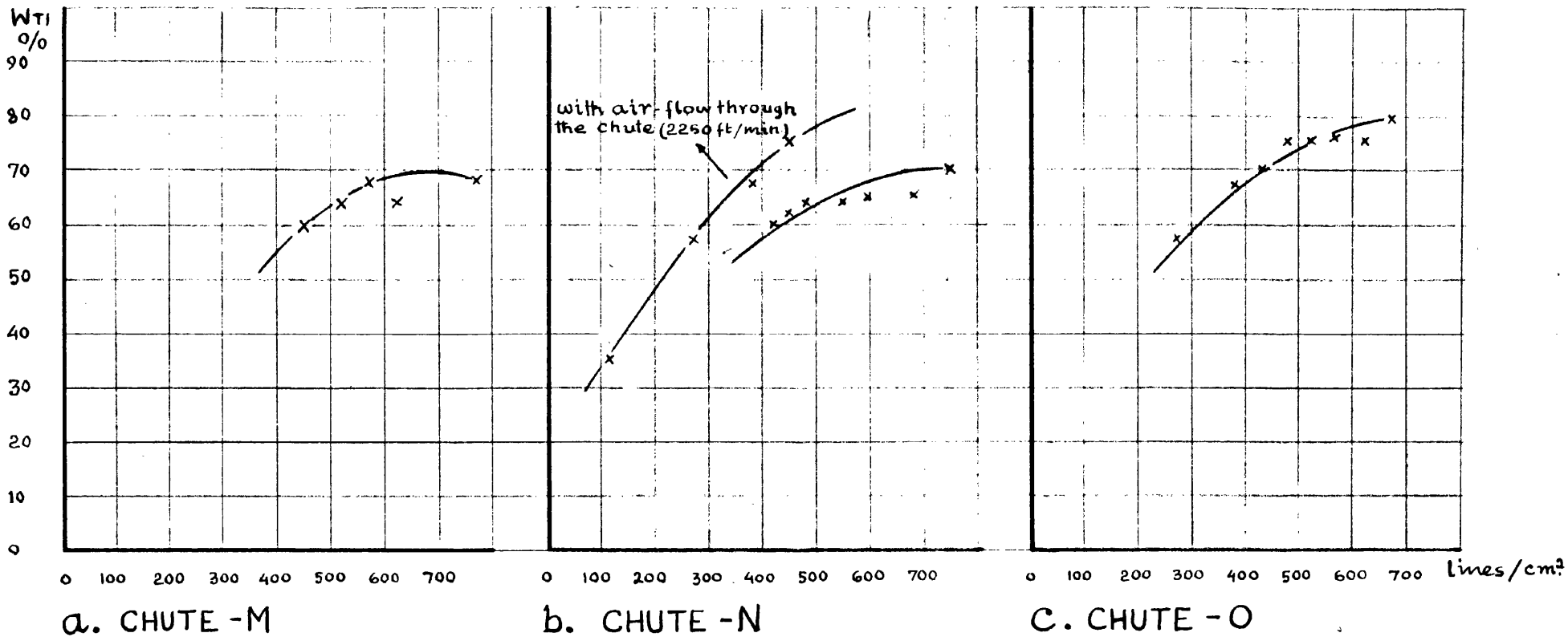

FIGS. 22 a-c : Showing variation of W_{TI} with d.c. blow-out field.

Initial conditions: Gap=1"; 7- arc barriers; V_c (max.) = 4400 V; I_L (max) = 1000 Amps..

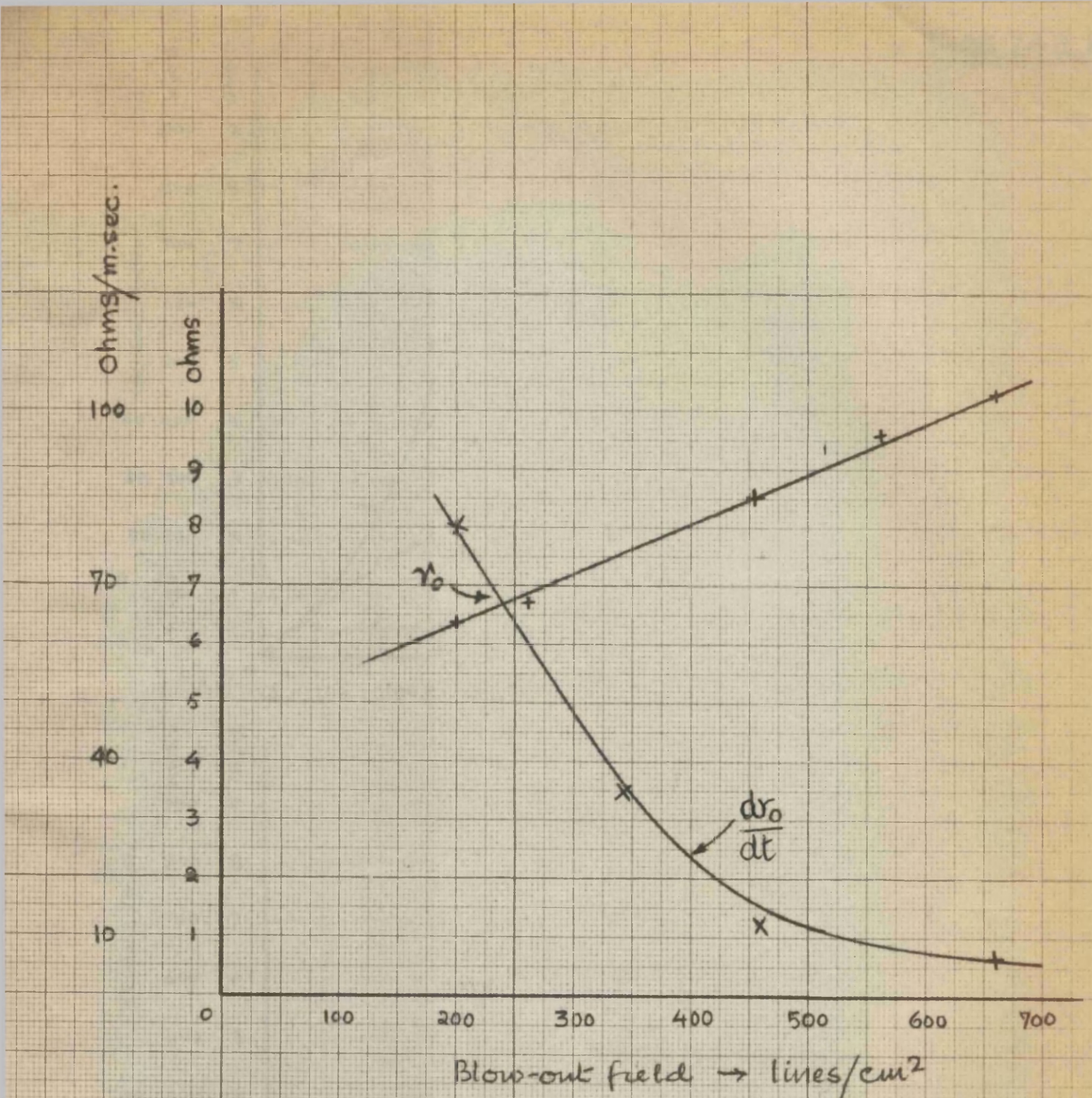

Fig. 23- Showing variation of r_o and dr_o/dt. with a.c. blow-out field.
(Chute O)

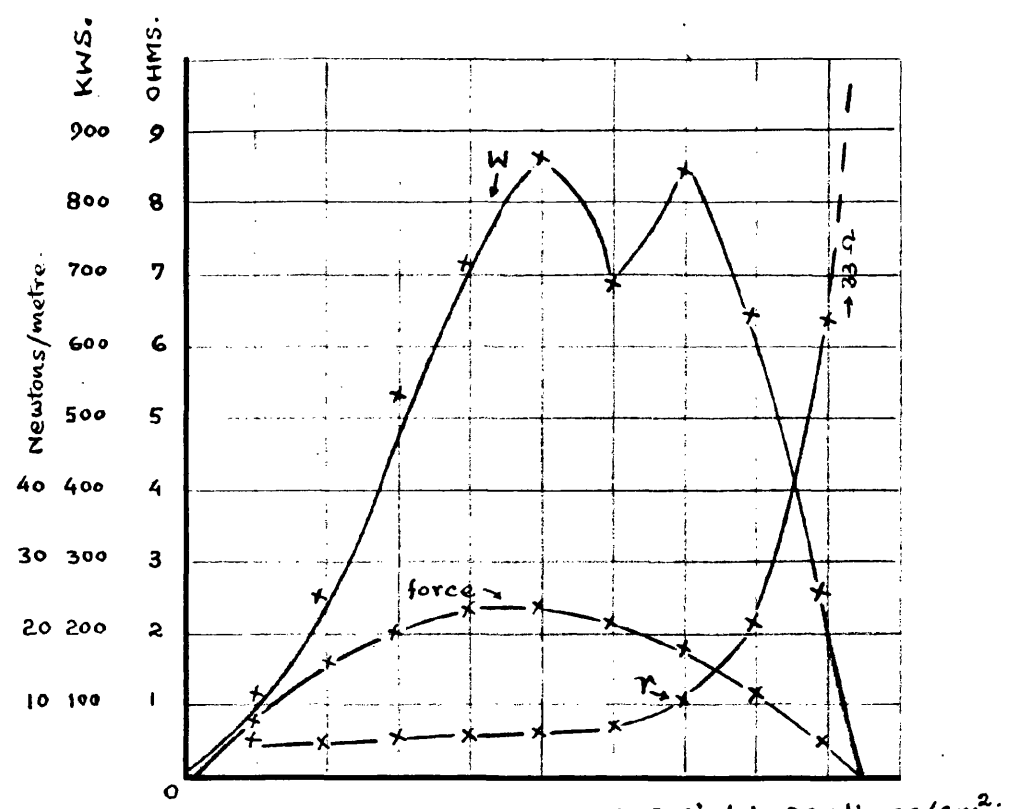

a. $V_{10} = 3100$ V ; $W_{T1} = 66\%$; d.C. field - 200 lines/cm^2.

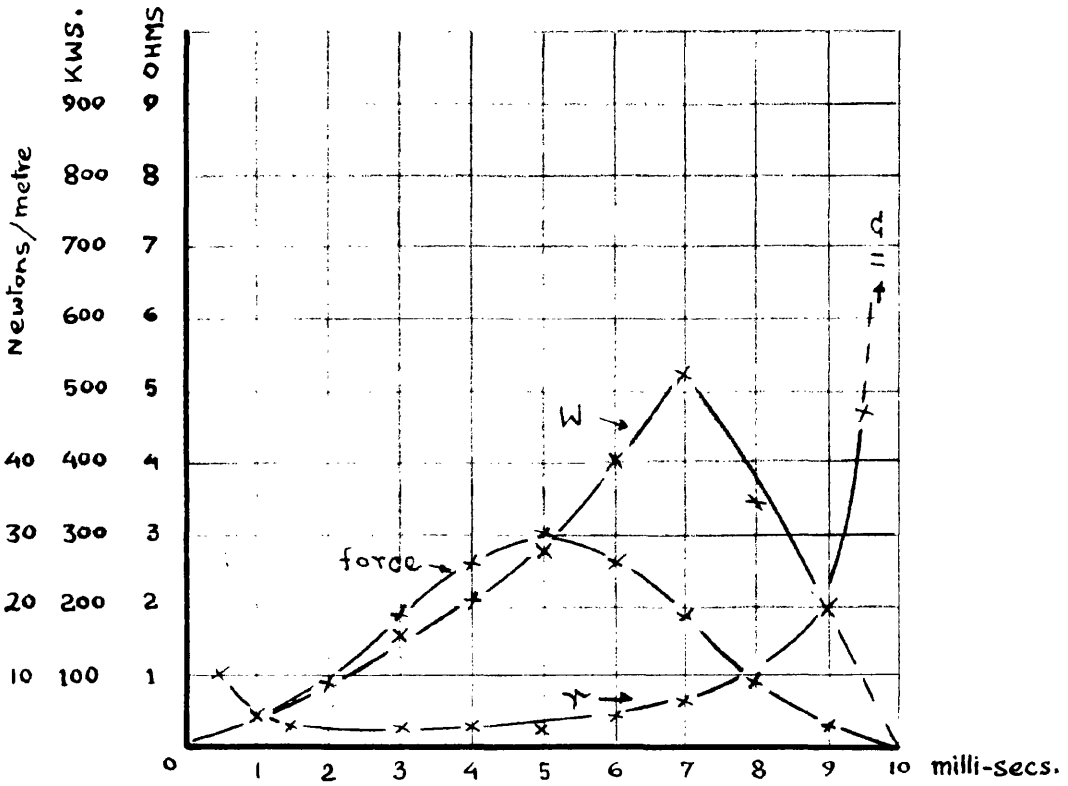

FIGS. 24 a,b: Shows the first half-cycle for experiments using d.c. and a.c. (in phase) blow-out fields with Chute N, using 7 arc-barriers.

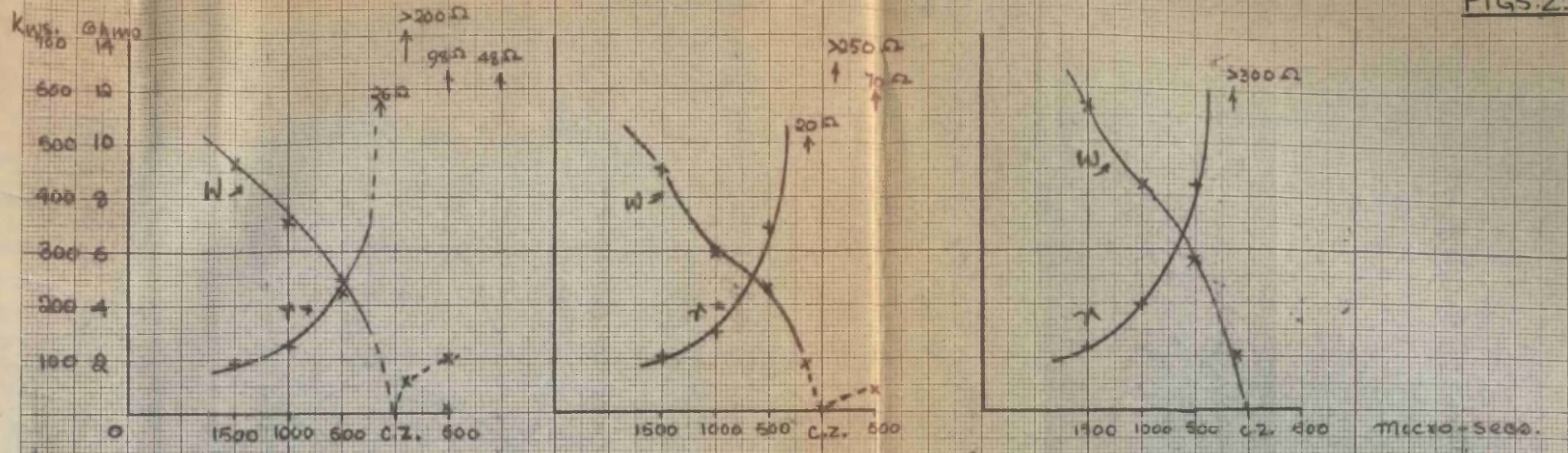

a. In phase, V_{10} = 2850V, W_{T1} = 57% b. 10° lag, V_{10} = 2640V, W_{T1} = 63% c. 25° lag, V_{10} = 2950V, W_{T1} = 51%

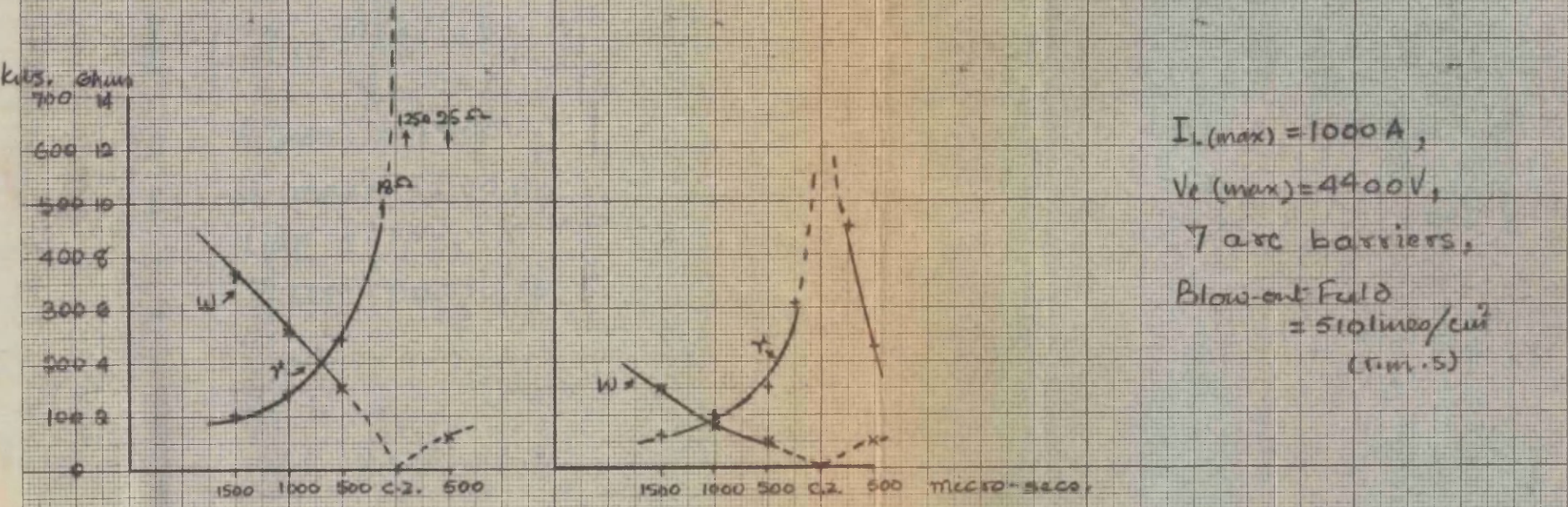

d. 8° lead, V_{10} = 2740V, 60%. e. 25° lead, V_{10} = 2640V, W_{T1} = 63%

$I_{L(max)}$ = 1000 A,
V_t (max) = 4400V,
7 arc barriers,
Blow-out Field
= 510 lines/cm²
(r.m.s.)

Figs. 25 a-e. – Chute M: Showing the variations of ω and r, towards the end of the First half-cycle of arcing.

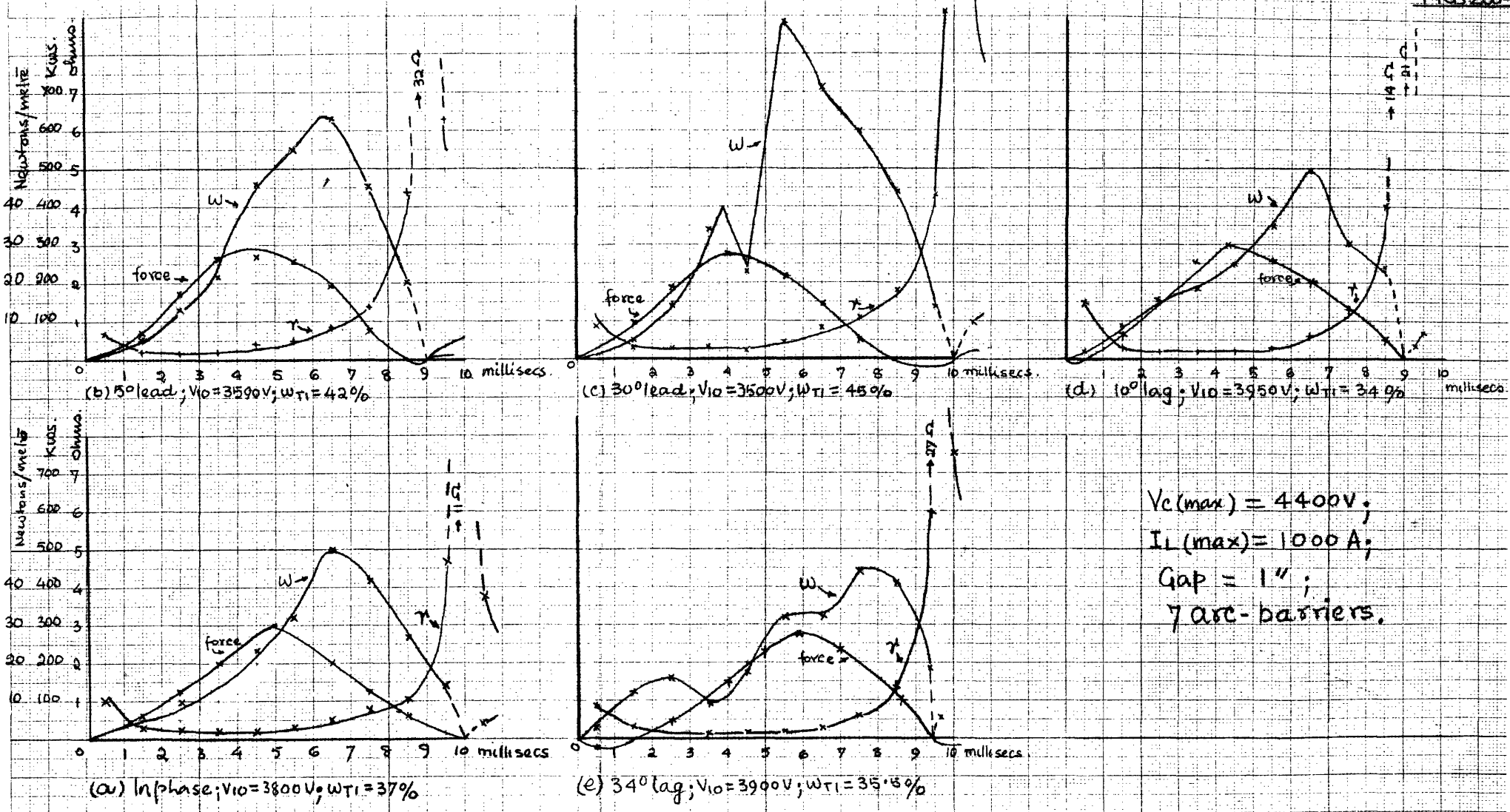

FIGS. 26a to e. Showing variation of arc resistance, energy input and blow-out force over the first half-cycle for Chute N, a.c. blow-out field – 268 lines/cm² (max.)

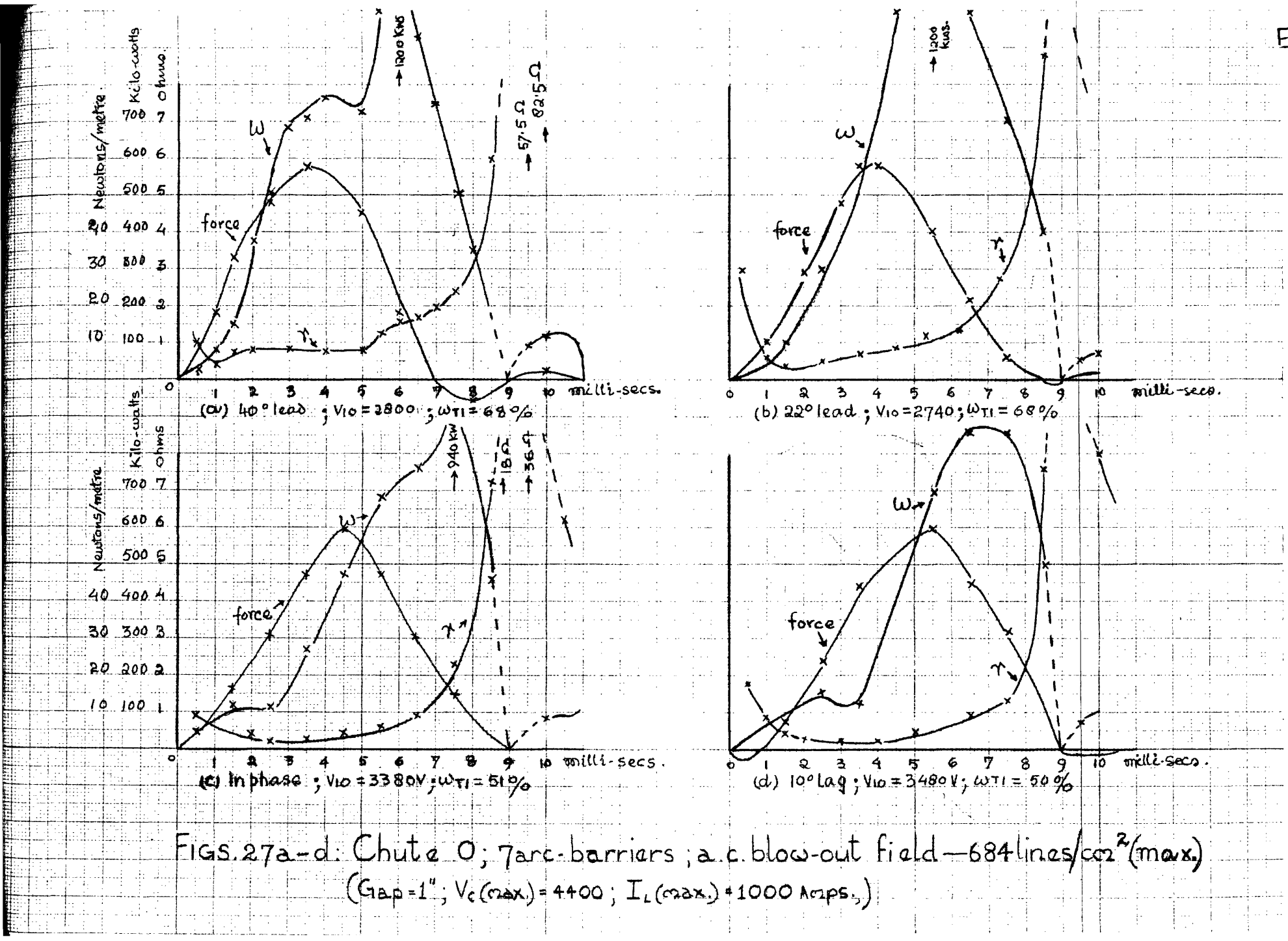

FIGS. 27a-d: Chute 0; 7 arc-barriers; a.c. blow-out field — 684 lines/cm² (max.)
(Gap = 1"; V_c (max.) = 4400; I_L (max.) = 1000 Amps.)

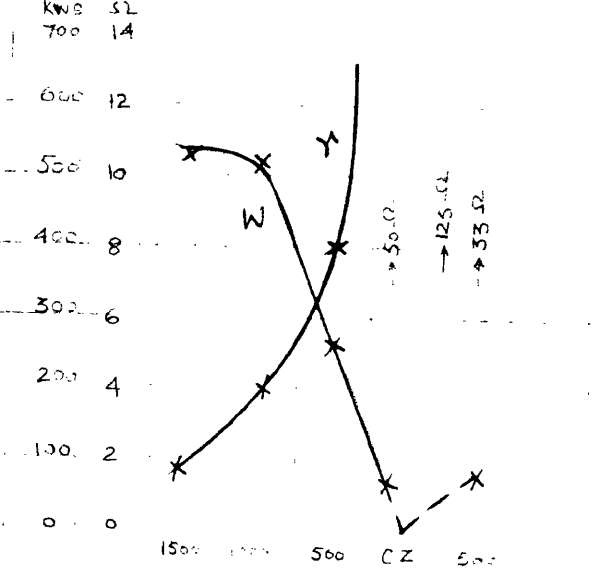

e. In phase
V_{10} = 3300v; W_{T1} = 40%

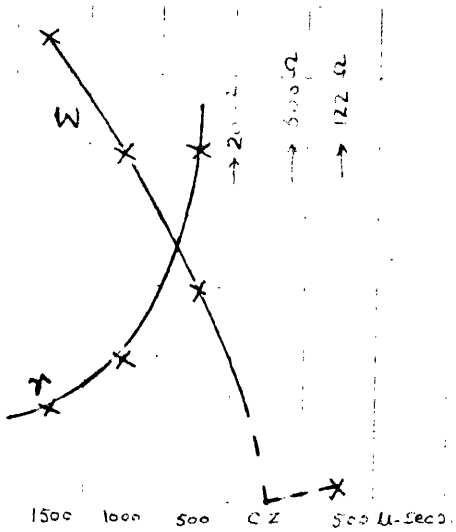

f. 13° lag
V_{10} = 2850v; W_{T1} = 56%

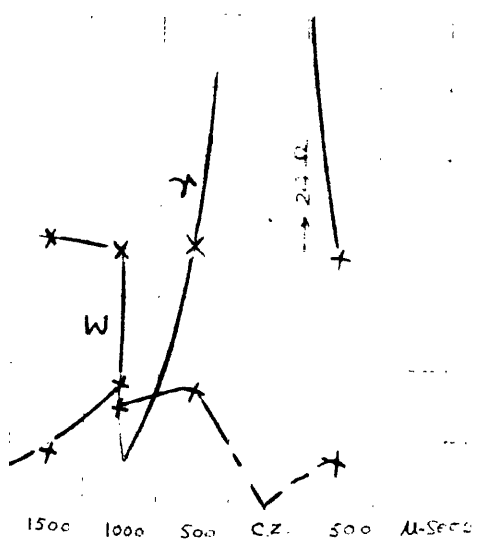

g. 33° lag
V_{10} = 3500v; W_{T1} = 35%

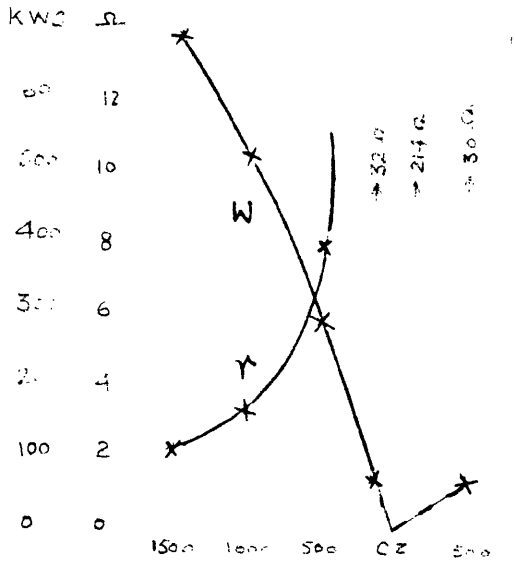

h. 12° lead
V_{10} = 3160v; W_{T1} = 55°

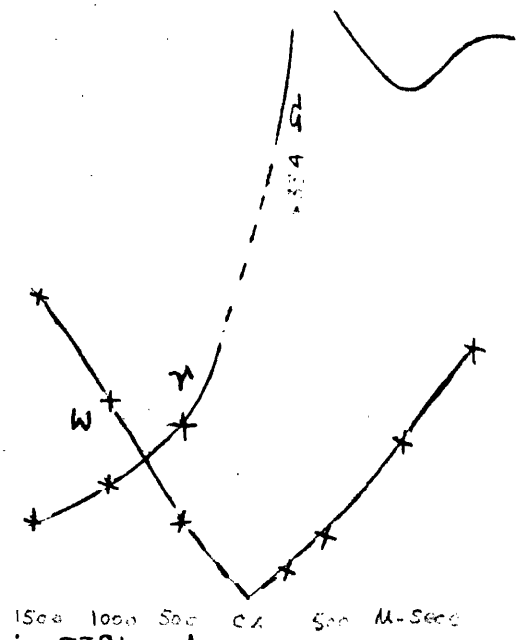

i. 33° lead
V_{10} = 3060; W_{T1} = 60%

FIG. 27 e-i: Chute O; 7 arc-barriers; a.c. blow-out field - 510 lines/cm² (r.m.s)

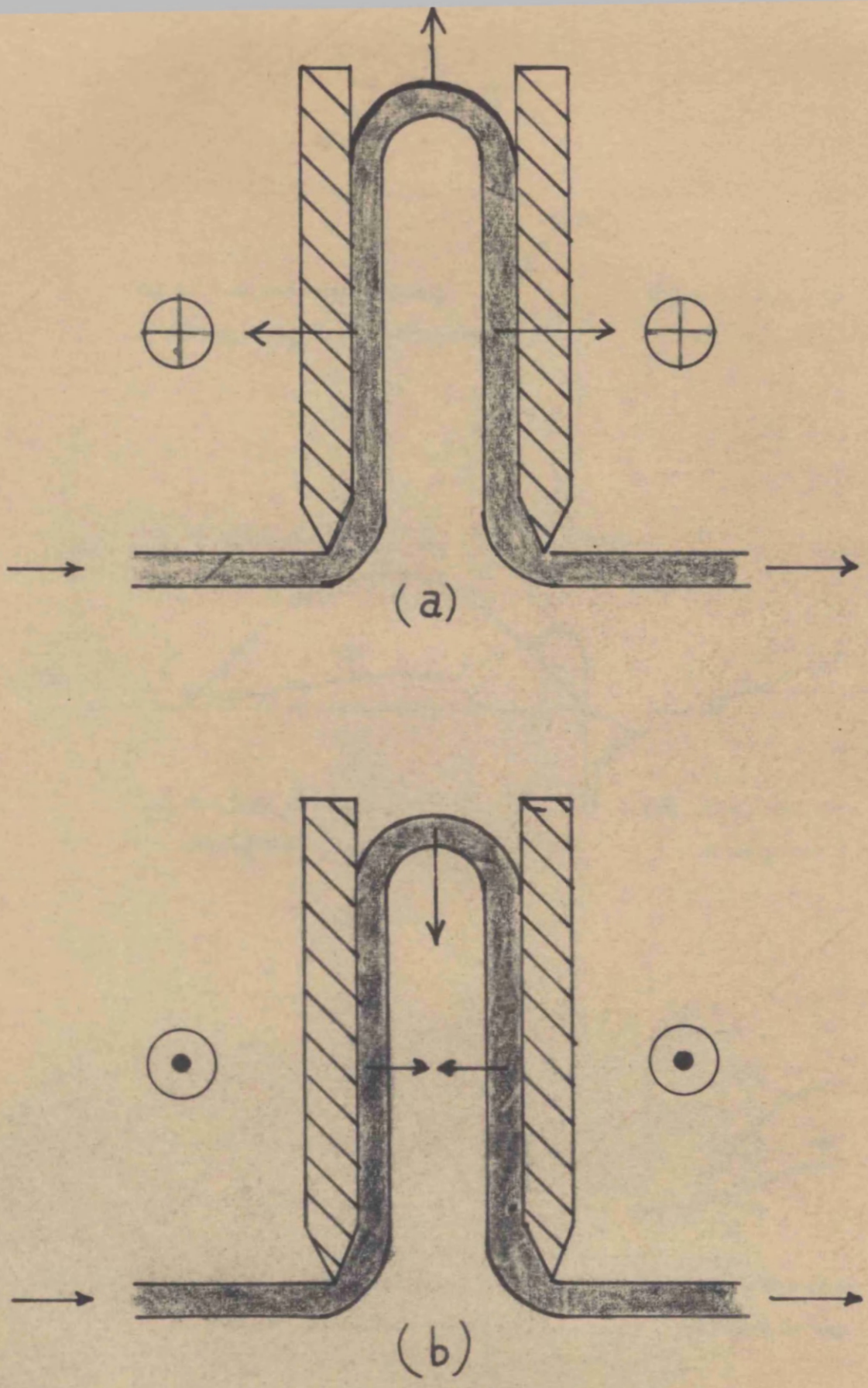

Fig. 28. Magnetic Blow-out force on an Arc Between Refractory Plates.

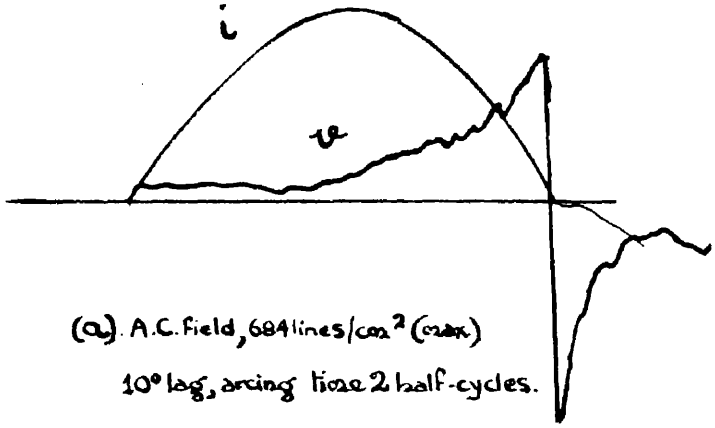

(a). A.C. field, 684 lines/cm² (max)
10° lag, arcing time 2 half-cycles.

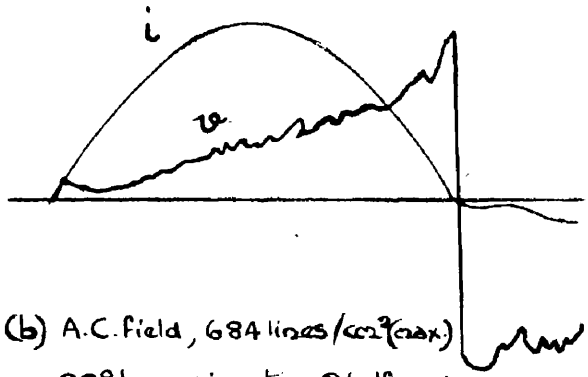

(b) A.C. field, 684 lines/cm² (max.)
22° lag, arcing time 2 half-cycles.

(c) D.C. field, 276 lines/cm²
arcing time 3 half-cycles.

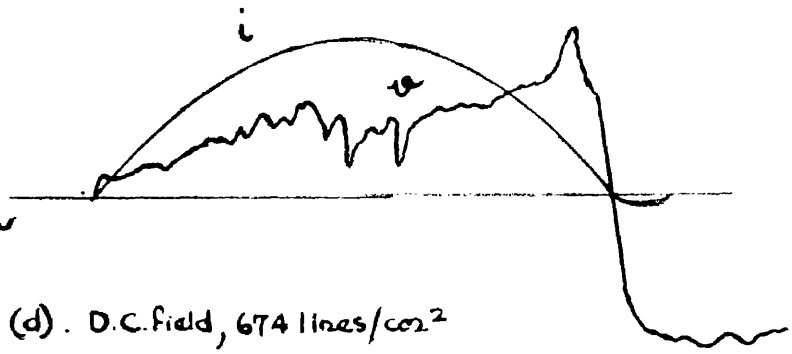

(d). D.C. field, 674 lines/cm²
arcing time 1 half-cycle.

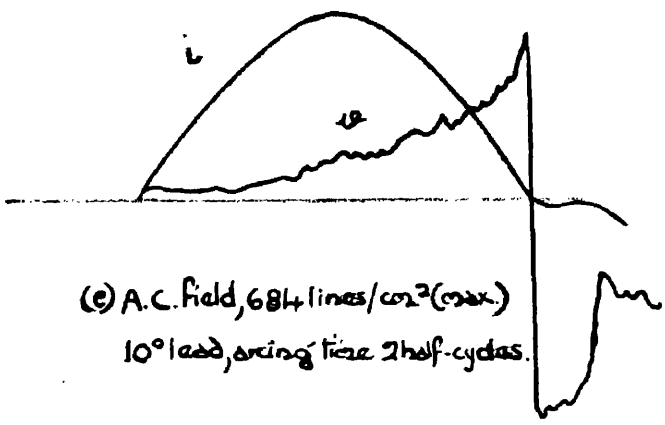

(e) A.C. field, 684 lines/cm² (max.)
10° lead, arcing time 2 half-cycles.

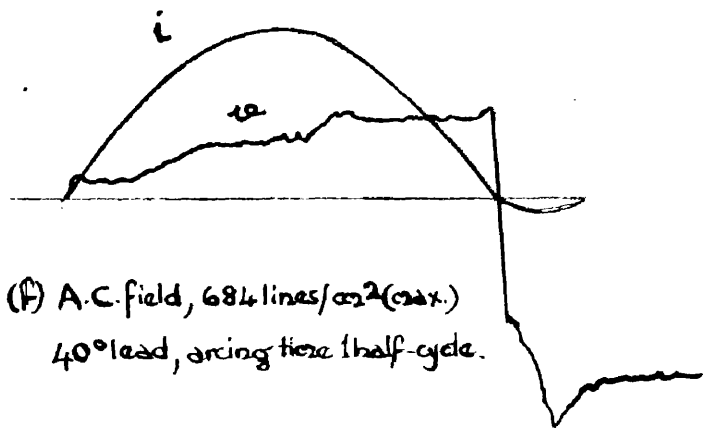

(f) A.C. field, 684 lines/cm² (max.)
40° lead, arcing time 1 half-cycle.

FIGS. 29 a to f. Tracings from typical oscillograms showing the first half-cycle of arcing with Chute O, 7 barriers.

(500 Amps ≡ 1 cm ≡ 1330 volts; time-scale is different for each test.)

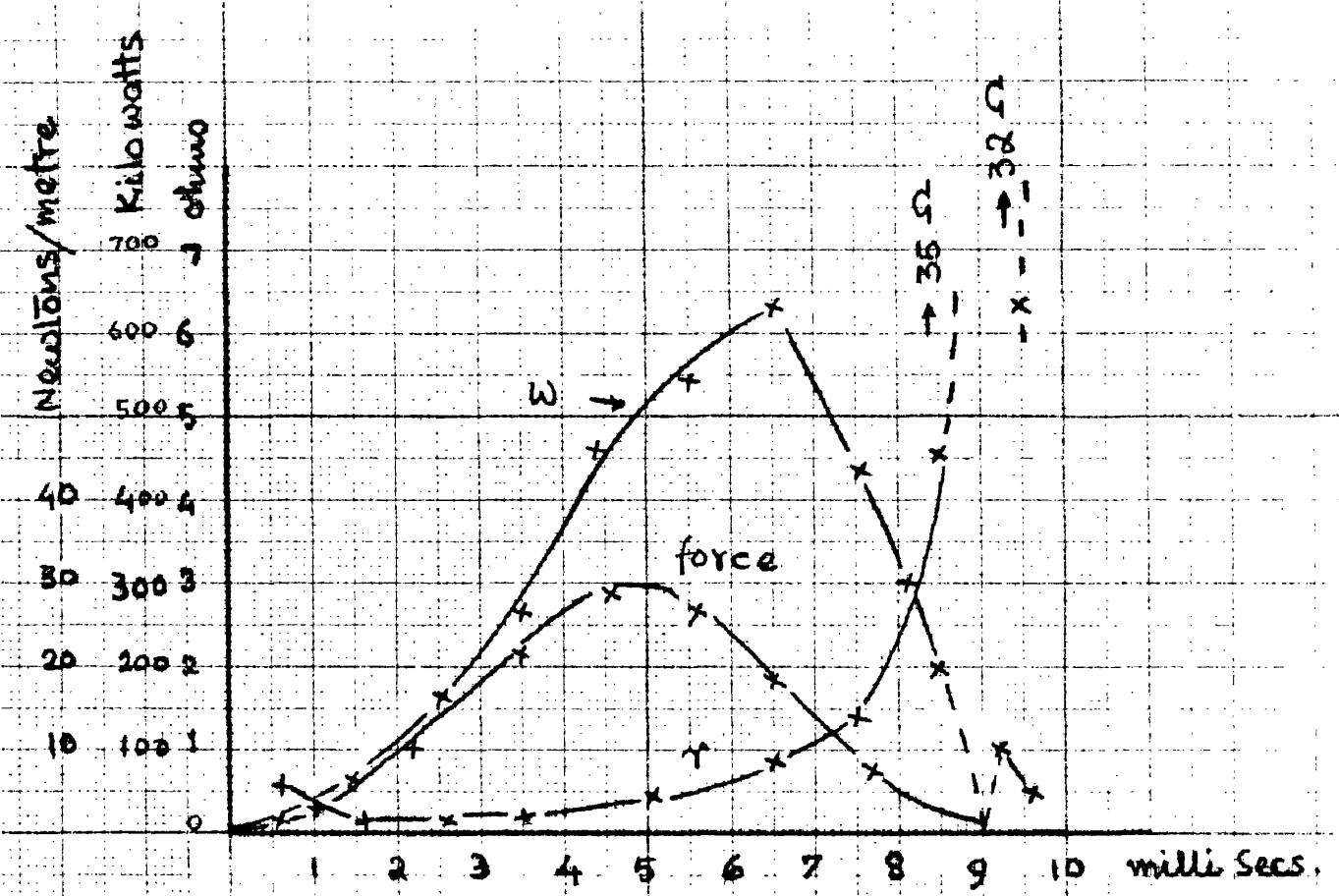

(a) $V_{IO} = 3590$ V; $W_{TI} = 42\%$

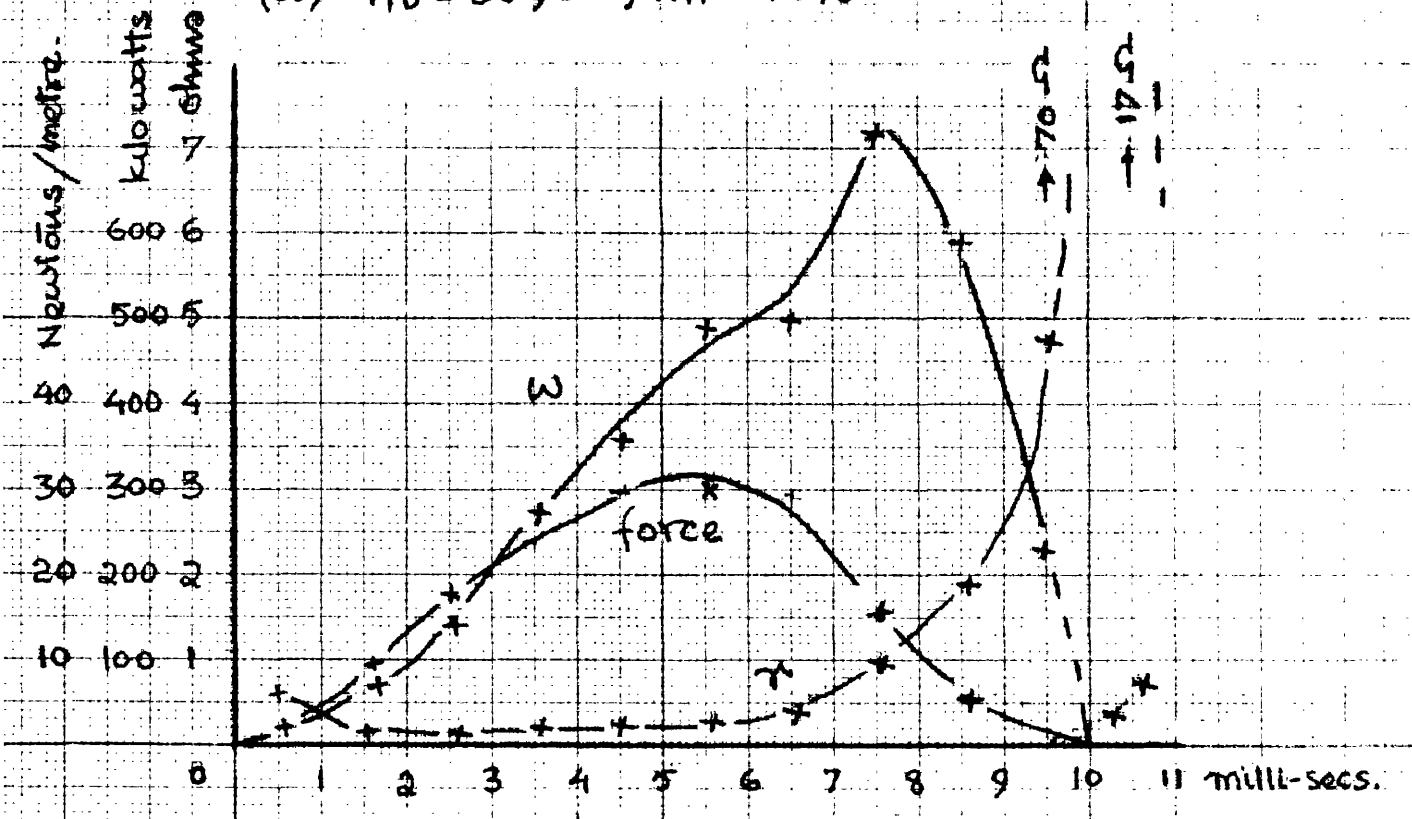

(b) $V_{IO} = 3610$V; $W_{TI} = 39\%$; air flow 2250 ft/min.

Fig. 30 a,b – Showing variation of arc resistance, energy input and out force over the first half-cycle for Chute N, with an air flow. (Gap = 1"; V_c(max) = 4400, I_L(max) 1000 Amps., 7 barriers) a.c. field = 26 lines/cm^2 (max.)

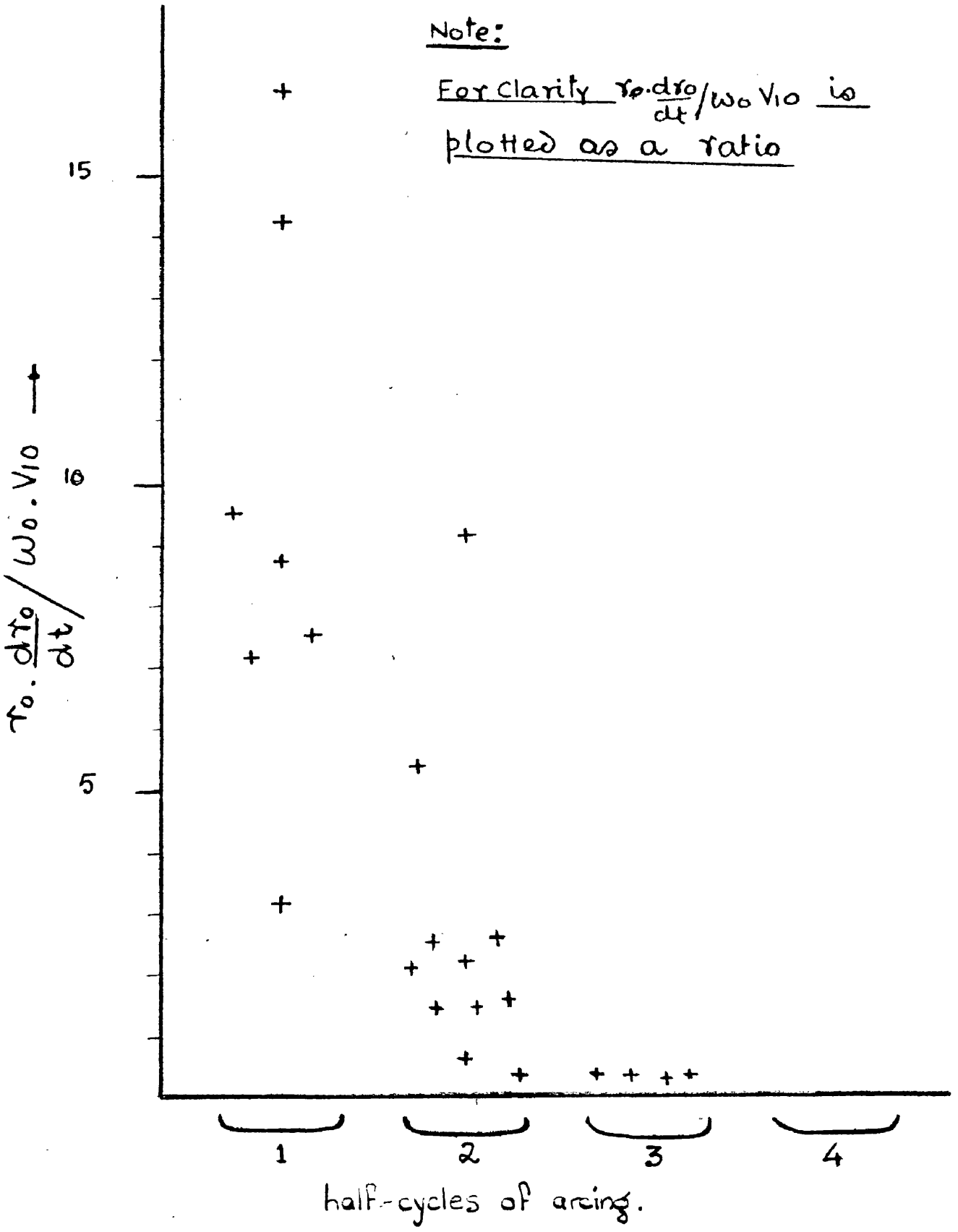

FIG.31 - Criteria of Arc Extinction.

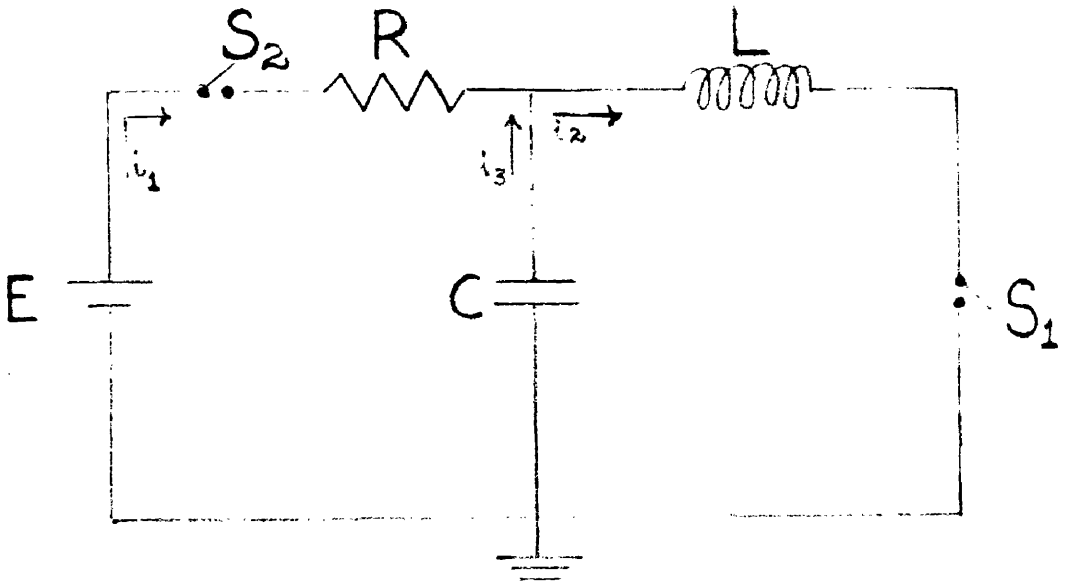

FIG. 3a

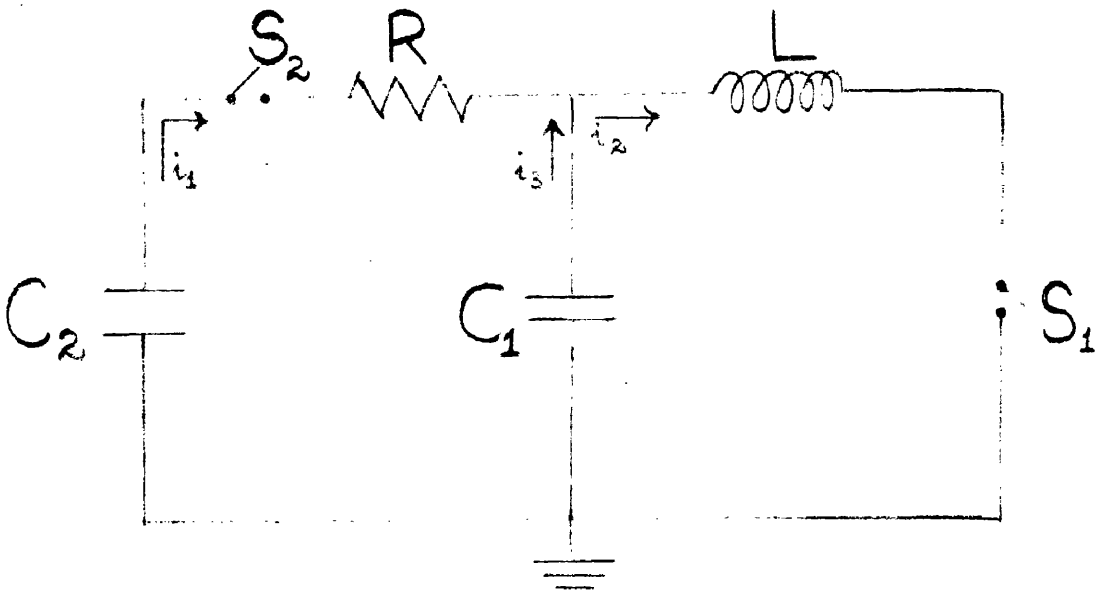

FIG. 3b.

POINT-ON-WAVE-SELECTION.

(Appendix I)

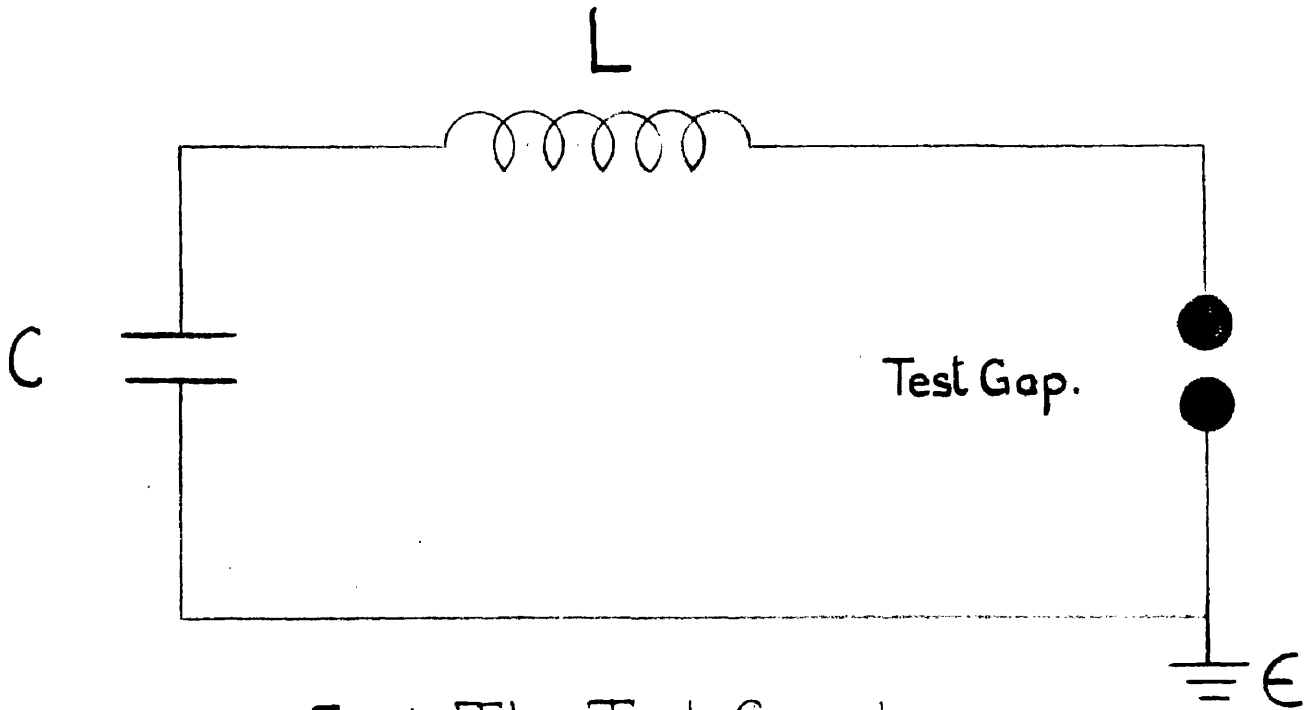

Fig.1. The Test Circuit.
(Appendix II)

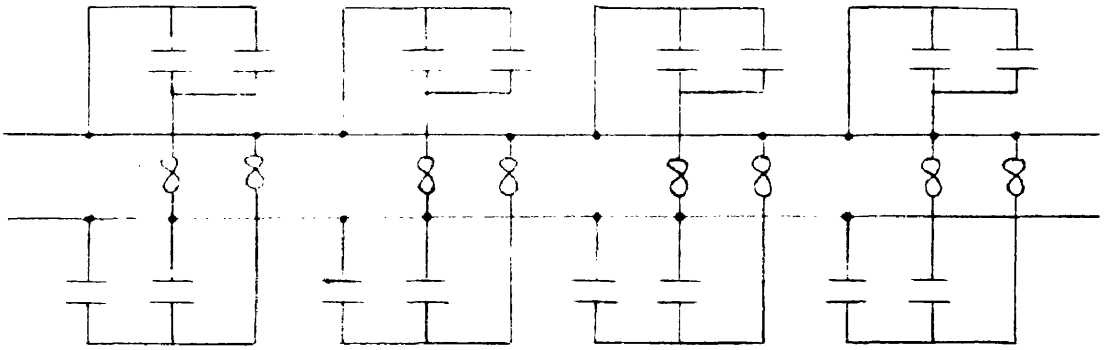

2200V ; 3000μF.

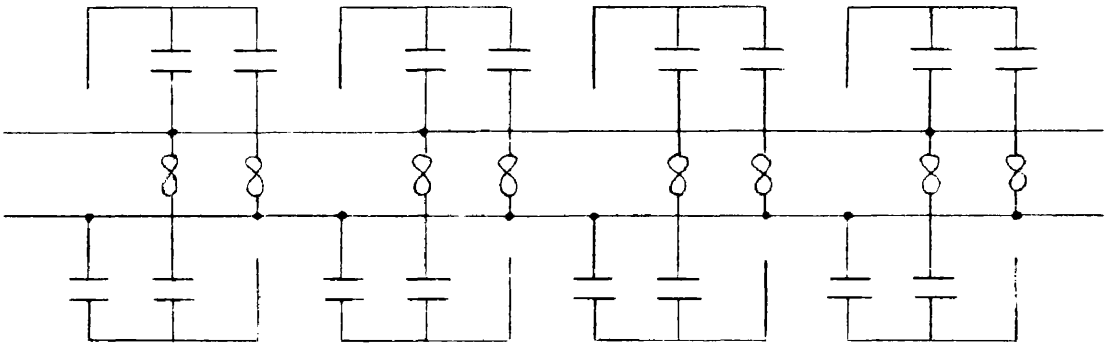

3300V ; 1250μF

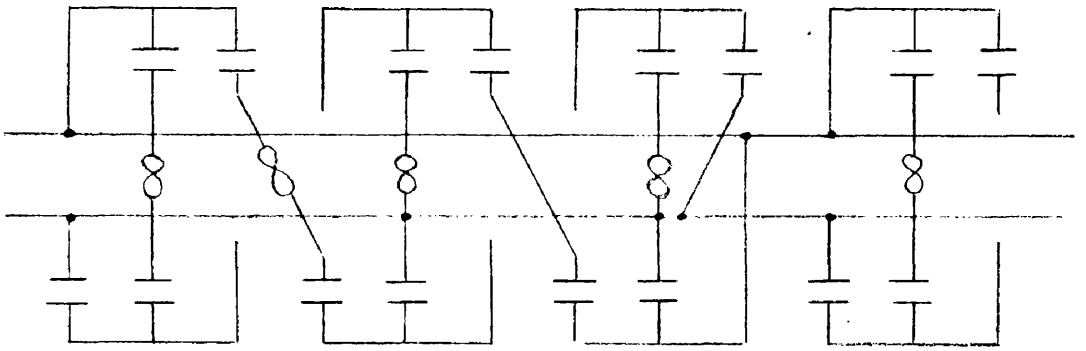

4400V ; 750μF

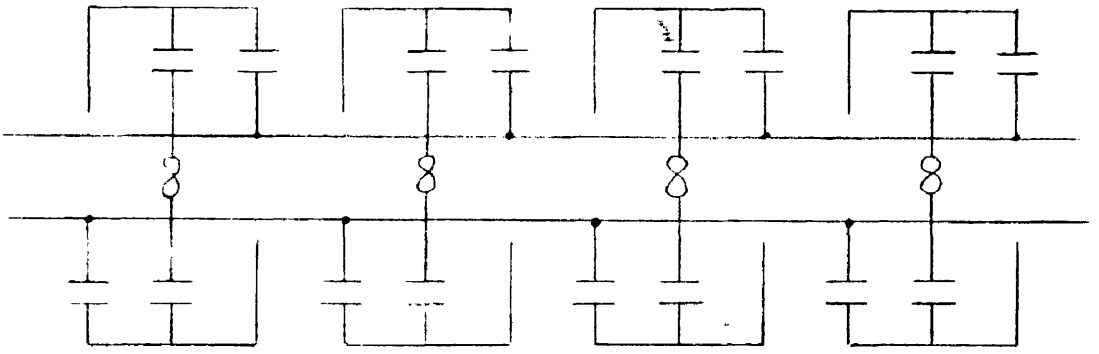

FIG. 2. Capacitor Bank.

(Appendix II.)

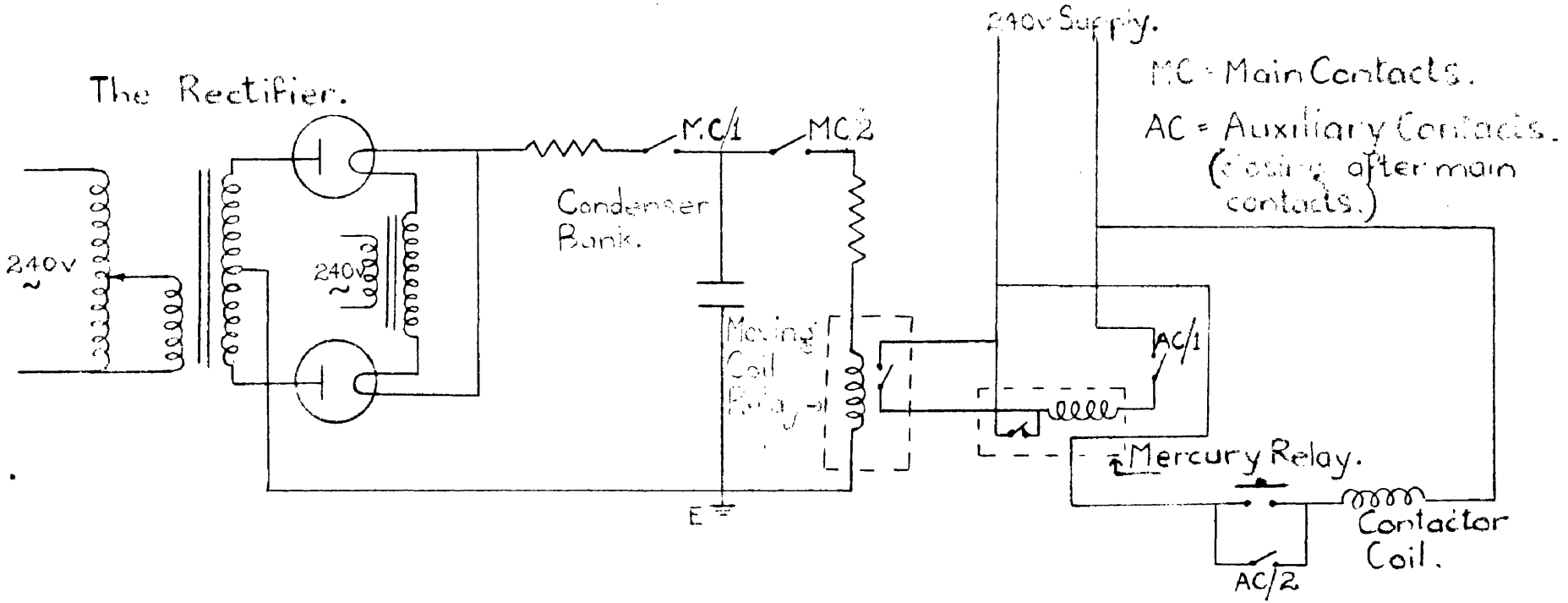

FIG.3. Charging Circuit.

(Appendix II.)

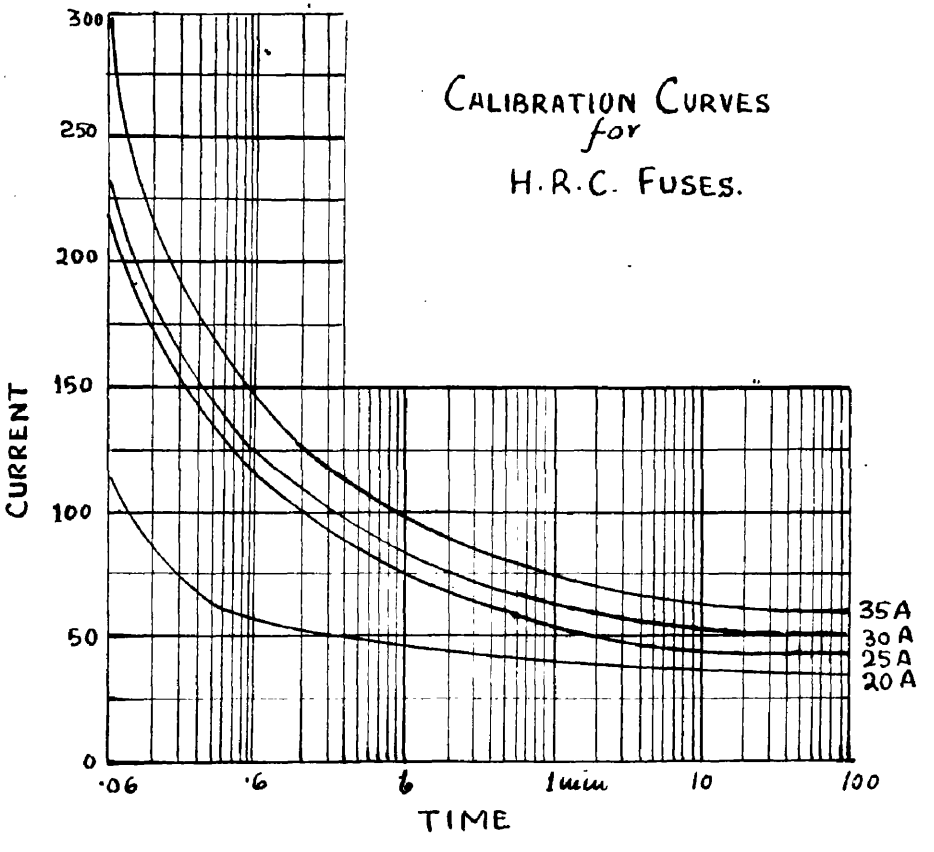

FIG. 4.
(Appendix II)

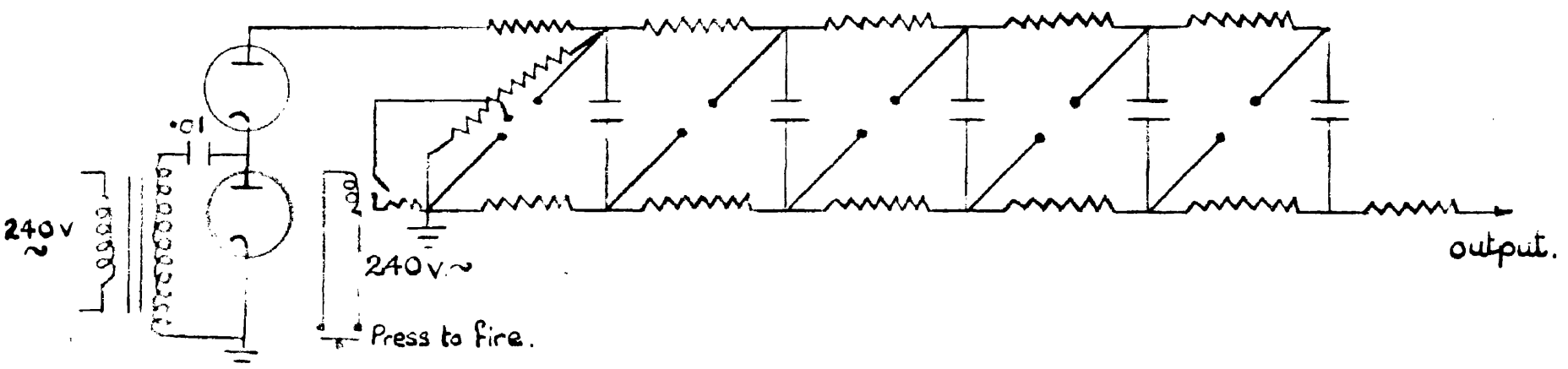

FIG.5. Impulse Generator (200 KV.)

(Appendix II.)

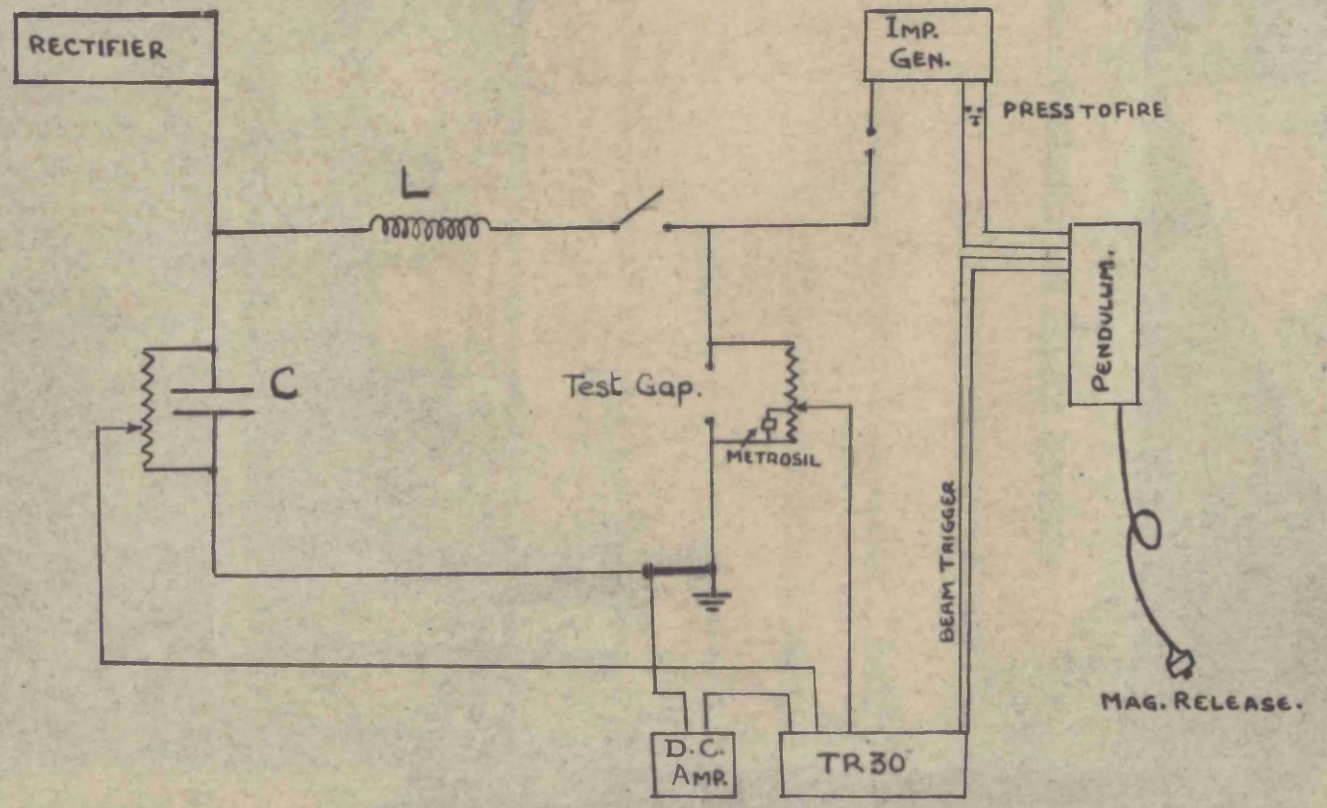

FIG. 6. Diagram of the Test Circuit.

(Appendix II.)

(Appendix II.)

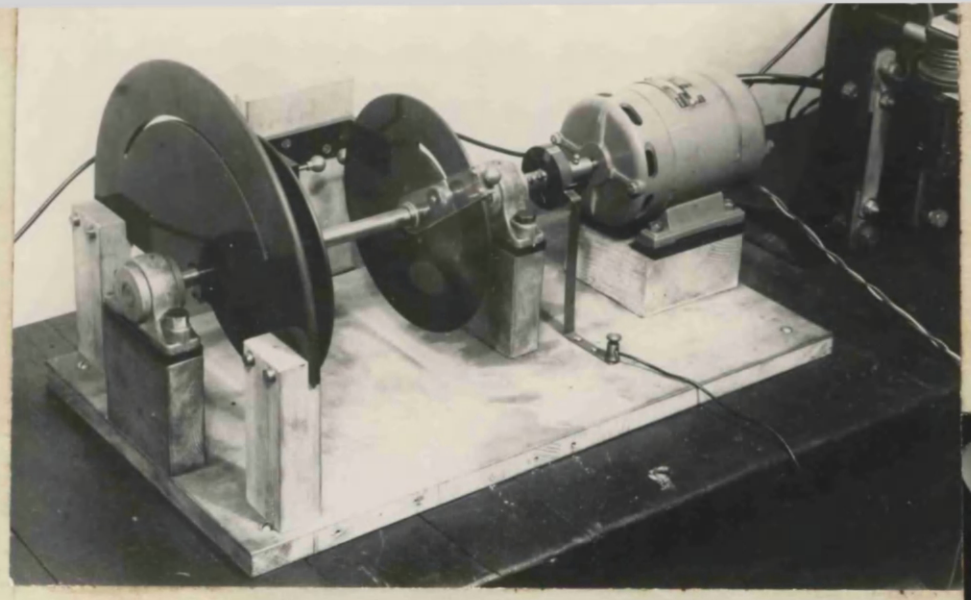

Fig 7d: The Synchronous Rotary Switch.

Fig. 7c: Transient Recorder TR 10 with camera and viewing hood ——— ——— ———→

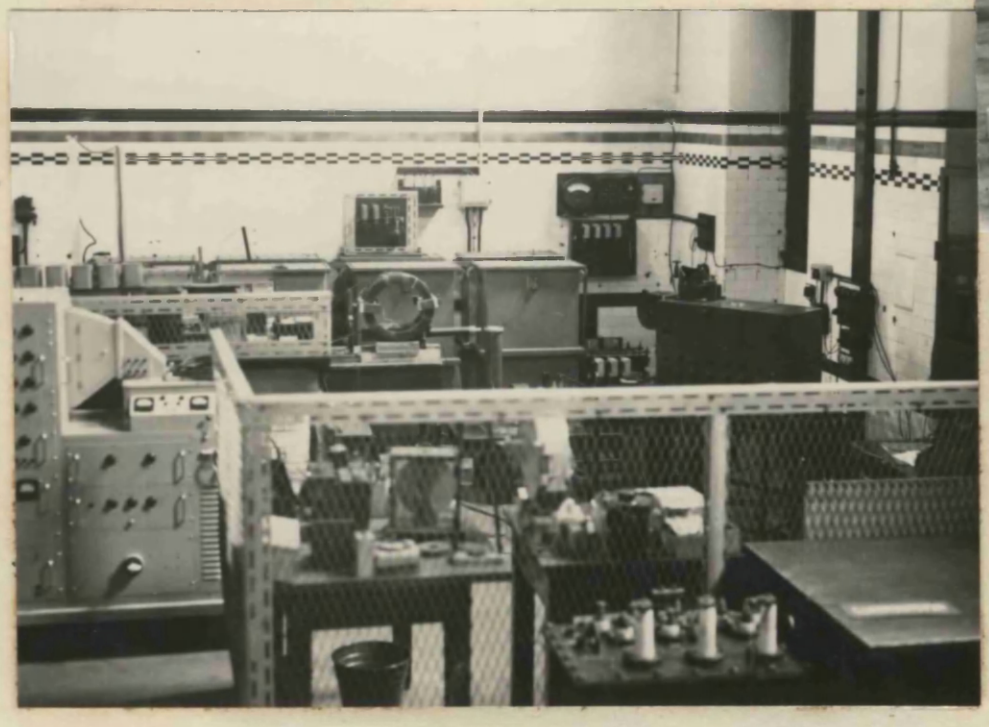

Fig. 7e: A general view showing:

(1) Capacitor Bank (2) Field coils and test gap.

(3) TR. 30 (4) Dudell oscillograph.

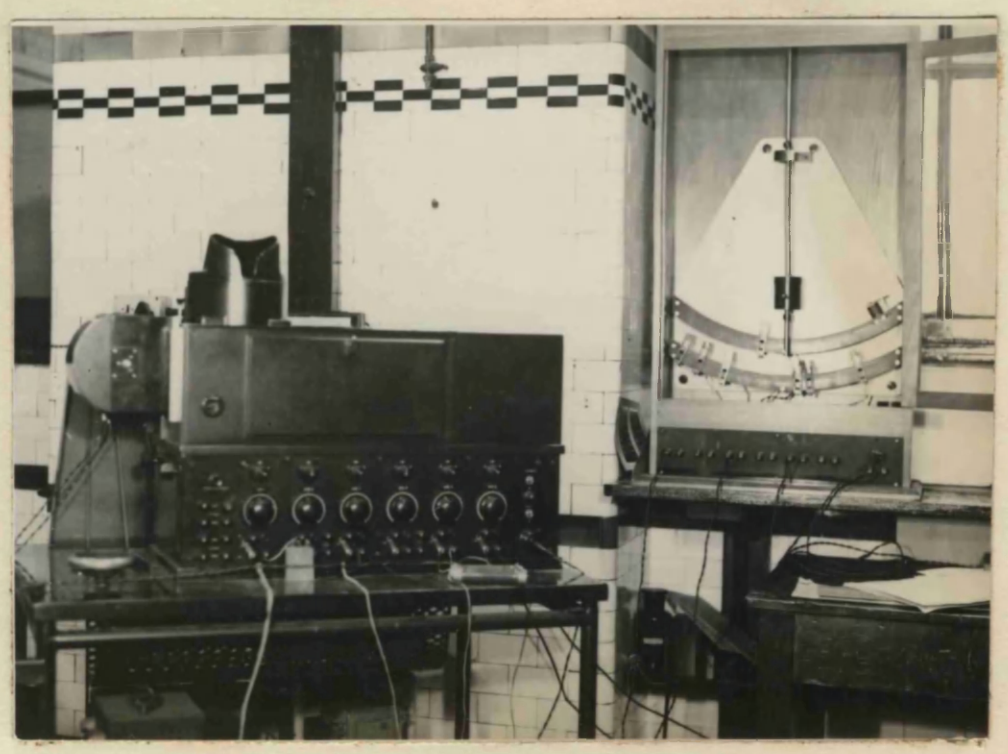

FIG. 7a : The Dudell oscillograph and the pendulum timing switch.

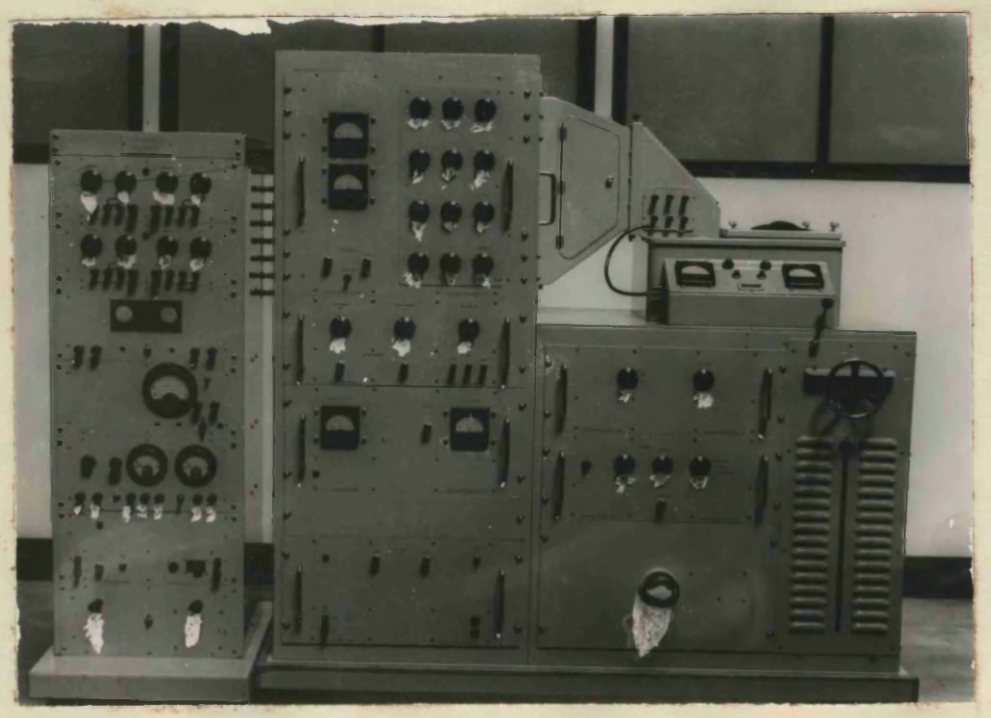

FIG. 7b : The Transient Recorder, TR 30, and the d.c. amplifier.

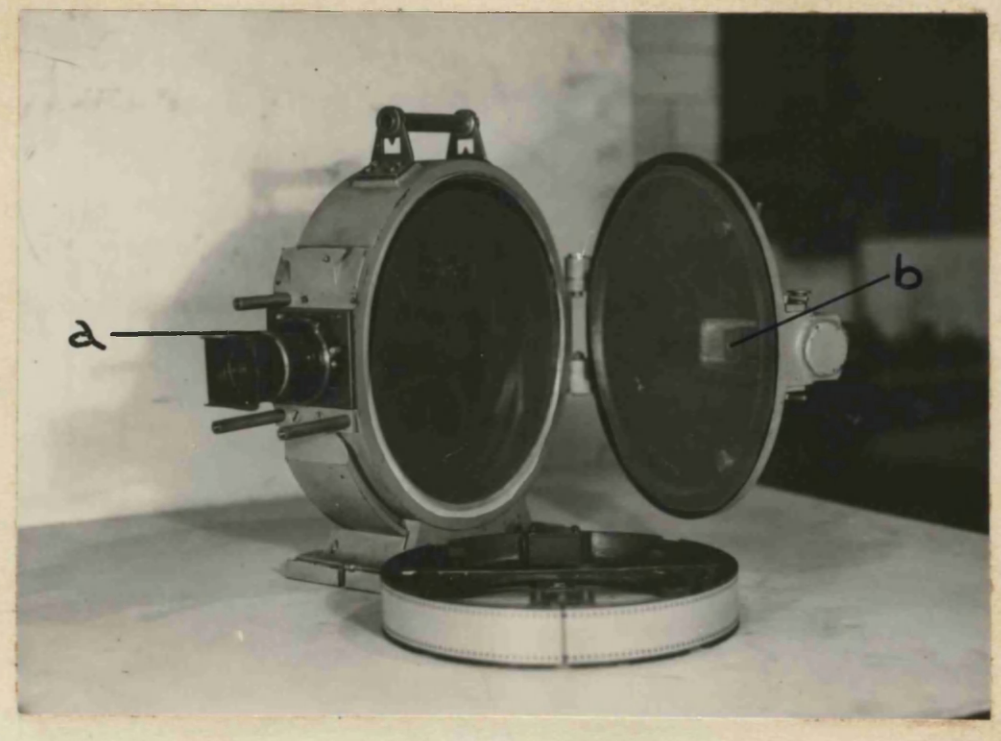

FIG. 1. Showing the ciné-camera used.

(a) lens assembly.

(b) focussing screen.

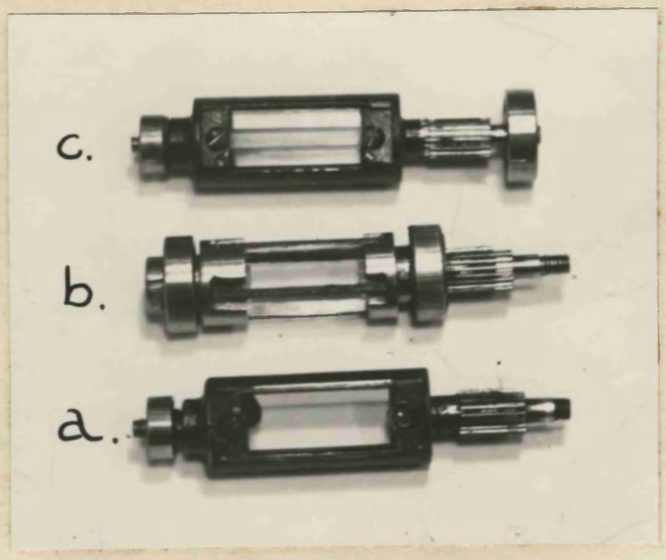

FIG. 2. Showing various compensating blocks used.

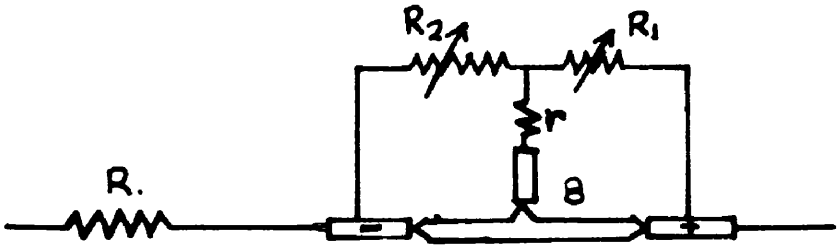

Fig. 1.

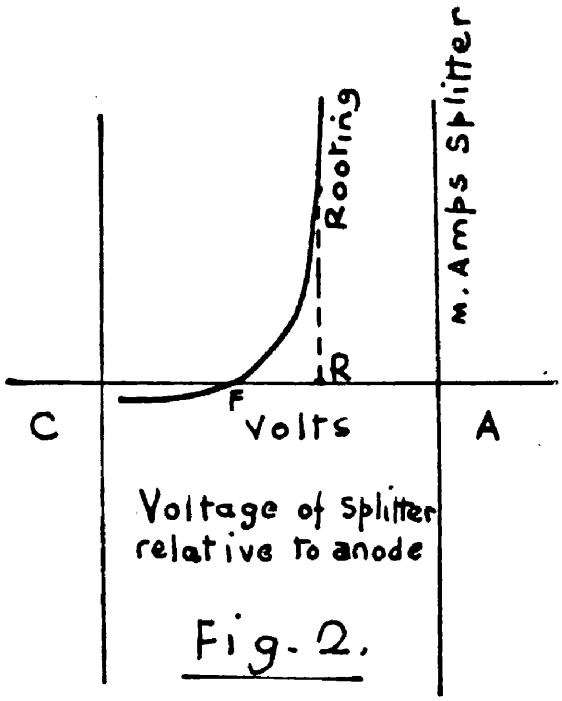

Fig. 2.

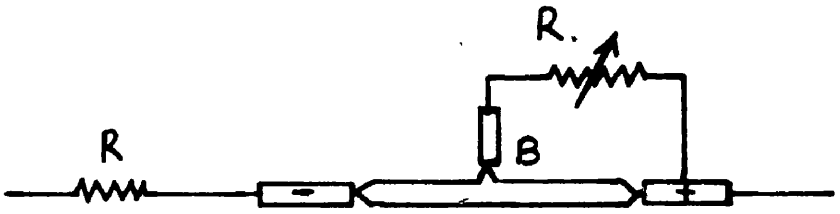

Fig. 3.

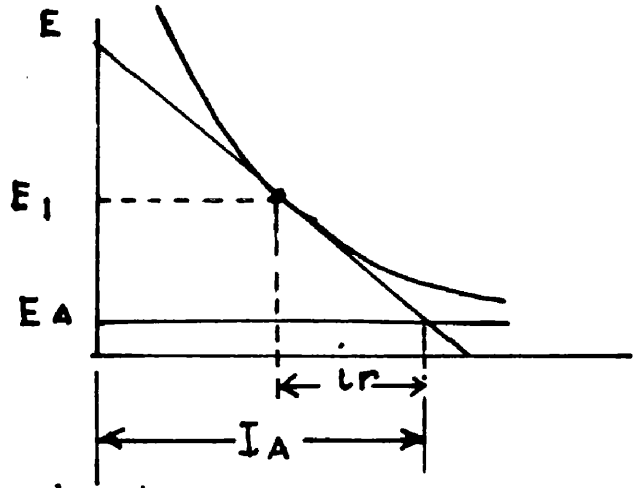

Fig. 4. Static Characteristic

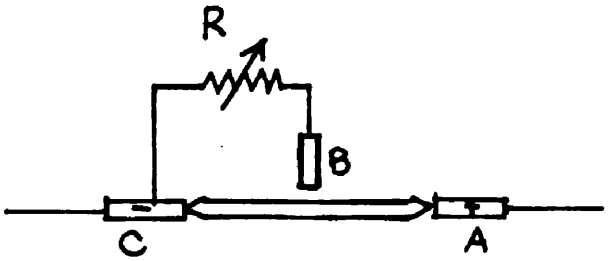

Fig. 5. Cathode Rooting.

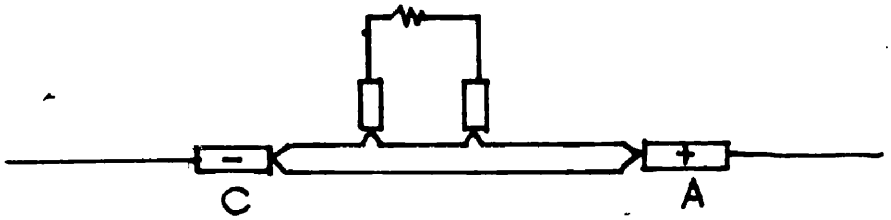

Fig. 6.

(Appendix IV.)